UNDERSTANDING GASTRIC SQUAMOUS-COLUMNAR JUNCTION CARCINOGENESIS

A Dissertation

Presented to the Faculty of the Graduate School

of Cornell University

In Partial Fulfillment of the Requirements for the Degree of

Doctor of Philosophy

by

Dah-Jiun Fu

December 2018

UNDERSTANDING GASTRIC SQUAMOUS-COLUMNAR JUNCTION CARCINOGENESIS

Dah-Jiun Fu, B.V.M., M.V.M., Ph. D.

Cornell University 2018

Areas of a junction between two types of epithelia are known to be cancer-prone in many organ systems. In some cases, this is attributed to stem cell niches located in such areas. However, mechanisms responsible for the preferential malignant transformation of cells at the junction areas, as compared to their counterparts in other regions of the same organ systems, remain insufficiently elucidated. Here we report that inactivation of tumor suppressor genes *Trp53* and *Rb1* in the gastric epithelium derived from $Lgr5^+$ stem cells results in preferential formation of metastatic poorly differentiated neoplasms, which are similar to human gastroesophageal junction (GEJ) carcinoma. Mouse carcinomas arise from the gastric squamous-columnar junction (SCJ), in spite of predominant presence of $Lgr5^+$ cells in the antrum. Unlike antral cells, SCJ cells comprise a highly proliferative pool of immature cancer-prone $Lgr5^-CD44^+$ cells. These cells express CD44 ligand osteopontin (OPN), which promotes organoid formation ability, stemness and tumorigenicity of gastric cells. OPN expression is downregulated in $Lgr5^+$ cells due to repression of the OPN encoding gene *Spp1* by a downstream effector of WNT signaling TCF-4. Supporting the key role of OPN-CD44 signaling in carcinogenesis, Lgr5 expression attenuates tumor growth and no $Lgr5^+$ neoplastic cells are present in mouse and human SCJ

carcinomas. In sum, OPN-responsive immature $Lgr5^{-}CD44^{+}$ cells represent the most susceptible target for the malignant transformation. Since OPN and CD44 overexpression correlate with the worst prognosis of human GEJ carcinoma, detection and selective targeting of active OPN-CD44 pathway may have direct clinical relevance.

BIOGRAPHICAL SKETCH

Dah-Jiun Fu was born on December 24, 1983, in Taipei, Taiwan. Dedicated to a career in Veterinary Medicine and Biomedical Sciences, Dah-Jiun obtained his Bachelor's and Mater's degree in Veterinary Medicine from the National Taiwan University. After the military service, Dah-Jiun worked in the Institute of Biomedical Sciences, Academia Sinica as a research assistant. In 2012, Dah-Jiun started to pursue his Ph. D. degree at Cornell University, Ithaca, New York, where he studied the mechanisms underlying the carcinogenesis of gastric squamous-columnar junctions under the guidance and supervision of Dr. Alexander Nikitin.

ACKNOWLEDGMENTS

I would like to express my deepest appreciation to my advisor, Dr. Alexander Nikitin for his guidance and encouragements during my Ph. D. training, giving me the opportunity to work on this exciting and challenging project. Without his persistent help and patience this dissertation would not have been possible. I would also like to thank my special committee members, Drs. Gerald Duhamel, Tudorita Tumbar, and Robert Weiss for their suggestions and help throughout my study.

I would like to thank all my former and current lab colleagues, especially Andrea, Lianghai, and Fouad, who have participated in this project. I would also like to thank Chieh-Yang, Chris, Aditi, Jacqueline, Ashley, Blaine, Ian, Arjun, and Tera for their support and help.

I am grateful to our collaborators, Dr. Andrew Miller for pathologic evaluation of our new mouse model; Dr. Feng Li for patient tissue collection; Dr. Frederic J. de Sauvage for providing *Lgr5*-DTR mice; Dr. John Schimenti and his student Robert Yamulla for preparing CRISP-related resources; Dr. Anton Berns for providing floxed *Trp53* and *Rb1* mice. I would also like to acknowledge Walter Iddings, Cornell Microbiology and Immunology Department for assistance with confocal imaging; Christian Abratte, Cornell Stem Cell and Transgenic Core for packaging lentivirus, Jennifer K. Grenier, Cornell RNA sequencing Core for providing RNA sequencing and analysis support, Adam P. Wojno, Cornell Biotechnology Resource Center for

assistance with FACS.

A very special gratitude goes out to the College of Veterinary Medicine, Cornell University for Graduate Research Assistantship, and Ministry of Education, Taiwan for Study Abroad Scholarship as a financial support during these years.

Last but not least, I would like to deeply thank my family and friends for their encouragement. Thank you to my significant other, Yi-An, for all her love and support.

TABLE OF CONTENTS

LIST OF FIGURES

LIST OF TABLES

LIST OF ABBREVIATIONS

ABC	Avidin-biotin complex
Ad-*Cre*	Adenovirus Cre recombinase
ALDH1	Aldehyde dehydrogenase 1
APC	Adenomatous polyposis coli
BrdU	5-Bromo-2'-deoxyuridine
CreERT2	Cre fused to a G400V/M543A/L544A triple mutation of the human estrogen receptor ligand-binding domain
CPC	Cancer-propagating cells
CRISPR	Clustered Regularly Interspaced Short Palindromic Repeats
DAB	Diaminobenzidine
DAPI	4',6-Diamidino-2- phenylinodole
DCLK1	Doublecortin-like kinase 1
DT	Diphtheria toxin
GEJ	Gastroesophageal junction
GE	Glandular epithelium
GFP	Green Fluorescent protein
GSEA	Gene set enrichment analysis
EGF	Epidermal growth factor
FACS	Fluorescence activated cell sorting
FGF	Fibroblast growth factor
HGF	Hepatocyte growth factor
HIF-2α	Hypoxic inducible factor-2α

IAP	Inhibitors of apoptosis protein
ICD	Intracellular domain
IHC	Immunohistochemistry
KRT	Keratin
Lgr5	Leucine-rich repeat-containing G-protein coupled receptor 5
MDR	Multidrug-resistance
OPN	Osteopontin
PBS	Phosphate-buffered saline
p.i.	Post injection
PI3K	Phosphatidylinositiol 3-kinase
PLCY	Phospholipase CY
RB1	Retinoblastoma 1
RFP	Red fluorescent protein
RT-PCR	Reverse transcriptase polymerase chain reaction
SCJ	Squamous-columnar junction
SDF-1α	Stromal-derived factor 1 alpha
SE	Squamous epithelium
shRNA	Short hairpin ribonucleic acid
STIC	Serous tubal intraepithelial carcinoma
TAC	Transit amplifying cell
TAM	Tamoxifen
TGF-β	Transforming growth factor beta
TIAM1	T-cell lymphoma invasion and metastasis-inducing protein 1

Trp53	Transformation related protein
TZ	Transitional zone
UTR	Untranslated region

CHAPTER 1

INTRODUCTION*

1.1 Epithelial transitional zone

1.1.1 Definition

An epithelial transitional zone (TZ; aka epithelial junction) is anatomically and histologically identified as the area where two different types of epithelia meet (Fu et al., 2018; McNairn and Guasch, 2011). These distinct structures occur at various places in human and animal bodies. The junction between the stomach and esophagus, for example, is a direct transition from the esophageal stratified squamous epithelium to the gastric glandular epithelium (Wang et al., 2011). Thus this region is also called the squamous-columnar junction (SCJ). The hilum region, which is a junction between the ovary and fimbria, has also been identified as an epithelial TZ (Flesken-Nikitin et al., 2013; Flesken-Nikitin et al., 2014; Ng and Barker, 2015). Other TZs have been found at the limbus region between cornea and conjunctiva in the eye, the junction between the anus and rectum, and the cervical area between the uterus and vagina epithelium (Fu et al., 2018; McNairn and Guasch, 2011).

*In part published as Fu, D.-J., Miller, A.D., Southard, T.L., Flesken-Nikitin, A., Ellenson, L.H., and Nikitin, A.Y. (2018). Stem Cell Pathology. Annu Rev Pathol *13*, 71-92.

1.1.2 Epithelial transitional zones and stem cells

Under normal physiological conditions, most epithelial TZs are subjected to more extensive and frequent damages than the other regions in the same or nearby organs (McNairn and Guasch, 2011). This notion is supported by the evidence that the junction epithelium naturally demonstrates some properties similar to those of the epidermis responding to wounding (Schäfer and Werner, 2007). For example, tissue-repairing marker Tenascin C and hyperproliferation-associated maker keratin 17 (KRT17) are highly expressed by the anal-rectal junction epithelium, accompanied with a large number of $Mac1^+$ macrophages present in the submucosa of this region. These findings suggest that this junction has a lesion-like state in normal physiological condition (Guasch et al., 2007). Similar to the anal-rectal junction, expression of pre-lesional markers, such as Tenascin C and K17, has also been observed in other TZs including the uterine-cervical junction, gastroesophageal junction (GEJ), and the corneal limbus region in the eye (Martens et al., 2004; McNairn and Guasch, 2011; Schlötzer-Schrehardt et al., 2007).

Stem cells are undifferentiated, long-living cells with the unique capacities of self-renewal and differentiation. These cells are required for tissue development, homeostasis, and repair. Because the epithelial TZs are lesion-prone sites in the body, these regions commonly contain the stem cell niches responsible for the tissue regeneration and repair upon injury (Fu et al., 2018; McNairn and Guasch, 2011). The anal-rectal junction, for instance, contains a reservoir of label-retaining population that is characterized by expression of well-known stem cell marker, CD34, and by the potential

capacity to give rise to the differentiated anal epithelium (Runck et al., 2010). In addition, the putative stem/progenitor cell population of cornea has been identified at the limbus region of the eye over four decades ago (Davanger and Evensen, 1971). Further studies supported the notion that this limbal stem/progenitor population, which is marked as ABCB5 and PAX6/p63, contributes to the maintenance of corneal epithelial homeostasis and wound healing (Ksander et al., 2015; Ouyang et al., 2014). The presence of putative stem/progenitor cell niche has also been demonstrated in other epithelial junctions such as GEJ, uterine-cervical junction, the hilum region of ovary-fimbriae junction (Fu et al., 2018) and tubal-peritoneal junction (Schmoeckel et al., 2017).

1.1.3 Epithelial transitional zone and cancer

Numerous studies have suggested that epithelial TZs are more predisposed to cancer than the other regions in the same organ (Cavaleiro-Pinto et al., 2011; Flesken-Nikitin et al., 2014; Fox and Wang, 2014; Herfs et al., 2012; McKelvie et al., 2002; McNairn and Guasch, 2011; Quante et al., 2012; Serra and Chetty, 2006). In one of the most compelling examples, 81% of ocular squamous cell carcinomas arise in the limbus region of the eye (McKelvie et al., 2002). In the anal region, the incidence of cancer arising from the junction between the rectum and anus is three times higher than that of the anal margin (McNairn and Guasch, 2011). In addition, the prognosis of the anal-rectal junction cancer is less favorable (Jemal et al., 2011; Serra and Chetty, 2006).

Unfortunately, the underlying molecular and cellular mechanisms predisposing the epithelial junction regions to cancer remain to be understood.

1.1.4 Stem cells and the cellular origin of cancer

Cancer is considered to be an evolutionary process propelled by the sequential accumulation of genetic and/or epigenetic mutations in the progeny of normal cells, leading to a selective proliferation advantage of these mutant cells, followed by a progression to an uncontrollable growth (Blanpain, 2013; Greaves and Maley, 2012; Kusano et al., 2008; Merlo et al., 2006). The cancer cell-of-origin, or the cancer-initiating cell, is defined as the first normal cell that accumulates enough loads of cancer-associated mutations leading to malignant transformation (Rycaj and Tang, 2015; White and Lowry, 2015). A better understanding of the cell of cancer origin may provide critical information for elucidating of carcinogenesis, predicting tumor behavior, as well as developing better earlier diagnostic methods and preventive therapeutics targeting at these specific cancer-prone populations (Visvader, 2011).

Numerous studies have indicate that stem cells are the most likely candidates to be the cells of origin in the majority of cancer types (Barker et al., 2009; Flesken-Nikitin et al., 2013; Liu et al., 2011; Wang et al., 2009; White et al., 2011); A number of key stem cell properties are likely contribute to their susceptibility to the malignant transformation. Firstly, stem cells usually demonstrate longer life spans than their progeny. This characteristic allows them to constitutively accumulate multiple oncogenic genetic

mutations and epigenetic (Visvader, 2011; White and Lowry, 2015). Second, stem cells are capable of self-renewal. This is a process by which stem cells produce unaltered progenies that inherit the functional role of the mother stem cell for the long-term maintenance of given tissue homeostasis. Self-renewing ability provides an opportunity to pass the oncogenic mutations to next generation of stem cells, resulting in a sequential accumulation of genetic alterations (Visvader, 2011). Third, most of stem cells are maintained in quiescent state resulting in a preferential execution of error-prone DNA repair mechanism in response to DNA damage. The two distinct pathways, such as non-homologous end joining (NHEJ) and homologous recombination (HR), are responsible for DNA damage repair and essential for cell survival and tissue homeostasis (Sancar et al., 2004). Importantly, during the G0/G1 phase, the damaged DNA is repaired through the NHEJ-mediated pathway, while during the S-G2/M phase, the damaged DNA is repaired through the HR-mediated pathway (Blanpain et al., 2011). A previous report has suggested that the quiescent hematopoietic stem cells preferentially perform the NHEJ-mediated DNA repair mechanism leading to their susceptibility to genomic instability associated with malignant transformation (Mohrin et al., 2010).

Previous studies in our laboratory have shown that the high-grade serous ovarian carcinoma may develop from cancer-prone stem cells located in the ovarian hilum region, which is epithelial TZ, connecting the ovarian surface epithelium, mesothelium, and uterine tube (Flesken-Nikitin et al., 2013; Flesken-Nikitin et al., 2014). The hilum cells express multiple stem cell markers, such as ALDH1, Lgr5, and LEF1, and are

responsible for the maintenance of epithelial homeostasis of the ovarian surface according to lineage tracing analysis. Notably, the hilum cells have proven to be more susceptible to the malignant transformation after losing tumor suppressor genes *Trp53* and *Rb1,* as compared to their progeny located in other ovarian regions. The transformation phenotypes, of the hilum cells included increased proliferation and decreased senescence (Flesken-Nikitin et al., 2013). Furthermore, mice transplanted with mutant hilum cells developed neoplasms much faster and more frequently than mice injected with mutant ovarian surface epithelium derived from other regions of the ovary (Flesken-Nikitin et al., 2013). Malignant tumors arising from the mutant hilum cells had extensive expression of certain markers of the high-grade serous ovarian carcinoma, such as keratin 8 (KRT8), PAX8, WT1, and estrogen receptor 1 (ER1), thereby closely resembling human disease (Flesken-Nikitin et al., 2013). Taken together these studies provided direct experimental evidence that stem cell niches residing in TZ may have preferential susceptibility to the malignant transformation.

In agreement with the observations in mice, the serous tubal intraepithelial carcinoma (STIC), which is regarded as the precursor of high-grade serous ovarian carcinoma, has been frequently located close to the tubal-peritoneal junction in human (Schmoeckel et al., 2017; Seidman, 2015). It is noteworthy that both the normal tubal peritoneal junction and the STIC express stem cell marker LEF1, supporting the idea that the STIC may arise from the putative stem/progenitor population in the TZ between the tubal epithelium and mesothelium (Schmoeckel et al., 2017). However, it remains uncertain

whether the existence of cancer-prone TZ stem cell niches can be generalized to other organs and tissues.

1.2 Stomach

1.2.1 Anatomic and histologic structure

The stomach is the expandable digestive organ located between the esophagus and small intestine in the upper gastrointestinal tract. Anatomically, the human stomach is divided into four distinct parts: the cardia which surrounds the esophageal entry, the fundus which lies above the horizontal line and forms the upper curvature of the stomach, the body which is the main part of stomach, and the antrum/pylorus which is a funnel-shaped area posteriorly linking to the duodenum. Histologically, the stomach is divided into three sections based on the type of glands composing each region: the cardia, corpus (fundus/body) and the antrum/pylorus (Figure 1.1).

The anatomic morphology of the mouse stomach differs from that of human. The mouse stomach is divided into two main compartments: the squamous epithelial forestomach part and the distal glandular part (Ghoshal and Bal, 1989). The squamous-columnar junction (SCJ), which occurs at the transition between the esophagus and stomach in humans, is shifted to the midline of the stomach in mice because the keratinized squamous epithelium posteriorly extends from the end of the esophagus to the median plane of the stomach (Kararli, 1995). The glandular part of the mouse stomach is more

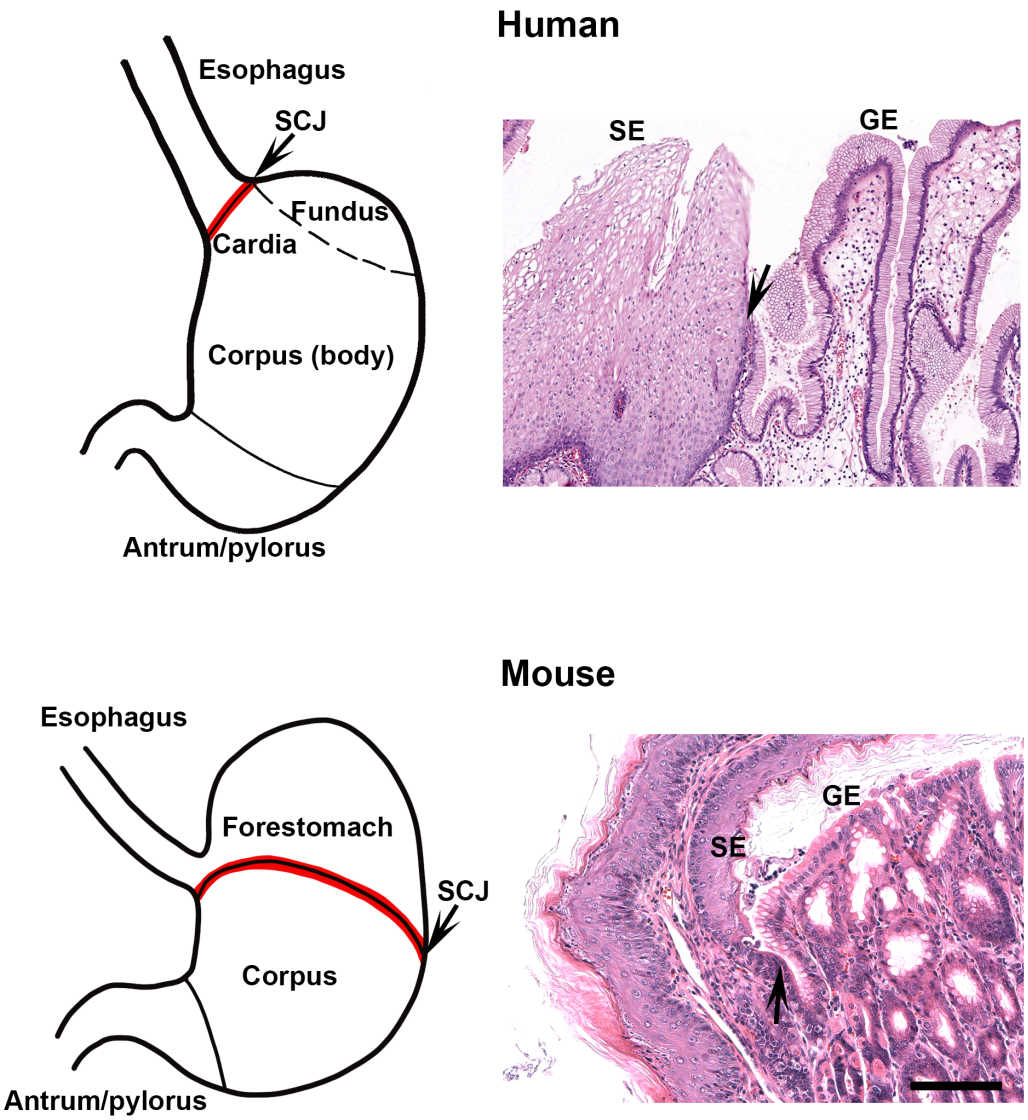

Figure 1.1 Anatomy and histology of human and mouse stomach. Arrows indicate the squamous-columnar junction (SCJ). SE, squamous epithelium. GE, glandular epithelium. The scale bar in bottom panel represents 210 μm (top panel) and 100 μm (bottom panel).

similar to humans, and that can be subdivided into three section; the cardia, corpus, and antrum/pylorus (Figure 1.1). Despite these differences in anatomic structure, the mouse gastric SCJ has been comparable to human GEJ in histology, physiology, molecular biology, and genetic analysis that allows for modeling human GEJ diseases, such as gastroesophageal reflux, intestine-like metaplasia, and cancer (Attwood et al., 2008; Kapoor et al., 2015; Kararli, 1995; Oh et al., 2009; Tétreault, 2015)

1.2.2 Putative gastric stem cell niches

Squamous-columnar junction (SCJ) and cardia

Recent studies have suggested that the leucine-rich-repeat-containing G protein-coupled receptor 5 (Lgr5) marks a putative stem/progenitor cell population present at the base of the first pit of glandular epithelium (Barker et al., 2010; O'Neil et al., 2017). These $Lgr5^+$ cells may contribute to the epithelial homeostasis of SCJ at the vicinity of esophageal entry (Barker et al., 2010). In addition, it was reported that overexpression of cytokine IL-1 accompanied by exposure to bile acid can induce the expansion and migration of $Lgr5^+$ cell progeny into the distal esophagus. This process potentially gives rise to Barrett's esophagus (BE) metaplasia, which is the likely precursor of GEJ carcinoma (Quante et al., 2012). Another study demonstrated that the SCJ region of mouse stomach contains a distinct $p63^+K5^+K7^+$ basal cell population serving as the progenitor of transitional epithelium (Jiang et al., 2017). Importantly, ectopic expression of CDX2 can induce the metaplasia of these transitional basal cells thereby resulting in

BE at the SCJ regions in both human and mouse (Jiang et al., 2017). These findings suggest that the SCJ region is maintained by its own stem/progenitor population and is potentially susceptible to malignant transformation. However, they do not provide definitive proof that stem/progenitor cell are the cells of origin of malignant carcinoma.

Corpus

Each corpus gland can be subdivided microscopically into four subcompartments. From bottom to top, these are base, neck, isthmus and the pit (foveolar) surface (Fu et al., 2018). Of these regions, the isthmus and the corpus have proven to contain different stem cell populations. In the isthmus, a putative stem/progenitor cell population is undifferentiated, frequently divides and lacks granules in the cytoplasm (Karam and Leblond, 1993). The subsequent studies demonstrated that these isthmal stem/progenitor cells could be identified by expression of transcription factor MIST1 (Muscle, Intestine, and stomach expression 1) (Hayakawa et al., 2015) and Runx1 enhancer element (eR1) (Matsuo et al., 2017). By lineage tracing analysis, these isthmal cells were shown to be the self-renewing, multipotent stem cells involved in the renewal of corpus epithelium over a long period of time under normal homeostasis condition (Hayakawa et al., 2015; Matsuo et al., 2017). In contrast to the actively proliferating isthmal stem cells, the base of corpus gland contains an alternative “reserve” stem/progenitor cells (Leushacke et al., 2017; Stange et al., 2013). These cells are quiescent, differentiated chief cells marked by expression of Lgr5 and Troy and capable to act as stem/progenitor cells in response to tissue damage (Leushacke et al., 2017; Stange et al., 2013). The isthmal stem/progenitor markers such as Mist1 and

eR1, are also expressed by some of the corpus base cells, suggesting the considerable plasticity between stem/progenitor cells and differentiated cells (Hayakawa et al., 2015; Leushacke et al., 2017; Matsuo et al., 2017; Stange et al., 2013).

Antrum/Pylorus

$Lgr5^+$ cells are present at the base of each antral gland and serve as active proliferating stem cell responsible for populating entire antral gland every 7 to 10 days (Barker et al., 2010). In the organoid cultures, $Lgr5^+$ cells show the self-renewal potential and multipotent capacity to differentiate into various types of mature cells. (Barker et al., 2010). Another putative stem/progenitor cell population, which is marked as $Villin^+$, resides at or below the isthmus region of antral gland (Qiao et al., 2007). Unlike the frequently dividing $Lgr5^+$ cell, the $Villin^+$ cell remains quiescent in normal homeostasis condition, but demonstrate high proliferative potential in response to inflammatory damage (Qiao et al., 2007). On the other hand, the cholecystokinin B receptor (CCK2R), which is the receptor for neuroendocrine peptide gastrin, marks the other distinct stem/progenitor population at the ishmus segment of antral gland (Hayakawa et al., 2015). These $CCK2R^+$ cells reside above the LGR5-high-expressing ($LGR5^{high}$) stem cell niches and overlap with the LGR5-low-expressing ($LGR5^{low}$) or LGR5-negative ($LGR5^{neg}$) cells in the antral glands (Hayakawa et al., 2015). Notably, the fate of isthmal $CCK2R^+$ cells is regulated by gastrin precursor progastrin, which is secreted by the neuroendocrine G-cell, promoting the neoplasia of antral region (Hayakawa et al., 2015). In addition, other stem cell markers, such as SOX2 and RUNX1, have been

shown to identify the putative stem/progenitor isthmal cells in the antral glands (Arnold et al., 2011; Matsuo et al., 2017).

1.3 Pathogenesis of gastric squamous-columnar junction cancer

1.3.1 Global epidemiology of gastric cancer

According to World Health Organization (WHO), gastric cancer is the fifth most common malignancy worldwide, with an estimated 952,000 new cases (6.8% of total) in 2012, behind the cancers of lung, breast, colorectum and prostate (Ferlay et al., 2015; Torre et al., 2015). Gastric cancer is also the third leading cause of cancer mortality with an estimated 723,000 deaths (8.8% of total) (Jemal et al., 2011; Torre et al., 2015). Of these cases, more than 70% are observed in developing countries Gastric cancer has a wide variability of incidence across countries (McLean and El-Omar, 2014). The highest incidence rate of gastric cancer occurs in East Asian countries such as Korea, with estimated 65.9 in men and 25.9 in women per 100,000 people. On the contrary, the lowest incidence rate is observed in North African countries like Egypt with estimated 3.3 in men and 2.0 in women per 100,000 people (Jemal et al., 2010).

Despite the advances in diagnosis and therapeutic methods of modern medicine, the patients with gastric cancer generally have a dismal prognosis with the overall 5-year survival rate being only 20% in most countries of the world (Karimi et al., 2014). This poor prognosis may be explained by the difficulty of early detection and the limited

response of gastric cancer to conventional chemotherapy and radiotherapy. Surgical resection is the most common therapeutic option for gastric cancer, however, the gastric resection leads to a number of the adverse effects, such as loss of appetite, heartburn, dysphagia, early satiety, and vomiting, thereby resulting in a poor quality of patients' life (Karanicolas et al., 2013). Therefore, development of approaches for early diagnosis, effective prevention and less debilitating treatments of gastric cancer is urgently needed.

1.3.2 Changing trends in the incidence rate of gastric cancer

Gastric cancer had been the most commonly diagnosed neoplasm worldwide in the past. However, the incidence rate has decreased by more than 80% since 1950s (Jemal et al., 2010; Parkin et al., 1984). The overall incidence rate for gastric cancer has particularly declined in developed western countries (Bertuccio et al., 2009)9. Reasons for this significant decrease in incidence rate remain to be elucidated, but it may be attributed to the improvement of dietary hygiene due to the invention of refrigerators, and the decline of *Helicobactor pylori* infection due to the application of antibiotics (Jemal et al., 2010; Parkin, 2006). The use of electric refrigerator, for instance, increased rapidly in most households between the 1960s to 1970s, consistent with the time when gastric cancer incidence started to decline (La Vecchia et al., 1990). Electric refrigerator provided a better way to keep food fresh, resulting in a decrease in use of potentially carcinogenic nitrites and excess salts, which were commonly used for food preservation (Jemal et al., 2010; La Vecchia et al., 1990). Furthermore, infection with

Helicobacter pylori has been considered as one of the most prominent causative factors for gastric cancer, and is estimated to be responsible for 65 to 80% of overall gastric cancer cases worldwide (Cavaleiro-Pinto et al., 2011; Fox and Wang, 2014; Ishimoto et al., 2014; Karimi et al., 2014; McNairn and Guasch, 2011). It was reported that the risk of gastric cancer in *Helicobacter pylori*-seropositive people is 2.1 to 16.7 times greater than that in the seronegative individuals (Crew and I Neugut, 2006). In addition, the countries with rapidly declined gastric cancer incidence rates typically have a reduction in the prevalence of *Helicobacter pylori* infection which is attributed to sanitation improvement and the availability of antibiotic treatment (Jemal et al., 2011).

Unfortunately, while the overall gastric cancer incidence rate has substantially declined in the past few decades, the incidence of cancer arising from the gastric SCJ and in the vicinity of distal esophagus has steadily increased in many countries such as the United State, Japan, Demark and the United Kingdom (Botterweck et al., 2000; Buas and Vaughan, 2013; Kusano et al., 2008). For example, the incidence of gastric SCJ cancer has risen nearly 2.5-fold in the United States from 1970s to 2000s, being responsible for approximately half of all gastric cancer cases in 2008 (Buas & Vaughan 2013). In Japan, the proportion of gastric cancer that is located at the gastric SCJ has risen from 2.8% to 10% between 1962 and 2005 (Kusano et al., 2008). Notably, the prognosis of the gastric SCJ cancer is generally worse than cancers located in other regions of the stomach. The 5-year survival rate of the patients with gastric SCJ cancer is approximately 2-12%, compared to 20-25% for all gastric cancers (Buas and Vaughan,

2013; Parkin, 2001). The underlying reasons for the increase in SCJ cancer frequency and poorer prognosis remain unknown.

1.3.3 Animal models of gastric cancer

Historically, animal models have been widely used in biomedical research to understand disease pathogenesis, to explore the molecular mechanisms of action, and to evaluate novel therapeutic agents against numerous types of diseases (Day et al., 2015; Dow and Lowe, 2012; Hayakawa et al., 2013; HogenEsch and Nikitin, 2012; McGonigle and Ruggeri, 2014) (Table 1). The earliest animal model for gastric cancer was developed by utilization of carcinogenic nitrosamines such as MNNG (*N*-methyl-*N*-nitro-*N*-nitrosoguanidine) in rat and MNU (*N*-methyl-*N*-nitrosourea) in mouse (Saito and Sugimura, 1973; Sugimura and Fujimura, 1967; Tatematsu et al., 1992). Treatment with MNU induces epithelial atrophy, inflammation, and neoplasm in the stomach of mice from a variety of genetic backgrounds (Yamamoto et al., 2002).

Subsequently, with the discovery of the strong link between gastric cancer and infection with *Helicobacter pylori*, subsequent studies started to shift their focus to the development of animal models on the basis of *Helicobacter* infection (Hayakawa et al., 2013). Mice have been shown to be resistant to colonization with *Helicobacter pylori* in the stomach. However, *Helicobacter felis*, another *Helicobactor* species derived from cat stomach, were identified as a potential agent to induce chronic gastritis, atrophic lesions and invasive adenocarcinoma in the mouse stomach

Table 1.1 Existing mouse models for gastric cancer

Model	Duration	Location	References
MNU	12 months	Antrum	(Saito and Sugimura, 1973)
MMTV	3-4 months	SCJ	(Koike et al., 1989)
HPV-16	246-352 days	Antrum	(Searle et al., 1994)
Smad4$^{-/-}$	12-18 months	Corpus	(Xu et al., 2000)
INS-GAS	20 months	Corpus	(Wang et al., 2000)
MTH1$^{-/-}$	18 months	Antrum	(Tsuzuki et al., 2001)
H. felis	18 months	SCJ	(Fox et al., 2002)
MNU + *H. pylori*	12 months	Antrum	(Han et al., 2002)
Gp130$^{-/-}$	6 months	Antrum	(Tebbutt et al., 2002)
CEA/SV40	50 days	Antrum	(Syder et al., 2004)
GAS$^{-/-}$	12 months	Antrum	(Zavros et al., 2005)
Wnt1/C2me	20 weeks	SCJ	(Oshima et al., 2006)
IL-1β + *H. felis*	12 months	Corpus/Antrum	(Tu et al., 2008)
CDH1$^{-/-}$ + MNU	40 weeks	Antrum	(Humar et al., 2009)
K19/K-ras	16 months	Corpus	(Okumura et al., 2010)
RUNX3$^{-/-}$ +MNU	52 weeks	Corpus/Antrum	(Ito et al., 2011)
MNU + *H. felis*	36 weeks	Antrum	(Tomita et al., 2011)
TFF1$^{-/-}$	5 months	Antrum	(Soutto et al., 2011)
GB-Smad4$^{-/-}$	12-18 months	Antrum	(Hahn et al., 2011)
Atp4a-CDH1$^{-/-}$p53$^{-/-}$	12 months	Corpus	(Shimada et al., 2012)
Villin-KLF4$^{-/-}$	80 weeks	Antrum	(Li et al., 2012)
L2-IL-1β	20-22 weeks	SCJ	(Quante et al., 2012)
Mist1-Kras^{G12D}APC$^{-/-}$	4 months	Corpus	(Hayakawa et al., 2015)
eR1-Kras^{G12D}	3 months	Corpus/Antrum	(Matsuo et al., 2017)
KRT5-CDX2	13 weeks	SCJ	(Jiang et al., 2017)

Abbreviations: MNU, *N*-methyl-*N*- MNU, *N*-methyl-*N*-nitrourea. *H. felis*, *Helicobacter felis*. *H. pylori*, *Helicobacter pylori.* CEA, carcinoembryonic antigen. MMTV, mouse mammary tumor virus. HPV, human papillomavirus. MTH, methuselah gene. TFF1, trefoil factor 1. GB, granzyme B promoter. INS, insulin promoter. GAS, gastrin. GP130, glycoprotein 130. C2me, cyclooxygenase-associated prostaglandin E 2. CDH1, E-cadherin encoding gene. RUNX3, runt-related transcription factor 3. KLF4, krupple-like factor 4. MIST1, muscle, intestine and stomach expression 1. eR1, Runx1 ehancer element. KRT5, cytokeratin 5.

(Cai et al., 2005; Fox et al., 2002). However, some limitations, such as slow time course and low incidence rate of advanced gastric cancer, have been reported in this *Helicobacter*-associated mouse model (Hayakawa et al., 2013).

Recent progress in genetic and genomic engineering has provided a powerful tool to develop genetically modified mouse models resembling an extensive variety of human diseases (Day et al., 2015; Dow and Lowe, 2012). By introduction of certain transgenes, several mouse models have been generated to explore the effect of hormones, growth factors and cytokines in cancer initiation and progression (Poh et al., 2016). For example, insulin-gastrin (INS-GAS) transgenic mice constitutively express human gastrin in the serum leading to an increase in secretion of gastric acid and parietal cell mass at the young age (Wang et al., 2000). Over time, the INS-GAS mice show loss of parietal cell mass, hypochloryhydria, and subsequently progress to gastric metaplasia, dysplasia and advanced invasive neoplasms (Hayakawa et al., 2013). Overexpression of WNT1 and prostaglandin E2 under the control of *Krt19* promoter is able to induce neoplasm at the gastric SCJ region (Oshima et al., 2006). Targeted mutation techniques

allow researchers to investigate the role of certain signaling pathways in the gastric carcinogenesis by inactivation of tumor suppressor genes and/or and overexpression of oncogenes. Mice with silent mutations in the tumor suppressor *Tff1*, for instance, show glandular hyperplasia at 3-week of age and subsequently progress to invasive adenocarcinoma in the antral region of the stomach in 5-months old mice (Lefebvre et al., 1996). Moreover, constitutive activation of oncogenic *Kras* in the eR1^{+} (RUNX1 enhancer-expressing) corpus isthmus stem cells can induce precancerous foveolar metaplasia potentially progressing to intestinal-type carcinoma in the corpus and antrum (Matsuo et al., 2017).

1.3.4 Models of the putative cell of gastric SCJ cancer origin

Barrett's esophagus, which is defined by replacement of esophageal stratified squamous epithelium with intestinal-like columnar epithelium at the distal end of the esophagus, has been highly considered as precursor lesion associated with initiation of low-grade dysplasia, high-grade dysplasia and adenocarcinoma in the GEJ region (Quante et al., 2012). Although this pre-neoplastic lesion has been identified more than 60 years ago, the cell of Barrett's esophagus origin remains debatable. One of the recent studies has suggested that the GEJ area contains unique embryonic residual cells that may be the source of precancerous Barrett's esophagus (Wang et al., 2011). In prenatal stage, the stomach is lined with a layer of distinct epithelium that expresses keratin 7 (KRT7). However, the majority of adult gastric epithelium shows an absence of CK7 expression and the positive cells remain only at the GEJ region. The retention of

this “embryonic epithelium” has been identified in the SCJ of mouse stomach and these $CK7^+$ embryonic residual cells can give rise to Barrett’s-like metaplasia in the *p63*-null mouse (Wang et al., 2011).

A distinct population of transitional zone basal cells, which may be the cells of Barrett’s esophagus origin, has been recently identified in the SCJ region of mouse stomach (Jiang et al., 2017). These cells are marked by simultaneous expression of p63, KRT7 and KRT5. Ectopic expression of oncogenic transcriptional factor CDX2 causes the $p63^+CK5^+CK7^+$ transition basal cells to generate goblet cell-containing intestinal-like metaplasia and Barrett’s esophagus lesions (Jiang et al., 2017). Consistent with the findings in mice, these $p63^+CK5^+CK7^+$ transitional basal cells have also been observed in the human GEJ (Jiang et al., 2017). Importantly, the expansion of these transitional basal cells is highly associated with the initiation of Barrett’s esophagus (Jiang et al., 2017).

Notably, a number of alternative putative cells of origin of Barrett’s esophagus has been proposed, such as the transdifferentiated squamous epithelial cells of the esophagus (Milano et al., 2007; Yu et al., 2005), the subpopulation of esophageal basal stem cells (Kalabis et al. 2008), the submucosal gland of esophagus (Leedham et al., 2008), the circulating bone marrow progenitor cells (Sarosi et al., 2008), the cardia glandular epithelial cells (Quante et al., 2012). Nevertheless, none of these experimental models provide direct evidence that Barrett’s esophagus-like lesions derived from these cellular candidates can progress to advanced malignancy. Furthermore, the cell of origin of SCJ

gastric cancers, which do not progress through Barrett's esophagus-like lesions, remains uncertain.

1.4 Osteopontin-CD44 signaling pathway

1.4.1 Osteopontin

Osteopontin (OPN), also known as secreted phosphoprotein 1 (SPP1), is a secreted, multifunctional, and matricellular phosphoglycoprotein that interacts with cell surface receptors, such as CD44 and integrins (Kahles et al., 2014; Shevde and Samant, 2014). OPN plays an important role in a wide range of physiological and pathological processes, such as cell adhesion, proliferation, survival, and angiogenesis. OPN was first identified as a sialoprotein present in the mineralized matrix of bovine bone (Franzén and Heinegård, 1985). The name "osteopontin" is a combined word from "osteo", which is a Greek word for bone, and "pons", which is a Latin word for "bridge", that reflects its function of linkage of cells to extracellular matrix (Reinholt et al., 1990). Besides the bone tissues, OPN is also synthesized by various types of cells and tissues including fibroblasts (Xie et al., 2003), hepatocytes (Tokairin et al., 2008), mammary glands (Nemir et al., 2000), kidney (Zhang et al., 2010), mononuclear leukocytes (Lund et al., 2009), endothelial cells (Singh et al., 1995), and brain (Shin et al., 1999).

OPN functionally contributes to the maintenance of stem cell properties, tissue homeostasis and wound repair in a number of tissues, such as bone marrow (Guidi et al., 2017), liver (Wang et al., 2015), and skin (Wang et al., 2017). During the

hematopoiesis, OPN is expressed by the endosteal surface of bone marrow cavity and regulates hematopoietic stem cell proliferation, aging, and migration (Guidi et al., 2017; Nilsson et al., 2005; Stier et al., 2005). In liver, autocrine OPN promotes the expansion and migration of hepatic progenitor cells and also controls the stem cell properties and differentiation through activation of WNT/β-catenin signaling (Liu et al., 2015). In addition, the OPN-associated signaling is also activated in differentiated hepatic cells, such as hepatocytes, pit cells, oval cells, and biliary epithelial cells that contributes to cell proliferation and activation during the liver regeneration (Wang et al., 2015).

Importantly, aberrant expression and abnormal splicing of OPN have been shown to play a pivotal role in promoting the pathogenesis of various diseases including obesity, diabetes, and cancers (Shevde and Samant, 2014). It has been reported that the expression of variant splicing isoforms of OPN is highly associated with the invasive phenotype of breast cancers (Shi et al., 2014). Another study has suggested that OPN secreted by tumor-associated cells can induce the stem cell marker CD44v6 expression in the colorectal cancer cells through activating WNT/β-catenin signaling pathway, thereby increasing the cell potential for migration and metastasis in colorectal cancer patients (Todaro et al., 2014). Moreover, OPN expression has been found to be a predictor of poorer overall survival of gastric cancer patients (Cheng et al., 2013).

1.4.2 CD44

CD44 is a ubiquitous, polymorphic, transmembrane glycoprotein widely expressed in multiple cell types (Zöller, 2011). This cell surface receptor participates in a wide variety of cellular functions, such as cell growth, differentiation, apoptosis and motility (Bourguignon et al., 2008; Schmitt et al., 2014). There are totally nine different splicing sites in the exons of *CD44* gene that provides multiple variable isoforms of the extracellular membrane domain (Alam et al., 2004). Expression of variant isoforms has been implicated in different cell types. For example, the CD44s is the smallest, standard isoforms that has been observed on the most of vertebrate cells**,** while CD44v expression is restricted to the epidermal ridge during embryonic development, and the cell membrane of some normal and malignant epithelial cells (Heider et al., 1993; Zöller, 2011). It is evident that the CD44 expression is correlated with the cancer prognosis of many organs, including the stomach, intestine, cervix, pancreas, and prostate (Alam et al., 2004; Ghaffarzadehgan et al., 2008; Morath et al., 2016; Noordzij et al., 1997).

Some isoforms of CD44 have been identified as stem/progenitor cell markers in various organs. CD44v4-v10 are expressed by the $LGR5^{+}$ stem cells in the intestinal crypts (Zeilstra et al., 2014). It is also used as the marker for mesenchymal stem cells and hematopoietic stem cells (D'Arena et al., 2014; Lv et al., 2014). CD44 plays an important role in the interaction between stem/progenitor cells and their microenvironment to modulate the fate of embryonic stem cells and adult hematopoietic stem cells by controlling their stemness and differentiation (Ruiz et al., 1995). Hyaluronan (HA), which is a polysaccharide abundantly present in the extracellular matrix, is the major ligand for CD44 that accounts for cell trafficking (Toole, 2004). The

homing migration of hematopoietic stem cells to the bone marrow requires the interaction between HA and CD44 (Avigdor et al., 2004). Moreover, the engagement of HA and CD44 may also participate in other stem/progenitor cell activities, such as cell-cell adhesion, proliferation, differentiation, apoptosis and survival (Toole, 2004; Zöller, 2011).

Similar to stem cells responsible for the normal tissue homeostasis, some cancer cells frequently acquire stem-like characteristics, such as self-renewal, frequently dormancy and relative resistance to conventional chemotherapies. (Chen et al., 2013; Fu et al., 2018). This subpopulation of cancer cells is responsible for the maintenance of tumor growth and is referred to as the cancer-propagating cells (CPC, also known as cancer stem cells) (Flesken-Nikitin et al., 2014; Rycaj and Tang, 2015). Importantly, CD44 has been found to be a frequent marker for the CPC in the cancers of many organs and tissues, such as breast, intestine, ovary, pancreas, and lung (Fillmore and Kuperwasser, 2007; Leung et al., 2010; Ringel et al., 2001; Rodriguez-Rodriguez et al., 2003; Takaishi et al., 2009; Wang et al., 2012). It has been reported that in some cases CD44 does not merely serve as a cell surface marker for CPC, but also plays an important role in the cancer metastasis and resistance to chemotherapy and radiotherapy (Morath et al., 2016); For instance, the metastatic ability of colorectal cancer cells has been diminished by their exposure to CD44v6 neutralizing antibody or by shRNA targeting *CD44v6* mRNA (Todaro et al., 2014). In addition, some cytokines and growth factors, such as stromal-derived factor 1α (SDF-1α), hepatocyte growth factor (HGF), and OPN, can increase the CD44v6 expression in colorectal cancer cells,

and promote tumor growth and migration to distal sites (Todaro et al., 2014). Furthermore, the drug resistance of CPC is also associated with CD44 (Bourguignon et al., 2008). HA-CD44 crosslinking increases the resistance of CPC to chemotherapy by activation of NANOG phosphorylation and its translocation to the nucleus, leading to overexpression of the inhibitor of apoptosis protein (IAP) and multidrug-resistance (MDR) protein that contribute to chemoresistence (Bourguignon et al., 2008).

In gastric cancer, CD44 has also been described as a functional marker involved in self-renewal, differentiation, and chemoresistance (Takaishi et al., 2009). CD44 expression in gastric cancer cells may enhance the protection against reactive oxygen species (ROS) by promoting the synthesis of intracellular antioxidant, thereby accounting for the resistance to chemo- and radiotherapy (Ishimoto et al., 2011). CD44 isoform variant 9 has been reported to be a potential marker for predicting recurrence of early gastric cancer after curative endoscopic dissection (Hirata et al., 2013). $CD44^+$ gastric cancer cells show greater organoid formation ability and tumorigenic potential than $CD44^-$ fraction (Takaishi et al., 2009). Moreover, $CD44^+$ cancer cells are able to give rise to more differentiated $CD44^-$ progeny (Takaishi et al., 2009). However, specific mechanisms linking CD44 to stem cell properties of gastric CPC remain insufficiently elucidated.

1.4.3 The role of osteopontin-CD44 signaling pathway in carcinogenesis

The interaction between OPN and CD44 involves multiple and varied signaling pathways that regulate a wide range of cellular activities and are increasingly implicated in tumor progression and metastasis. First, the OPN-CD44 binding activates the kinase cascades involving phospholipase CΥ (PLCΥ), phosphatidylinositiol 3-kinase (PI3K) and the serine/threonine kinase (Akt) that enhances tumor migration and promotes cell survival through anti-apoptotic signaling (Figure 1.2) (Bellahcène et al., 2008; Lin and Yang-Yen, 2001). Second, OPN-CD44 interaction has been identified as a critical mediator of bladder cancer invasion via activation of T cell lymphoma antigen (TIAM1)-Rac1 signaling pathway (Figure 1.2) (Ahmed et al., 2016). TIAM1, which connects to the cytoplasmic tail of CD44, can be activated once OPN binds to CD44 extracellular domain (Bourguignon et al., 2000). The activated TIAM1 functions as a guanine nucleotide-exchange factor (GEF). It accelerates the exchange of bound GDP for GTP on Rho-GTPase, which contributes to several cellular processes, such as regulation of gene expression, cell cycle progression, and cell migration during the cancer progression (Haga and Ridley, 2016; Mertens et al., 2003). Administration of the CD44 neutralizing antibody or Rho-GDP dissociation inhibitor suppresses the metastatic potential of bladder cancer through blocking of the OPN-CD44-TIAM1-Rac1 signaling (Ahmed et al., 2016). Third, OPN has been shown to promote the stemness and invasiveness of glioma cells by triggering an alternative signaling pathway (Pietras et al., 2014). After binding to CD44, OPN induces proteolytic cleavage of CD44 via activation of presenilin-1/γ-secretase, resulting in the release of CD44 intracellular domain (ICD) (Figure 1.2) (Pietras et al., 2014). The CD44 ICD fragment can

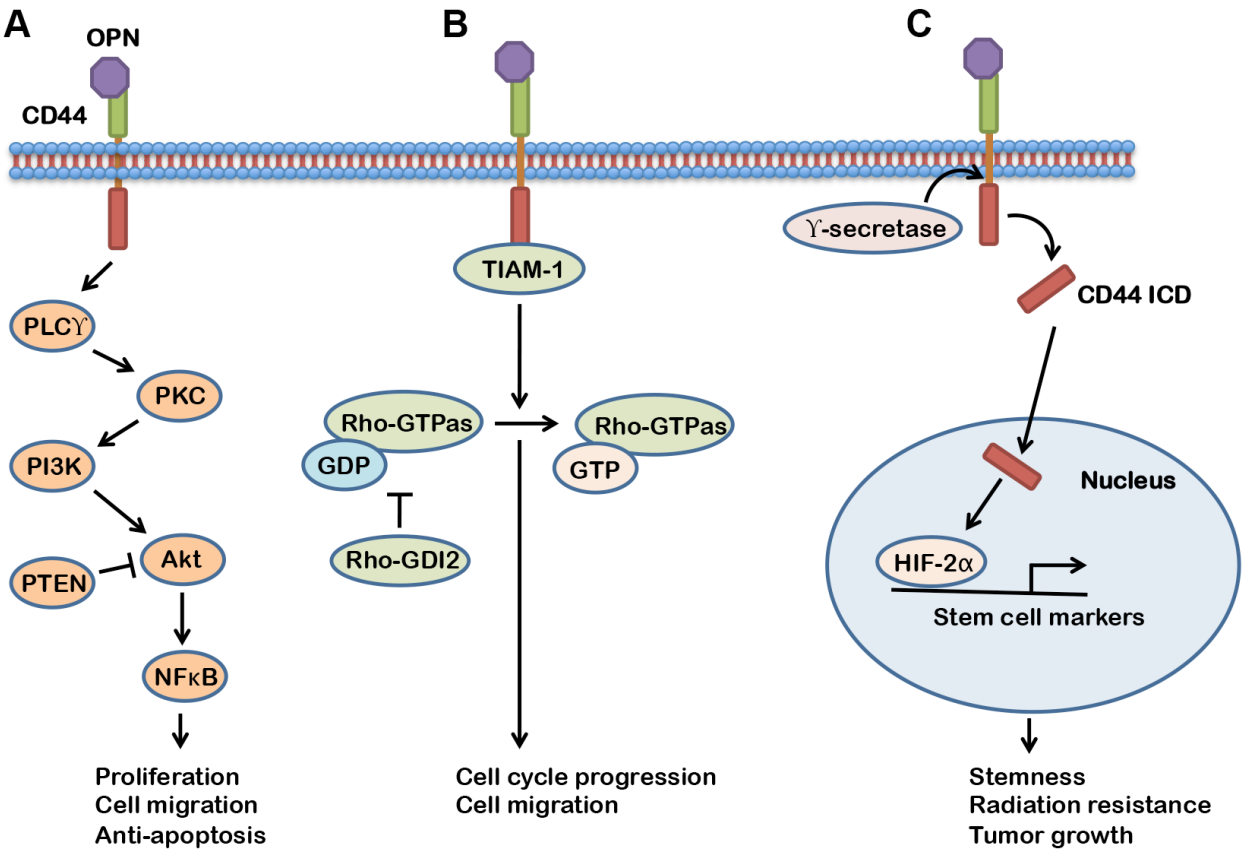

Figure 1.2 OPN-CD44 signaling pathways. Upon binding of CD44 extracellular domain, OPN can induce multiple cellular reactions including proliferation, migration, stemness, and resistance to radiation through variable signaling pathways. PLCϒ, phospholipase Cϒ. PI3K, phosphatidylinositiol 3-kinase. NFκB, nuclear factor kappa-light-chain-enhancer of activated B cells. TIAM1, T cell lymphoma antigen. GDI, guanine nucleotide dissociation inhibitors. ICD, intracellular domain. HIF-2α, hypoxia-inducible factor 2 alpha.

translocate from the membrane to nucleus and act as a transcriptional factor to stimulate multiple gene expression via CBP/p300 coactivator family-mediated transcription (Okamoto et al., 2001). This signaling pathway is highly associated with the tumor aggressive growth, radiation resistance and the prognosis for cancer patients (Pietras et al., 2014). Therefore, OPN-CD44 signaling may be a potential target for preventive or therapeutic intervention of cancers. However its role in gastric cancer remains insufficiently elucidated.

1.5 Concluding remarks and project overview

Areas of the junctions between two types of epithelium are known to be cancer-prone in many organs systems. However, the cell of origin of these malignancies and the mechanisms by which the junction areas are preferentially susceptible to the malignant transformation remain poorly investigated. Importantly, although the overall incidence of gastric cancer has shown a tendency to decrease over the past few decades the incidence of gastroesophageal cancers has been rising over the same period. Thus exploring the cellular origin and identifying the critical signaling pathways responsible for the preferential transformation in SCJ areas may provide new critical information essential for the development of novel diagnostic, preventive and treatment approaches.

In Chapter 2, we describe establishment of a novel mouse model of gastric SCJ cancer closely resembling human disease. After conditional inactivation of tumor suppressor

genes *Trp53* and *Rb1* in $Lgr5^+$ stem cells, cancers preferentially arise from the SCJ between the forestomach squamous epithelium and the glandular stomach columnar epithelium. Notably, SCJ has only a limited number of $Lgr5^+$ stem cells compared to the antral region. In this mouse model, the junction cancers are characterized by poor differentiation, aggressive invasion, highly metastatic potential, and prevalent formation in males, the features that are similar to human GEJ cancers. These finding are further supported by close similarity in gene expression profiles of human and mouse SCJ cancers according to GSEA. We have also found that the Lgr5 expression may be dispensable during the cancer progression and metastasis, while the other stem/progenitor cell marker, CD44, is consistently expressed by the gastric SCJ cancer cells. This mouse model provides a useful tool for further in-depth studies of the mechanism underlying the preferential malignant transformation of junction areas.

In Chapter 3, we described a novel distinct immature cell population that may represent the cell of gastric SCJ cancer origin. These cells express CD44 but not Lgr5 and are predominantly positioned in the first pit of mouse gastric glandular epithelium. By characterizing the early stage lesions and utilizing the organoid culture system, we have found that $Lgr5^-CD44^+$ immature cells represent the most susceptible target for the malignant transformation following oncogenic mutations in all cell populations. These findings provide a new insight into the cellular origin of gastric SCJ cancer and form the firm basis for further studies of the preferential malignant transformation tendency in the junction areas.

Finally, in Chapter 4, we have shown that OPN-CD44 signaling pathway plays a key role in gastric SCJ carcinogenesis and may be a potential target for preventing cancer initiation and progression. Our findings indicate that OPN-CD44 signaling promotes the growth, stemness, and tumorigenicity of gastric SCJ cells. We have also found the OPN expression is downregulated in $Lgr5^{+}$ cells due to the repressive effect of WNT signaling on OPN-encoding gene *Spp1* expression mediated by the downstream effector TCF-4. Moreover, expression of CD44 and its ligand OPN correlates with the poor survival of gastric SCJ cancer patients. These findings support the idea that selective targeting of OPN-CD44 signaling may have clinical relevance for the development of effective therapeutics. Furthermore, they caution against application of Lgr5-targeted therapies in cancers with active CD44-OPN pathway.

References

Ahmed, M., Sottnik, J.L., Dancik, G.M., Sahu, D., Hansel, D.E., Theodorescu, D., and Schwartz, M.A. (2016). An Osteopontin/CD44 Axis in RhoGDI2-Mediated Metastasis Suppression. Cancer Cell *30*, 432-443.

Alam, T.N., O'Hare, M.J., Laczkó, I., Freeman, A., Al-Beidh, F., Masters, J.R., and Hudson, D.L. (2004). Differential expression of CD44 during human prostate epithelial cell differentiation. Journal of Histochemistry & Cytochemistry *52*, 1083-1090.

Arnold, K., Sarkar, A., Yram, M.A., Polo, J.M., Bronson, R., Sengupta, S., Seandel, M., Geijsen, N., and Hochedlinger, K. (2011). Sox2+ adult stem and progenitor cells are important for tissue regeneration and survival of mice. Cell Stem Cell *9*, 317-329.

Attwood, S.E., Harrison, L.-A., Preston, S.L., and Jankowski, J.A. (2008). Esophageal adenocarcinoma in "mice and men": back to basics! The American Journal of Gastroenterology *103*, 2367-2372.

Avigdor, A., Goichberg, P., Shivtiel, S., Dar, A., Peled, A., Samira, S., Kollet, O., Hershkoviz, R., Alon, R., and Hardan, I. (2004). CD44 and hyaluronic acid cooperate with SDF-1 in the trafficking of human CD34+ stem/progenitor cells to bone marrow. Blood *103*, 2981-2989.

Barker, N., Huch, M., Kujala, P., van de Wetering, M., Snippert, H.J., van Es, J.H., Sato, T., Stange, D.E., Begthel, H., van den Born, M*., et al.* (2010). Lgr5(+ve) stem cells drive self-renewal in the stomach and build long-lived gastric units in vitro. Cell stem cell *6*, 25-36.

Barker, N., Ridgway, R.A., van Es, J.H., van de Wetering, M., Begthel, H., van den Born, M., Danenberg, E., Clarke, A.R., Sansom, O.J., and Clevers, H. (2009). Crypt stem cells as the cells-of-origin of intestinal cancer. Nature *457*, 608-611.

Bellahcène, A., Castronovo, V., Ogbureke, K.U.E., Fisher, L.W., and Fedarko, N.S. (2008). Small integrin-binding ligand N-linked glycoproteins (SIBLINGs): multifunctional proteins in cancer. Nature reviews Cancer *8*, 212-226.

Bertuccio, P., Chatenoud, L., Levi, F., Praud, D., Ferlay, J., Negri, E., Malvezzi, M., and La Vecchia, C. (2009). Recent patterns in gastric cancer: a global overview. Int J Cancer *125*, 666-673.

Blanpain, C. (2013). Tracing the cellular origin of cancer. Nature cell biology *15*, 126-134.

Blanpain, C., Mohrin, M., Sotiropoulou, P.A., and Passegué, E. (2011). DNA-Damage Response in Tissue-Specific and Cancer Stem Cells. Stem Cell *8*, 16-29.

Botterweck, A.A., Schouten, L.J., Volovics, A., Dorant, E., and van Den Brandt, P.A. (2000). Trends in incidence of adenocarcinoma of the oesophagus and gastric cardia in ten European countries. International journal of epidemiology *29*, 645-654.

Bourguignon, L.Y., Zhu, H., Shao, L., and Chen, Y.W. (2000). CD44 interaction with tiam1 promotes Rac1 signaling and hyaluronic acid-mediated breast tumor cell migration. J Biol Chem *275*, 1829-1838.

Bourguignon, L.Y.W., Peyrollier, K., Xia, W., and Gilad, E. (2008). Hyaluronan-CD44 interaction activates stem cell marker Nanog, Stat-3-mediated MDR1 gene expression, and ankyrin-regulated multidrug efflux in breast and ovarian tumor cells. J Biol Chem *283*, 17635-17651.

Buas, M.F., and Vaughan, T.L. (2013). Epidemiology and risk factors for gastroesophageal junction tumors: understanding the rising incidence of this disease. Seminars in radiation oncology *23*, 3-9.

Cai, X., Carlson, J., Stoicov, C., Li, H., Wang, T.C., and Houghton, J. (2005). Helicobacter felis eradication restores normal architecture and inhibits gastric cancer progression in C57BL/6 mice. YGAST *128*, 1937-1952.

Cavaleiro-Pinto, M., Peleteiro, B., Lunet, N., and Barros, H. (2011). Helicobacter pylori infection and gastric cardia cancer: systematic review and meta-analysis. Cancer causes & control : CCC *22*, 375-387.

Chen, K., Huang, Y.-h., and Chen, J.-l. (2013). Understanding and targeting cancer stem cells: therapeutic implications and challenges. Acta Pharmacologica Sinica *34*, 732.

Cheng, H.-C., Liu, Y.-P., Shan, Y.-S., Huang, C.-Y., Lin, F.-C., Lin, L.-C., Lee, L., Tsai, C.-H., Hsiao, M., and Lu, P.-J. (2013). Loss of RUNX3 increases osteopontin expression and promotes cell migration in gastric cancer. Carcin *34*, 2452-2459.

Crew, K., and I Neugut, A. (2006). Crew KD, Neugut AIEpideiology of gastric cancer. World J Gastroenterol 12: 354-362, Vol 12.

D'Arena, G., Calapai, G., and Deaglio, S. (2014). Anti-CD44 mAb for the treatment of B-cell chronic lymphocytic leukemia and other hematological malignancies: evaluation of WO2013063498. Expert Opin Ther Pat *24*, 821-828.

Davanger, M., and Evensen, A. (1971). Role of the pericorneal papillary structure in renewal of corneal epithelium. Nature *229*, 560-561.

Day, C.-P., Merlino, G., and Van Dyke, T. (2015). Preclinical mouse cancer models: a maze of opportunities and challenges. Cell *163*, 39-53.

Dow, L.E., and Lowe, S.W. (2012). Life in the fast lane: mammalian disease models in the genomics era. Cell *148*, 1099-1109.

Ferlay, J., Soerjomataram, I., Dikshit, R., Eser, S., Mathers, C., Rebelo, M., Parkin, D.M., Forman, D., and Bray, F. (2015). Cancer incidence and mortality worldwide: sources, methods and major patterns in GLOBOCAN 2012. Int J Cancer *136*, E359-386.

Fillmore, C., and Kuperwasser, C. (2007). Human breast cancer stem cell markers CD44 and CD24: enriching for cells with functional properties in mice or in man? Breast cancer research *9*, 303.

Flesken-Nikitin, A., Hwang, C.-I., Cheng, C.-Y., Michurina, T.V., Enikolopov, G., and Nikitin, A.Y. (2013). Ovarian surface epithelium at the junction area contains a cancer-prone stem cell niche. Nature *495*, 241-245.

Flesken-Nikitin, A., Odai-Afotey, A.A., and Nikitin, A.Y. (2014). Role of the stem cell niche in the pathogenesis of epithelial ovarian cancers. Molecular & cellular oncology *1*, e963435.

Fox, J.G., Sheppard, B.J., Dangler, C.A., Whary, M.T., Ihrig, M., and Wang, T.C. (2002). Germ-line p53-targeted disruption inhibits helicobacter-induced premalignant lesions and invasive gastric carcinoma through down-regulation of Th1 proinflammatory responses. Cancer research *62*, 696-702.

Fox, J.G., and Wang, T.C. (2014). Dietary Factors Modulate Helicobacter-associated Gastric Cancer in Rodent Models. Toxicologic pathology *42*, 162-181.

Franzén, A., and Heinegård, D. (1985). Isolation and characterization of two sialoproteins present only in bone calcified matrix. Biochem J *232*, 715-724.

Fu, D.-J., Miller, A.D., Southard, T.L., Flesken-Nikitin, A., Ellenson, L.H., and Nikitin, A.Y. (2018). Stem Cell Pathology. Annu Rev Pathol *13*, 71-92.

Ghaffarzadehgan, K., Jafarzadeh, M., Raziee, H.R., Sima, H.R., Esmaili-Shandiz, E., Hosseinnezhad, H., Taghizadeh-Kermani, A., Moaven, O., and Bahrani, M. (2008). Expression of cell adhesion molecule CD44 in gastric adenocarcinoma and its prognostic importance. World journal of gastroenterology: WJG *14*, 6376.

Ghoshal, N.G., and Bal, H.S. (1989). Comparative morphology of the stomach of some laboratory mammals. Lab Anim *23*, 21-29.

Greaves, M., and Maley, C.C. (2012). Clonal evolution in cancer. Nature *481*, 306.

Guasch, G., Schober, M., Pasolli, H.A., Conn, E.B., Polak, L., and Fuchs, E. (2007). Loss of TGFbeta signaling destabilizes homeostasis and promotes squamous cell carcinomas in stratified epithelia. Cancer Cell *12*, 313-327.

Guidi, N., Sacma, M., Ständker, L., Soller, K., Marka, G., Eiwen, K., Weiss, J.M., Kirchhoff, F., Weil, T., Cancelas, J.A.*, et al.* (2017). Osteopontin attenuates aging-associated phenotypes of hematopoietic stem cells. The EMBO journal *36*, 840-853.

Haga, R.B., and Ridley, A.J. (2016). Rho GTPases: Regulation and roles in cancer cell biology. Small GTPases *7*, 207-221.

Hahn, J.N., Falck, V.G., and Jirik, F.R. (2011). Smad4 deficiency in T cells leads to the Th17-associated development of premalignant gastroduodenal lesions in mice. J Clin Invest *121*, 4030-4042.

Han, S.-U., Kim, Y.-B., Joo, H.-J., Hahm, K.-B., Lee, W.-H., Cho, Y.-K., Kim, D.-Y., and Kim, M.-W. (2002). Helicobacter pylori infection promotes gastric carcinogenesis in a mice model. Journal of gastroenterology and hepatology *17*, 253-261.

Hayakawa, Y., Ariyama, H., Stancikova, J., Sakitani, K., Asfaha, S., Renz, B.W., Dubeykovskaya, Z.A., Shibata, W., Wang, H., Westphalen, C.B.*, et al.* (2015). Mist1 Expressing Gastric Stem Cells Maintain the Normal and Neoplastic Gastric Epithelium and Are Supported by a Perivascular Stem Cell Niche. Cancer cell *28*, 800-814.

Hayakawa, Y., Fox, J.G., Gonda, T., Worthley, D.L., Muthupalani, S., and Wang, T.C. (2013). Mouse models of gastric cancer. Cancers *5*, 92-130.

Heider, K.-H., Dämmrich, J., Skroch-Angel, P., Müller-Hermelink, H.-K., Vollmers, H.P., Herrlich, P., and Ponta, H. (1993). Differential expression of CD44 splice variants in intestinal-and diffuse-type human gastric carcinomas and normal gastric mucosa. Cancer research *53*, 4197-4203.

Herfs, M., Yamamoto, Y., Laury, A., Wang, X., Nucci, M.R., McLaughlin-Drubin, M.E., Münger, K., Feldman, S., McKeon, F.D., Xian, W.*, et al.* (2012). A discrete population of squamocolumnar junction cells implicated in the pathogenesis of cervical cancer. Proceedings of the National Academy of Sciences of the United States of America *109*, 10516-10521.

Hirata, K., Suzuki, H., Imaeda, H., Matsuzaki, J., Tsugawa, H., Nagano, O., Asakura, K., Saya, H., and Hibi, T. (2013). CD44 variant 9 expression in primary early gastric cancer as a predictive marker for recurrence. British journal of cancer *109*, 379.

HogenEsch, H., and Nikitin, A.Y. (2012). Challenges in pre-clinical testing of anti-cancer drugs in cell culture and in animal models. Journal of controlled release *164*, 183-186.

Humar, B., Blair, V., Charlton, A., More, H., Martin, I., and Guilford, P. (2009). E-cadherin deficiency initiates gastric signet-ring cell carcinoma in mice and man. Cancer research *69*, 2050-2056.

Ishimoto, T., Izumi, D., Watanabe, M., Yoshida, N., Hidaka, K., Miyake, K., Sugihara, H., Sawayama, H., Imamura, Y., Iwatsuki, M.*, et al.* (2014). Chronic inflammation with Helicobacter pylori infection is implicated in CD44 overexpression through miR-328 suppression in the gastric mucosa. Journal of gastroenterology.

Ishimoto, T., Nagano, O., Yae, T., Tamada, M., Motohara, T., Oshima, H., Oshima, M., Ikeda, T., Asaba, R., and Yagi, H. (2011). CD44 variant regulates redox status in cancer cells by stabilizing the xCT subunit of system xc− and thereby promotes tumor growth. Cancer Cell *19*, 387-400.

Ito, K., Chuang, L.S.H., Ito, T., Chang, T.L., Fukamachi, H., Salto-Tellez, M., and Ito, Y. (2011). Loss of Runx3 is a key event in inducing precancerous state of the stomach. Gastroenterology *140*, 1536-1546.e1538.

Jemal, A., Bray, F., Center, M.M., Ferlay, J., Ward, E., and Forman, D. (2011). Global cancer statistics. CA: a cancer journal for clinicians *61*, 69-90.

Jemal, A., Center, M.M., DeSantis, C., and Ward, E.M. (2010). Global patterns of cancer incidence and mortality rates and trends. Cancer epidemiology, biomarkers & prevention : a publication of the American Association for Cancer Research, cosponsored by the American Society of Preventive Oncology *19*, 1893-1907.

Jiang, M., Li, H., Zhang, Y., Yang, Y., Lu, R., Liu, K., Lin, S., Lan, X., Wang, H., Wu, H.*, et al.* (2017). Transitional basal cells at the squamous-columnar junction generate Barrett's oesophagus. Nature *550*, 529-533

Kahles, F., Findeisen, H.M., and Bruemmer, D. (2014). Osteopontin: A novel regulator at the cross roads of inflammation, obesity and diabetes. Molecular metabolism *3*, 384-393.

Kapoor, H., Lohani, K.R., Lee, T.H., Agrawal, D.K., and Mittal, S.K. (2015). Animal Models of Barrett's Esophagus and Esophageal Adenocarcinoma–Past, Present, and Future. Clinical And Translational Science *8*, 841-847.

Karam, S.M., and Leblond, C.P. (1993). Dynamics of epithelial cells in the corpus of the mouse stomach. I. Identification of proliferative cell types and pinpointing of the stem cell. The Anatomical Record *236*, 259-279.

Karanicolas, P.J., Graham, D., Gönen, M., Strong, V.E., Brennan, M.F., and Coit, D.G. (2013). Quality of life after gastrectomy for adenocarcinoma: a prospective cohort study. Annals of surgery *257*, 1039.

Kararli, T.T. (1995). Comparison of the gastrointestinal anatomy, physiology, and biochemistry of humans and commonly used laboratory animals. Biopharm Drug Dispos *16*, 351-380.

Karimi, P., Islami, F., Anandasabapathy, S., Freedman, N.D., and Kamangar, F. (2014). Gastric cancer: descriptive epidemiology, risk factors, screening, and prevention. Cancer epidemiology, biomarkers & prevention : a publication of the American Association for Cancer Research, cosponsored by the American Society of Preventive Oncology *23*, 700-713.

Koike, K., Hinrichs, S.H., Isselbacher, K.J., and Jay, G. (1989). Transgenic mouse model for human gastric carcinoma. Proceedings of the National Academy of Sciences *86*, 5615-5619.

Ksander, B.R., Kolovou, P.E., Wilson, B.J., Saab, K.R., Guo, Q., Ma, J., McGuire, S.P., Gregory, M.S., Vincent, W.J.B., Perez, V.L.*, et al.* (2015). ABCB5 is a limbal stem cell gene required for corneal development and repair. Nature *511*, 353-357.

Kusano, C., Gotoda, T., Khor, C.J., Katai, H., Kato, H., Taniguchi, H., and Shimoda, T. (2008). Changing trends in the proportion of adenocarcinoma of the esophagogastric junction in a large tertiary referral center in Japan. Journal of gastroenterology and hepatology *23*, 1662-1665.

La Vecchia, C., Negri, E., d'Avanzo, B., and Franceschi, S. (1990). Electric refrigerator use and gastric cancer risk. British journal of cancer *62*, 136.

Leedham, S.J., Preston, S.L., McDonald, S.A., Elia, G., Bhandari, P., Poller, D., Harrison, R., Novelli, M.R., Jankowski, J.A., and Wright, N.A. (2008). Individual crypt genetic heterogeneity and the origin of metaplastic glandular epithelium in human Barrett's oesophagus. Gut *57*, 1041-1048.

Lefebvre, O., Chenard, M.-P., Masson, R., Linares, J., Dierich, A., LeMeur, M., Wendling, C., Tomasetto, C., Chambon, P., and Rio, M.-C. (1996). Gastric mucosa abnormalities and tumorigenesis in mice lacking the pS2 trefoil protein. Science *274*, 259-262.

Leung, E.L.-H., Fiscus, R.R., Tung, J.W., Tin, V.P.-C., Cheng, L.C., Sihoe, A.D.-L., Fink, L.M., Ma, Y., and Wong, M.P. (2010). Non-small cell lung cancer

cells expressing CD44 are enriched for stem cell-like properties. PLoS ONE *5*, e14062.

Leushacke, M., Tan, S.H., Wong, A., Swathi, Y., Hajamohideen, A., Tan, L.T., Goh, J., Wong, E., Denil, S., Murakami, K.*, et al.* (2017). Lgr5-expressing chief cells drive epithelial regeneration and cancer in the oxyntic stomach. Nature cell biology *19*, 774-786.

Li, Q., Jia, Z., Wang, L., Kong, X., Li, Q., Guo, K., Tan, D., Le, X., Wei, D., Huang, S.*, et al.* (2012). Disruption of Klf4 in villin-positive gastric progenitor cells promotes formation and progression of tumors of the antrum in mice. Gastroenterology *142*, 531-542.

Lin, Y.-H., and Yang-Yen, H.-F. (2001). The osteopontin-CD44 survival signal involves activation of the phosphatidylinositol 3-kinase/Akt signaling pathway. Journal of Biological Chemistry *276*, 46024-46030.

Liu, C., Sage, J.C., Miller, M.R., Verhaak, R.G.W., Hippenmeyer, S., Vogel, H., Foreman, O., Bronson, R.T., Nishiyama, A., Luo, L.*, et al.* (2011). Mosaic analysis with double markers reveals tumor cell of origin in glioma. Cell *146*, 209-221.

Liu, Y., Cao, L., Chen, R., Zhou, X., Fan, X., Liang, Y., Jia, R., Wang, H., Liu, G., Guo, Y.*, et al.* (2015). Osteopontin Promotes Hepatic Progenitor Cell Expansion and Tumorigenicity via Activation of beta-Catenin in Mice. Stem Cells *33*, 3569-3580.

Lund, S.A., Giachelli, C.M., and Scatena, M. (2009). The role of osteopontin in inflammatory processes. J Cell Commun Signal *3*, 311-322.

Lv, F.-J., Tuan, R.S., Cheung, K.M.C., and Leung, V.Y.L. (2014). Concise review: the surface markers and identity of human mesenchymal stem cells. Stem cells (Dayton, Ohio) *32*, 1408-1419.

Martens, J.E., Arends, J., Van der Linden, P.J.Q., De Boer, B.A.G., and Helmerhorst, T.J.M. (2004). Cytokeratin 17 and p63 are markers of the HPV target cell, the cervical stem cell. Anticancer Res *24*, 771-775.

Matsuo, J., Kimura, S., Yamamura, A., Koh, C.P., Hossain, M.Z., Heng, D.L., Kohu, K., Voon, D.C.-C., Hiai, H., and Unno, M. (2017). Identification of stem cells in the epithelium of the stomach corpus and antrum of mice. Gastroenterology *152*, 218-231. e214.

McGonigle, P., and Ruggeri, B. (2014). Animal models of human disease: challenges in enabling translation. Biochem Pharmacol *87*, 162-171.

McKelvie, P.A., Daniell, M., McNab, A., Loughnan, M., and Santamaria, J.D. (2002). Squamous cell carcinoma of the conjunctiva: a series of 26 cases. Br J Ophthalmol *86*, 168-173.

McLean, M.H., and El-Omar, E.M. (2014). Genetics of gastric cancer. Nature reviews Gastroenterology & hepatology *11*, 664-674.

McNairn, A.J., and Guasch, G. (2011). Epithelial transition zones: merging microenvironments, niches, and cellular transformation. European journal of dermatology : EJD *21 Suppl 2*, 21-28.

Merlo, L.M., Pepper, J.W., Reid, B.J., and Maley, C.C. (2006). Cancer as an evolutionary and ecological process. Nature Reviews Cancer *6*, 924.

Mertens, A.E., Roovers, R.C., and Collard, J.G. (2003). Regulation of Tiam1-Rac signalling. FEBS Lett *546*, 11-16.

Milano, F., van Baal, J.W.P.M., Buttar, N.S., Rygiel, A.M., de Kort, F., DeMars, C.J., Rosmolen, W.D., Bergman, J.J.G.H.M., van Marle, J., Wang, K.K.*, et al.* (2007). Bone morphogenetic protein 4 expressed in esophagitis induces a columnar phenotype in esophageal squamous cells. YGAST *132*, 2412-2421.

Mohrin, M., Bourke, E., Alexander, D., Warr, M.R., Barry-Holson, K., Le Beau, M.M., Morrison, C.G., and Passegué, E. (2010). Hematopoietic stem cell quiescence promotes error-prone DNA repair and mutagenesis. Cell Stem Cell *7*, 174-185.

Morath, I., Hartmann, T.N., and Orian-Rousseau, V. (2016). CD44: more than a mere stem cell marker. The international journal of biochemistry & cell biology *81*, 166-173

Nemir, M., Bhattacharyya, D., Li, X., Singh, K., Mukherjee, A.B., and Mukherjee, B.B. (2000). Targeted inhibition of osteopontin expression in the mammary gland causes abnormal morphogenesis and lactation deficiency. J Biol Chem *275*, 969-976.

Ng, A., and Barker, N. (2015). Ovary and fimbrial stem cells: biology, niche and cancer origins. Nature reviews Molecular cell biology *16*, 625.

Nilsson, S.K., Johnston, H.M., Whitty, G.A., Williams, B., Webb, R.J., Denhardt, D.T., Bertoncello, I., Bendall, L.J., Simmons, P.J., and Haylock, D.N. (2005). Osteopontin, a key component of the hematopoietic stem cell niche and regulator of primitive hematopoietic progenitor cells. Blood *106*, 1232-1239.

Noordzij, M.A., van Steenbrugge, G.J., Verkaik, N.S., Schröder, F.H., and van der Kwast, T.H. (1997). The prognostic value of CD44 isoforms in prostate

cancer patients treated by radical prostatectomy. Clin Cancer Res *3*, 805-815.

O'Neil, A., Petersen, C.P., Choi, E., Engevik, A.C., and Goldenring, J.R. (2017). Unique Cellular Lineage Composition of the First Gland of the Mouse Gastric Corpus. Journal of Histochemistry & Cytochemistry *65*, 47-58.

Oh, D.S., DeMeester, S.R., Dunst, C.M., Mori, R., Lehman, B.J., Kuramochi, H., Danenberg, K., Danenberg, P., Hagen, J.A., Chandrasoma, P.*, et al.* (2009). Validation of a rodent model of Barrett's esophagus using quantitative gene expression profiling. Surg Endosc *23*, 1346-1352.

Okamoto, I., Kawano, Y., Murakami, D., Sasayama, T., Araki, N., Miki, T., Wong, A.J., and Saya, H. (2001). Proteolytic release of CD44 intracellular domain and its role in the CD44 signaling pathway. J Cell Biol *155*, 755-762.

Okumura, T., Ericksen, R.E., Takaishi, S., Wang, S.S.W., Dubeykovskiy, Z., Shibata, W., Betz, K.S., Muthupalani, S., Rogers, A.B., Fox, J.G.*, et al.* (2010). K-ras mutation targeted to gastric tissue progenitor cells results in chronic inflammation, an altered microenvironment, and progression to intraepithelial neoplasia. Cancer research *70*, 8435-8445.

Oshima, H., Matsunaga, A., Fujimura, T., Tsukamoto, T., Taketo, M.M., and Oshima, M. (2006). Carcinogenesis in mouse stomach by simultaneous activation of the Wnt signaling and prostaglandin E2 pathway. Gastroenterology *131*, 1086-1095.

Ouyang, H., Xue, Y., Lin, Y., Zhang, X., Xi, L., Patel, S., Cai, H., Luo, J., Zhang, M., Zhang, M.*, et al.* (2014). WNT7A and PAX6 define corneal epithelium homeostasis and pathogenesis. Nature *511*, 358-361.

Parkin, D.M. (2001). Global cancer statistics in the year 2000. The lancet oncology *2*, 533-543.

Parkin, D.M. (2006). The global health burden of infection-associated cancers in the year 2002. International journal of cancer *118*, 3030-3044.

Parkin, D.M., Stjernswärd, J., and Muir, C.S. (1984). Estimates of the worldwide frequency of twelve major cancers. Bull World Health Organ *62*, 163-182.

Pietras, A., Katz, A.M., Ekstrom, E.J., Wee, B., Halliday, J.J., Pitter, K.L., Werbeck, J.L., Amankulor, N.M., Huse, J.T., and Holland, E.C. (2014). Osteopontin-CD44 signaling in the glioma perivascular niche enhances cancer stem cell phenotypes and promotes aggressive tumor growth. Cell Stem Cell *14*, 357-369.

Poh, A.R., O'Donoghue, R.J.J., Ernst, M., and Putoczki, T.L. (2016). Mouse models for gastric cancer: Matching models to biological questions. Journal of gastroenterology and hepatology *31*, 1257-1272.

Qiao, X.T., Ziel, J.W., McKimpson, W., Madison, B.B., Todisco, A., Merchant, J.L., Samuelson, L.C., and Gumucio, D.L. (2007). Prospective identification of a multilineage progenitor in murine stomach epithelium. Gastroenterology *133*, 1989-1998. e1983.

Quante, M., Bhagat, G., Abrams, J.A., Marache, F., Good, P., Lee, M.D., Lee, Y., Friedman, R., Asfaha, S., Dubeykovskaya, Z*., et al.* (2012). Bile acid and inflammation activate gastric cardia stem cells in a mouse model of Barrett-like metaplasia. Cancer Cell *21*, 36-51.

Reinholt, F.P., Hultenby, K., Oldberg, A., and Heinegård, D. (1990). Osteopontin--a possible anchor of osteoclasts to bone. Proceedings of the National Academy of Sciences *87*, 4473-4475.

Ringel, J., Jesnowski, R., Schmidt, C., Ringel, J., Köhler, H.J., Rychly, J., Batra, S.K., and Löhr, M. (2001). CD44 in normal human pancreas and pancreatic carcinoma cell lines. Teratogenesis Carcinogenesis and Mutagenesis *21*, 97-106.

Rodriguez-Rodriguez, L., Sancho-Torres, I., Mesonero, C., Gibbon, D., Shih, W., and Zotalis, G. (2003). The CD44 receptor is a molecular predictor of survival in ovarian cancer. Medical Oncology *20*, 255-263.

Ruiz, P., Schwärzler, C., and Günthert, U. (1995). CD44 isoforms during differentiation and development. Bioessays *17*, 17-24.

Runck, L.A., Kramer, M., Ciraolo, G., Lewis, A.G., and Guasch, G. (2010). Identification of epithelial label-retaining cells at the transition between the anal canal and the rectum in mice. Cell cycle (Georgetown, Tex) *9*, 3039-3045.

Rycaj, K., and Tang, D.G. (2015). Cell-of-origin of cancer versus cancer stem cells: assays and interpretations. Cancer research *75*, 4003-4011.

Saito, T., and Sugimura, T. (1973). Biochemical studies on carcinogenesis in the glandular stomach of rats with N-methyl-N'-nitro-N-nitrosoguanidine. Gan *64*, 373-381.

Sancar, A., Lindsey-Boltz, L.A., Ünsal-Kaçmaz, K., and Linn, S. (2004). Molecular mechanisms of mammalian DNA repair and the DNA damage checkpoints. Annu Rev Biochem *73*, 39-85.

Sarosi, G., Brown, G., Jaiswal, K., Feagins, L., Lee, E., Crook, T., Souza, R., Zou, Y., Shay, J., and Spechler, S.J. (2008). Bone marrow progenitor cells

contribute to esophageal regeneration and metaplasia in a rat model of Barrett's esophagus. Diseases of the Esophagus *21*, 43-50.

Schäfer, M., and Werner, S. (2007). Transcriptional control of wound repair. Annu Rev Cell Dev Biol *23*, 69-92.

Schlötzer-Schrehardt, U., Dietrich, T., Saito, K., Sorokin, L., Sasaki, T., Paulsson, M., and Kruse, F.E. (2007). Characterization of extracellular matrix components in the limbal epithelial stem cell compartment. Exp Eye Res *85*, 845-860.

Schmitt, M., Metzger, M., Gradl, D., Davidson, G., and Orian-Rousseau, V. (2014). CD44 functions in Wnt signaling by regulating LRP6 localization and activation. Cell Death & Differentiation, 1-13.

Schmoeckel, E., Odai-Afotey, A.A., Schleißheimer, M., Rottmann, M., Flesken-Nikitin, A., Ellenson, L.H., Kirchner, T., Mayr, D., and Nikitin, A.Y. (2017). LEF1 is preferentially expressed in the tubal-peritoneal junctions and is a reliable marker of tubal intraepithelial lesions. Nature Publishing Group *30*, 1241-1250.

Searle, P.F., Thomas, D.P., Faulkner, K.B., and Tinsley, J.M. (1994). Stomach cancer in transgenic mice expressing human papillomavirus type 16 early region genes from a keratin promoter. J Gen Virol *75 (Pt 5)*, 1125-1137.

Seidman, J.D. (2015). Serous tubal intraepithelial carcinoma localizes to the tubal-peritoneal junction: a pivotal clue to the site of origin of extrauterine high-grade serous carcinoma (ovarian cancer). Int J Gynecol Pathol *34*, 112-120.

Serra, S., and Chetty, R. (2006). Tumours of the anal canal. Current Diagnostic Pathology *12*, 136-151.

Shevde, L.A., and Samant, R.S. (2014). Role of osteopontin in the pathophysiology of cancer. Matrix Biol *37*, 131-141.

Shi, Z., Mirza, M., Wang, B., Kennedy, M.A., and Weber, G.F. (2014). Osteopontin-a alters glucose homeostasis in anchorage-independent breast cancer cells. Cancer letters *344*, 47-53.

Shimada, S., Mimata, A., Sekine, M., Mogushi, K., Akiyama, Y., Fukamachi, H., Jonkers, J., Tanaka, H., Eishi, Y., and Yuasa, Y. (2012). Synergistic tumour suppressor activity of E-cadherin and p53 in a conditional mouse model for metastatic diffuse-type gastric cancer. Gut *61*, 344-353.

Shin, S.L., Cha, J.H., Chun, M.H., Chung, J.W., and Lee, M.Y. (1999). Expression of osteopontin mRNA in the adult rat brain. Neurosci Lett *273*, 73-76.

Singh, K., Balligand, J.L., Fischer, T.A., Smith, T.W., and Kelly, R.A. (1995). Glucocorticoids increase osteopontin expression in cardiac myocytes and microvascular endothelial cells. Role in regulation of inducible nitric oxide synthase. J Biol Chem *270*, 28471-28478.

Soutto, M., Belkhiri, A., Piazuelo, M.B., Schneider, B.G., Peng, D., Jiang, A., Washington, M.K., Kokoye, Y., Crowe, S.E., Zaika, A.*, et al.* (2011). Loss of TFF1 is associated with activation of NF-κB–mediated inflammation and gastric neoplasia in mice and humans. J Clin Invest *121*, 1753-1767.

Stange, D.E., Koo, B.-K., Huch, M., Sibbel, G., Basak, O., Lyubimova, A., Kujala, P., Bartfeld, S., Koster, J., Geahlen, J.H.*, et al.* (2013). Differentiated Troy(+) Chief Cells Act as Reserve Stem Cells to Generate All Lineages of the Stomach Epithelium. Cell *155*, 357-368.

Stier, S., Ko, Y., Forkert, R., Lutz, C., Neuhaus, T., Grunewald, E., Cheng, T., Dombkowski, D., Calvi, L.M., Rittling, S.R.*, et al.* (2005). Osteopontin is a hematopoietic stem cell niche component that negatively regulates stem cell pool size. The Journal of experimental medicine *201*, 1781-1791.

Sugimura, T., and Fujimura, S. (1967). Tumour production in glandular stomach of rat by N-methyl-N′-nitro-N-nitrosoguanidine. Nature *216*, 943.

Syder, A.J., Karam, S.M., Mills, J.C., Ippolito, J.E., Ansari, H.R., Farook, V., and Gordon, J.I. (2004). A transgenic mouse model of metastatic carcinoma involving transdifferentiation of a gastric epithelial lineage progenitor to a neuroendocrine phenotype. Proceedings of the National Academy of Sciences *101*, 4471-4476.

Takaishi, S., Okumura, T., Tu, S., Wang, S.S., Shibata, W., Vigneshwaran, R., Gordon, S.A., Shimada, Y., and Wang, T.C. (2009). Identification of gastric cancer stem cells using the cell surface marker CD44. Stem cells *27*, 1006-1020.

Tatematsu, M., Ogawa, K., Hoshiya, T., Shichino, Y., Kato, T., Imaida, K., and Ito, N. (1992). Induction of adenocarcinomas in the glandular stomach of BALB/c mice treated with N-methyl-N-nitrosourea. Cancer Science *83*, 915-918.

Tebbutt, N.C., Giraud, A.S., Inglese, M., Jenkins, B., Waring, P., Clay, F.J., Malki, S., Alderman, B.M., Grail, D., Hollande, F.*, et al.* (2002). Reciprocal regulation of gastrointestinal homeostasis by SHP2 and STAT-mediated trefoil gene activation in gp130 mutant mice. Nature medicine *8*, 1089-1097.

Tétreault, M.-P. (2015). Esophageal Cancer: Insights From Mouse Models. Cancer Growth Metastasis *8*, 37-46.

Todaro, M., Gaggianesi, M., Catalano, V., Benfante, A., Iovino, F., Biffoni, M., Apuzzo, T., Sperduti, I., Volpe, S., Cocorullo, G.*, et al.* (2014). CD44v6 is a marker of constitutive and reprogrammed cancer stem cells driving colon cancer metastasis. Cell Stem Cell *14*, 342-356.

Tokairin, T., Nishikawa, Y., Watanabe, H., Doi, Y., Omori, Y., Yoshioka, T., Yamamoto, Y., Yoshida, M., Nishimura, T., Li, Q.*, et al.* (2008). Osteopontin expression in the liver with severe perisinusoidal fibrosis: autopsy case of Down syndrome with transient myeloproliferative disorder. Pathol Int *58*, 64-68.

Tomita, H., Takaishi, S., Menheniott, T.R., Yang, X., Shibata, W., Jin, G., Betz, K.S., Kawakami, K., Minamoto, T., Tomasetto, C.*, et al.* (2011). Inhibition of gastric carcinogenesis by the hormone gastrin is mediated by suppression of TFF1 epigenetic silencing. Gastroenterology *140*, 879-891.

Toole, B.P. (2004). Hyaluronan: from extracellular glue to pericellular cue. Nature Reviews Cancer *4*, 528.

Torre, L.A., Bray, F., Siegel, R.L., Ferlay, J., Lortet-Tieulent, J., and Jemal, A. (2015). Global cancer statistics, 2012. CA: a cancer journal for clinicians *65*, 87-108.

Tsuzuki, T., Egashira, A., Igarashi, H., Iwakuma, T., Nakatsuru, Y., Tominaga, Y., Kawate, H., Nakao, K., Nakamura, K., Ide, F.*, et al.* (2001). Spontaneous tumorigenesis in mice defective in the MTH1 gene encoding 8-oxo-dGTPase. Proceedings of the National Academy of Sciences *98*, 11456-11461.

Tu, S., Bhagat, G., Cui, G., Takaishi, S., Kurt-Jones, E.A., Rickman, B., Betz, K.S., Penz-Oesterreicher, M., Bjorkdahl, O., Fox, J.G.*, et al.* (2008). Overexpression of Interleukin-1β Induces Gastric Inflammation and Cancer and Mobilizes Myeloid-Derived Suppressor Cells in Mice. CCELL *14*, 408-419.

Visvader, J.E. (2011). Cells of origin in cancer. Nature *469*, 314-322.

Wang, C., Xie, J., Guo, J., Manning, H.C., Gore, J.C., and Guo, N. (2012). Evaluation of CD44 and CD133 as cancer stem cell markers for colorectal cancer. Oncology reports *28*, 1301-1308.

Wang, G., Li, X., Chen, S., Zhao, W., Yang, J., Chang, C., and Xu, C. (2015). Expression profiles uncover the correlation of OPN signaling pathways with rat liver regeneration at cellular level. Cell biology international *39*, 1329-1340.

Wang, T.C., Dangler, C.A., Chen, D., Goldenring, J.R., Koh, T., Raychowdhury, R., Coffey, R.J., Ito, S., Varro, A., Dockray, G.J.*, et al.* (2000). Synergistic

interaction between hypergastrinemia and Helicobacter infection in a mouse model of gastric cancer. YGAST *118*, 36-47.

Wang, W., Li, P., Li, W., Jiang, J., Cui, Y., Li, S., and Wang, Z. (2017). Osteopontin activates mesenchymal stem cells to repair skin wound. PLoS ONE *12*, e0185346.

Wang, X., Kruithof-de Julio, M., Economides, K.D., Walker, D., Yu, H., Halili, M.V., Hu, Y.-P., Price, S.M., Abate-Shen, C., and Shen, M.M. (2009). A luminal epithelial stem cell that is a cell of origin for prostate cancer. Nature *461*, 495-500.

Wang, X., Ouyang, H., Yamamoto, Y., Kumar, P.A., Wei, T.S., Dagher, R., Vincent, M., Lu, X., Bellizzi, A.M., Ho, K.Y.*, et al.* (2011). Residual embryonic cells as precursors of a Barrett's-like metaplasia. Cell *145*, 1023-1035.

White, A.C., and Lowry, W.E. (2015). Refining the role for adult stem cells as cancer cells of origin. Trends in cell biology *25*, 11-20.

White, A.C., Tran, K., Khuu, J., Dang, C., Cui, Y., Binder, S.W., and Lowry, W.E. (2011). Defining the origins of Ras/p53-mediated squamous cell carcinoma. Proceedings of the National Academy of Sciences of the United States of America *108*, 7425-7430.

Xie, Z., Singh, M., Siwik, D.A., Joyner, W.L., and Singh, K. (2003). Osteopontin Inhibits Interleukin-1-stimulated Increases in Matrix Metalloproteinase Activity in Adult Rat Cardiac Fibroblasts. Journal of Biological Chemistry *278*, 48546-48552.

Xu, X., Brodie, S.G., Yang, X., Im, Y.-H., Parks, W.T., Chen, L., Zhou, Y.-X., Weinstein, M., Kim, S.-J., and Deng, C.-X. (2000). Haploid loss of the tumor suppressor Smad4/Dpc4 initiates gastric polyposis and cancer in mice. Oncogene *19*, 1868-1874.

Yamamoto, M., Furihata, C., Ogiu, T., Tsukamoto, T., Inada, K.i., Hirano, K., and Tatematsu, M. (2002). Independent variation in susceptibilities of six different mouse strains to induction of pepsinogen-altered pyloric glands and gastric tumor intestinalization by N-methyl-N-nitrosourea. Cancer letters *179*, 121-132.

Yu, W.-Y., Slack, J.M., and Tosh, D. (2005). Conversion of columnar to stratified squamous epithelium in the developing mouse oesophagus. Developmental biology *284*, 157-170.

Zavros, Y., Eaton, K.A., Kang, W., Rathinavelu, S., Katukuri, V., Kao, J.Y., Samuelson, L.C., and Merchant, J.L. (2005). Chronic gastritis in the

hypochlorhydric gastrin-deficient mouse progresses to adenocarcinoma. Oncogene *24*, 2354.

Zeilstra, J., Joosten, S., Van Andel, H., Tolg, C., Berns, A., Snoek, M., Van De Wetering, M., Spaargaren, M., Clevers, H., and Pals, S. (2014). Stem cell CD44v isoforms promote intestinal cancer formation in Apc (min) mice downstream of Wnt signaling. Oncogene *33*, 665.

Zhang, Z.-X., Shek, K., Wang, S., Huang, X., Lau, A., Yin, Z., Sun, H., Liu, W., Garcia, B., and Rittling, S. (2010). Osteopontin expressed in tubular epithelial cells regulates NK cell-mediated kidney ischemia reperfusion injury. The Journal of Immunology *185*, 967-973.

Zöller, M. (2011). CD44: can a cancer-initiating cell profit from an abundantly expressed molecule? Nature Reviews Cancer *11*, 254.

CHAPTER 2

MODELING GASTRIC SQUAMOUS-COLUMNAR JUNCTION CANCER IN THE MOUSE*

2.1 Abstract

The incidence of the cancer arising from the squamous-columnar junction (SCJ) between the esophagus and the stomach has been increasing over the past few decades. Our refined analysis with tdTomato reporter confirms previous reports that a fraction of cells at the gastric SCJ and antral region express a member of WNT-pathway, leucine-rich repeat-containing G-protein coupled receptor 5 (Lgr5). However, at variance with previous studies, we show that $Lgr5^+$ cells gastric SCJ are present not only at the esophageal entry, but also distributed along the entire junction line. According to the cell lineage tracing analysis these Lgr5-expressing ($Lgr5^+$) cells represent a stem cell population, which contributes to daily renewal of the glandular epithelium in both gastric SCJ and antral region. Conditional knockout of the common tumor suppressor genes *Trp53* (*p53)* and *Rb1* (*Rb)* in these $Lgr5^+$ stem cells leads to malignancies preferentially arising from the gastric SCJ. Similar to human gastroesophageal junction (GEJ) carcinomas, mouse SCJ carcinomas metastasize to lymph nodes and liver and have faster progression in males. These carcinomas are also similar to their human counterparts according to gene set enrichment analysis (GSEA). Notably, Lgr5 expression has not been detected in either primary or

metastatic neoplasms, thereby suggesting that Lgr5+ cells do not represent cancer-propagating cells. On the other hand, some cancer cells expressed another stem/progenitor cell-associated marker, CD44, which is frequently present cancers in stomach cancer, as well as in cancers of other organs, such as the prostate, ovary, liver, and intestine. Taken together, the newly established mouse model should be a very valuable tool to further studies of the pathogenesis of SCJ cancers. It also may facilitate understanding the mechanisms underlying the susceptibility of the epithelial junction area to malignant transformation.

*In part submitted as Fu, D.-J., Wang, L., Chouairi, F.K., Rose, I.M., Miller, A.D., Yamulla, R.J., Schimenti, J.C., Flesken-Nikitin, A., Nikitin, A.Y., Osteopontin-CD44 signaling keeps progeny of Lgr5^{+} cells in immature cancer-prone state at the gastric squamous-columnar junction (2018).

Author contributions: Dah-Jiun Fu and Alexander Yu. Nikitin designed the study, interpreted data and wrote the manuscript. Dah-Jiun Fu and Andrea Flesken-Nikitin performed experiments and analyzed data. Dah-Jiun Fu, Andrew D. Miller, and Alexander Yu. Nikitin were responsible for pathologic analysis. Alexander Yu. Nikitin supervised the project.

2.2 Introduction

Gastric cancer is the fourth most common malignancy, with nearly 1 million people diagnosed annually. It is also the third leading cause of cancer death worldwide, with a death toll of approximately 700,000 people annually (Jemal et al., 2011; McLean and El-Omar, 2014). The overall incidence rate of gastric cancer has declined over past decades. However, the incidence of the cancer arising from the anatomically defined junction region between the esophagus and the stomach, squamous-columnar junction (SCJ) has been steadily rising (Botterweck et al., 2000; Buas and Vaughan, 2013; Kusano et al., 2008). This observation is particularly alarming because cancers located in this junction area have worse prognosis compared to those in other areas of stomach. Unfortunately, the mechanisms underlying the carcinogenesis of this epithelial junction area remain unclear (Buas and Vaughan, 2013; Kim et al., 2005).

Gastric SCJ is one of the epithelial transitional zones (TZs), which are defined as the region where one type of epithelia transit to another forming a distinct junction structure (Fu et al., 2018; McNairn and Guasch, 2011). It is well established that many TZs, such as gastric SCJ, uterine cervix, corneal limbus, anal-rectal junction, ovarian hilum and tubal peritoneal junction are highly predisposed to cancer (Cavaleiro-Pinto et al., 2011; Flesken-Nikitin et al., 2013; Flesken-Nikitin et al., 2014; Fox and Wang, 2014; Herfs et al., 2012; Jiang et al., 2017; Karimi et al., 2014; McKelvie et al., 2002; McNairn and Guasch, 2011; Quante et al., 2012; Schmoeckel

et al., 2017; Serra and Chetty, 2006). The majority of TZs contain stem/progenitor cells responsible for tissue regeneration required to compensate for the increased frequency of damages typical for such areas. (Flesken-Nikitin et al., 2013; Ksander et al., 2014; McNairn and Guasch, 2011; Runck et al., 2010; Wang et al., 2011). Adult stem cells are commonly considered to be the most compelling target of malignant transformation. Their key properties, such as self-renewal, longevity and high proliferation potential, allow them to sequentially accumulate oncogenic genetic and/or epigenetic alterations (Visvader, 2011; White and Lowry, 2015). The cancer-prone character of stem cells at the TZ has been directly shown in the mouse ovarian hilum (Flesken-Nikitin et al., 2013). However, direct experimental evidence that stem cells in TZs of other organs have similar preferential susceptibility to the malignant transformation is missing.

Cancer is considered to be an evolutionary process initiated by a sequential accumulation of multiple genetic, epigenetic, and transcriptional alterations (Blanpain, 2013). A broad spectrum of mutations has been reported to be involved in the carcinogenesis of human gastric SCJ (aka GEJ) (Dulak et al., 2013; Hayakawa et al., 2016; Network, 2014, 2017). According to genome-wide studies, *TP53* and *CDKN2A* have been identified as the most common targets for mutation, deletion or epigenetic silence in human gastric SCJ cancer. This finding is consistent with the earlier reports that the frequent mutations in *TP53* and *CDKN2A* were observed in the Barrett's esophagus, which is a dysplastic precursor for the gastroesophageal cancer (Contino et al., 2016; Hardie et al., 2005; Stachler et al., 2015; Wong et al., 2001). *CDKN2A*

Table 2.1 Distinct genetic alterations in GEJ cancer

Signaling pathway	Gene	Mechanism of aberrancy	Frequency of alteration	Reference
p53 signaling	*TP53*	Mutation and deletion	70-83%	Ross-Innes et al., 2015 Dulak et al., 2013
	MDM2	Mutation and amplification	5%	Dulak et al., 2012
RB signaling	*CDKN2A*	Mutation and deletion	32-81%	Network et al., 2017 Hayakawa et al., 2016
	CDK4	Mutation and amplification	3%	Dulak et al., 2013 Dulak et al., 2012
	CCND1	Mutation and amplification	10-15%	
	CCNE1	Mutation and amplification	12-14%	
	CDK6	Mutation and amplification	14-17%	
	RB1	Mutation and amplification	1-5%	
RTK-RAS-PI3K signaling	*KRAS*	Mutation and amplification	14-21%	Network et al., 2017 Dulak et al., 2013
	PTEN	Mutation and deletion	5-7%	
	ERBB2	Mutation and amplification	19-32%	
WNT signaling	*CTNNB1*	Mutation and amplification	2-4%	Network et al., 2017 Dulak et al., 2013
	APC	Mutation and deletion	3-15%	
TGF-β/SMAD4 signaling	*SMAD4*	Mutation and deletion	24-34%	Network et al., 2017 Dulak et al., 2013
	SMAD2	Mutation and deletion	7-29%	
	TGFBR1	Mutation and deletion	5%	

gene encodes p16 protein, which functions as a negative regulator in cell cycling integral to the RB pathway. P16 inhibits cycling dependent kinase 4 and 6 (CDK4 and 6) and thereby prevents RB phosphorylation, resulting in intervening the progression from G1 to S phase. In addition, p16 expression is also regulated by RB (Rayess et al., 2012). It is therefore likely that aberrations of p53- and RB-signaling play important role are in the pathogenesis of gastric SCJ cancer.

Recently, mouse models with inducible genetic alterations specifically targeted to stem cells have been used to study the connection between the stem/progenitor cells and cancers (Cheng et al., 2010; Visvader, 2011; White and Lowry, 2015). Conditional inactivation of the tumor suppressor *Apc* in Lgr5-expressing intestinal stem cell can lead to benign tumors, adenomas, whereas no tumors were observed in the more differentiated progenies carrying the same oncogenic alteration (Barker et al., 2009). Similarly, the keratin 15 (K15)-expressing hair follicle stem cells have preferential susceptibility to formation of squamous cell carcinoma after expression of oncogenic *Kras* and *p53* inactivation (White et al., 2011). These findings support the notion that at least in some organs, the stem/progenitor cells are the most favorable target for malignant transformation as compared to their committed and/or differentiated progenies. However, it remains to be shown if the stem/progenitor cells are also implicated in gastric SCJ carcinogenesis. To address this question, we established a new mouse model of gastric SCJ cancer associated with alterations in the p53- and RB-signaling in $Lgr5^{+}$ stem cells.

2.3 Materials and Methods

Experimental animals. The *Lgr5*$^{tm1(cre/ERT2)Cle}$*/J* (*Lgr5*$^{eGFP\text{-}Ires\text{-}CreERT2}$) knock in mice (Stock number 008875), *Gt(ROSA)26Sor*$^{tm9(CAG\text{-}tdTomato)Hze}$ (*Rosa-loxp-stop-loxp*-tdTomato/Ai9) mice (Stock number 007909) and NOD.Cg-*Prkdc*^{scid} *Il2rg*^{tm1wjl}/SzJ (NSG) mice (Stock number 005557 were obtained from The Jackson Laboratory (Bar Harbor, ME, USA). The *Trp53*$^{loxP/loxP}$ and *Rb1*$^{loxP/loxP}$ mice, which have *Trp53* and *Rb1* genes flanked by *loxP* alleles, respectively, were a gift from Dr. Anton Berns. All the experiments and maintenance of the mice were following with the recommendations of the Guide for the Institutional Laboratory Animal Use and Care Committee.

Tamoxifen induction. Administration of tamoxifen was carried out as previously described (Flesken-Nikitin et al., 2013). Briefly, for lineage tracing experiments, 6 week-old *Lgr5*$^{eGFP\text{-}Ires\text{-}CreERT2}$Ai9 mice received a single dose (8 µl/g body weight) of tamoxifen (25 mg/ml in corn oil, Sigma-Aldrich, St. Louis, MO, USA, T5648) by intraperitoneal injection. At 1, 4, 10 and 200 days after induction, the tamoxifen-pulsed mice were euthanized by CO_2 and further analyses were carried out. For tumor induction experiments, 6 to 10 week-old *Lgr5*$^{eGFP\text{-}Ires\text{-}CreERT2}$*Trp53*$^{loxP/loxP}$ *Rb1*$^{loxP/loxP}$ mice and control mice were intraperitoneally injected with tamoxifen (25 mg/ml in corn oil, 8 µl/g body weight) three times, every other day for a total of 6 days to maximize the Cre-recombination efficiency.

Lineage tracing analysis. Mice were humanely euthanized with carbon dioxide (CO_2) at indicated days after tamoxifen administration. Tissue of interest were collected and fixed in buffered 4% paraformaldehyde overnight at 4°C. The fixed tissue were washed with PBS and immersed in 30% sucrose in PBS at 4°C for at least 2 hours until the tissue sink to the bottom of tubes for cryopreservation. All tissues were subsequently placed in cassettes for Tissue-Plus O.C.T. embedding. Prepared 15 μm cryosections were counterstained with DAPI and subjected to fluorescence microscopic evaluation. Transverse sections of the whole stomach were scanned using Aperio Scanscope FL (Leica Biosystems, Vista, CA, USA) with 20X objective lens.

Pathologic analysis. Mice were subjected to careful evaluation during necropsy and the tissue of interest, including brain, lung, thymus, stomach, small and large intestines, anus, liver, kidney, adrenal gland, ovary, uterus, prostate, testicle, spleen, pancreas, salivary gland, skin, thigh muscle, and heart, were collected for histopathologic analysis. All tissues were fixed in buffered 4% paraformaldehyde overnight at 4°C, followed by tissue processing and paraffin embedding. To facilitate detection of stem-cell associated pathological lesions, organs with anatomically defined stem cell niches, such as stomach, intestine, prostate, ovary, brain, and skin, were carefully oriented during embedding in paraffin as described previously (Fu et al., 2018). Paraffin section were cut at 4 μm, stained with Mayer's hematoxylin and

eosin, and subjected to histopathologic evaluation by experienced pathologists. Age- and sex-matched littermates without tamoxifen administration were used as control.

Immunohistochemistry. All tissues were fixed in buffered 4% paraformaldehyde overnight at 4°C followed by standard tissue processing and paraffin embedding. Immunohistochemistry staining were carried out on 4 μm-thick paraffin sections by modified ABC techniques as described previously (Nikitin and Lee 1996). Briefly, antigen retrieval was performed by incubation of deparaffinized and rehydrated tissue sections in boiling 10 mM sodium citrate buffer (pH 6.0) for 10 minutes. The primary antibodies against CD44 (Santa Cruz Biotechnologies, Dallas, TX, USA; sc-18849), GFP (NOVUS biological, Littleton, CO, USA; NB600-303), ALDH1A1 (Abcam, ab23375), CK5 (Covance, PRB-160P), DCLK1 (Abgent, AP20304B), and KLF4 (Santa Cruz, sc-20691) were incubated at room temperature (RT) for 1 hour, followed by incubation with secondary biotinylated antibodies (30 minutes, RT). Modified Elite avidin-biotin peroxidase (ABC) technique (Vector Laboratories, Burlingame, CA, USA; pk-6100) was performed at RT for 30 minutes. Hematoxylin was used as the counterstain. All antibodies used for immunostaining are listed in Table 2.1.

Laser microdissection and polymerase chain reaction (PCR). Prepared 4-μm-thick paraffin sections were placed on steel-framed polyethylene terephthalate (PET)-membrane slides (Leica microsystems, Buffalo Grove, IL, USA; 1505151), followed

Table 2.2 List of antibodies used for immunohistochemistry and immunofluorescence staining

Antigen	Antibody source, catalogue number	Clone	Dilution	Detection system
GFP	Novus biological, NB600-303	PC*	1:8000	Vectastain Elite ABC-HRP Kit
ALDH1A1	Abcam, ab23375	PC*	1:2000	Vectastain Elite ABC-HRP Kit
KLF4	Santa Cruz Sc-20691	PC*	1:500	Vectastain Elite ABC-HRP Kit
DCLK1	Abgent, AP20304B	PC*	1:2000	Vectastain Elite ABC-HRP Kit
CK5	Covance, PRB-160P	PC*	1:200	Vectastain Elite ABC-HRP Kit
SOX2	Abcam, ab97959	PC*	1:200	Vectastain Elite ABC-HRP Kit

PC*: Polyclonal.

by deparaffinization in xylene and staining with Mayer's hematoxylin and eosin (H&E). Microscopically selected areas were microdissected with UV laser (Laser Microdissection System, Leica AS, Heidelberg, Germany), followed by collections into caps of Eppendorf tubes located beneath the tissue sections. Collected cells were digested in proteinase K lysis buffer at 56°C for 1 hour, followed by inactivation of proteinase K at 95°C for 10 minutes.

PCR analyses were performed for detection of Cre-mediated recombination in collected cells as described previously (Flesken-Nikitin et al., 2003; Nikitin and Lee, 1996). Briefly, wild-type, floxed, and excised *Trp53* sequences were identified with primers 1F5' (5'-GTG CCC TCC GTC CTT TTT CGC AAT C-3'), 103,3' (CCA TGA GAC AGG GTC TTG CTA TTG T-3'), and 10F5' (GTT AAG GGG TAT GAG GGA CAA GGT A-3'), resulting in 163-bp, 316-bp and 198-bp DNA fragments, respectively. PCR amplification of wild type, floxed, and excised *Rb1* sequences were identified with primers Rb18M3' (5'- GGA ATT CCG GCG TGT GCC ATC AAT G-3'), Rb19EM5' (5'-AGC TCT CAA GAG CTCAGA CTC ATG G-3'), and Rb212M5' (5'-CGA AAG GAA AGT CAG GGA CAT TGG G-3'), resulting in 247-bp, 296-bp and 269-bp DNA fragments, respectively.

Image acquisition and equipment. For gross lineage-tracing tissue imaging, all tissue were fixed in buffered 4% paraformaldehyde overnight at 4°C followed by PBS buffer washing twice. The tissue was immersed in PBS on 6 cm cell culture dish while

imaging. MVI Dissecting microscope (Micro Video Instruments Inc., Avon, MA, USA) and SPOT 2MP CCD camera (SPOT imaging, Sterling Heights, MI, USA) were used for gross imaging.

For bright field tissue section imaging, all sections with either hematoxylin and eosin staining or immunohistochemistry (IHC) staining were mounted with Canada Balsam medium (Polysciences Inc., Warrington, PA), and scanned by ScanScope CS2 (Leica). All images were further analyzed using HALO Image Analysis Software (PerkinElmer Inc., Shelton, CT, USA) or Aperio ImageScope Software (Leica).

For confocal imaging, all sections with indicated fluorescence markers and DAPI counterstaining were mounted with Fluoro-Gel (Electron Microscopy Sciences, Hatfield, PA, USA; 17985-10). The confocal images were acquired using Leica TCS SP5 confocal laser-scanning microscope (Leica) and all image stacks were further merged and analyzed with ImageJ software (National Institutes of Health, Bethesda, MD, USA).

RNA sequencing. SCJ tumors (n=5) were dissected from stomachs of *Lgr5*$^{eGFP\text{-}Ires\text{-}CreERT2}$*Trp53*$^{loxP/loxP}$*Rb1*$^{loxP/loxP}$Ai9 mice at least 250 days after tamoxifen induction. The tumor borders were delineated based on tdTomato expression. The wild-type control stomachs (n=3) were isolated from age-paired mice and separated into squamous forestomach, transitional zone (SCJ) and antral compartments. All the

tumors and gastric tissue were minced on ice using pre-autoclaved glass tissue grinder. The total RNA was purified from digested tissue using mirVana miRNA Isolation Kit (Thermo Fischer Scientific; AM1560). Following quality assessment by Agilent BioAnalyzer, samples with RNA Quality Number (RQN) greater than 7.0 were submitted to the Cornell RNA Sequencing Core (RSC) to generate standard library using the next generation high throughput sequencing by Illumina TruSeq system (Illumina, San Diego, CA, USA).

Statistical analyses. Statistical comparisons were performed using a two-tailed unpaired *t* test with InStat 3 and Prism 6 software (GraphPad Software Inc., La Jolla, CA, USA). Survival curves were computed using the Kaplan-Meier method and the survival comparisons were analyzed by log-rank tests. Significance was determined as $P<0.05$.

2.4 Results

2.4.1 Lgr5 marks the active stem/progenitor cells at the glands base of gastric squamous-columnar junction (SCJ)

Leucine-rich repeat-containing G-protein coupled receptor 5 (Lgr5) is a well-known stem/progenitor cell marker in the epithelium of multiple organs such as intestine, ovary, skin and stomach (Barker et al., 2010; Barker et al., 2007; Flesken-Nikitin et al., 2013; Jaks et al., 2008; Ng et al., 2014). A previous study has identified a limited number of $Lgr5^{+}$ cells located at the vicinity of the esophageal entry of stomach (Barker et al., 2010). This study was based on the lineage tracing experiment in *Lgr5-eGFP-IRESCreERT2* knock-in (*Lgr5*$^{EGFP\text{-}Ires\text{-}CRERT2}$) mice crossed with the enzyme-mediated *R26R-LacZ* (β-gal) reporter mice. In *Lgr5*$^{EGFP\text{-}Ires\text{-}CreERT2}$Ai9 mice, inducible Cre recombinase is synthesized in Lgr5-expressing ($Lgr5^{+}$) cells. When the mice are treated with single injection of tamoxifen, Cre excises the floxed "STOP" gene leading to the expression of LacZ encoded β-galactosidase (β-gal). In this system, visualization of the $Lgr5^{+}$ stem cells and their progeny requires the substrate X-gal (5-bromo-4-chloro-3-indolyl-β-D-galactopyranoside) to infiltrate into the tissue and cause an enzymatic staining reaction (Snippert and Clevers, 2011; Vorhagen et al., 2015). Such approach may result in significant background staining in some tissues and may also miss some minute cell populations. To avoid these artifacts we conducted a refined lineage tracing analysis by crossing the *Lgr5*$^{EGFP\text{-}Ires\text{-}CRERT2}$ mice

with *Rosa-loxp-stop-loxp-tdTomato* (Ai9) reporter mice. In these *Lgr5*$^{EGFP\text{-}Ires\text{-}CreERT2}$Ai9 mice, cells with present and past tamoxifen-induced Cre recombinase activity are detected by tdTomato expression, which is a modified dsRed fluorescent marker (Figure 2.1). This system has no detectable background and, unlike β-gal assay, does not require any additional tissue treatments.

Twenty-four hours post-induction (p.i.), tdTomato-expressing (tdTomato$^+$) cells were observed at the SCJ, the anatomic boundary between squamous epithelial forestomach and glandular stomach (Figure 2.2A and B). Unlike the finding in previous study (Barker et al., 2010), the progeny of Lgr5$^+$ lineage is not only restrictedly present at the esophageal entry, but also distributed along the entire SCJ line of the stomach (Figure 2.2B). Microscopically, the majority of tdTomato$^+$ cells were co-expressing Lgr5-eGFP at the base of first gastric pit at the SCJ 24-hour p.i. (Figure 2.2C). At 10 days p.i., the tdTomato$^+$ progeny were observed in the lower half of the first gastric gland unit at the SCJ, suggesting that the Lgr5$^+$ cells and/or their progeny are actively proliferating. At 21 day p.i., the tdTomato$^+$ cells populate the entire first gland of SCJ. This finding shows that the first gland of SCJ is actively renewed approximately every 10-21 days. In agreement with previous observation (Barker et al., 2010), the antral epithelium also contains Lgr5$^+$ cells that are located at the base of each antral gland (Figure 2.2D). These Lgr5$^+$ cells serve as actively proliferating stem/progenitor cells responsible for the entire antral epithelium homeostasis with relatively faster turnover rate (4-10 days; Figure 2.2D) and (Barker et al., 2010). The tdTomato$^+$ progeny lasts for at least 200 days throughout the first

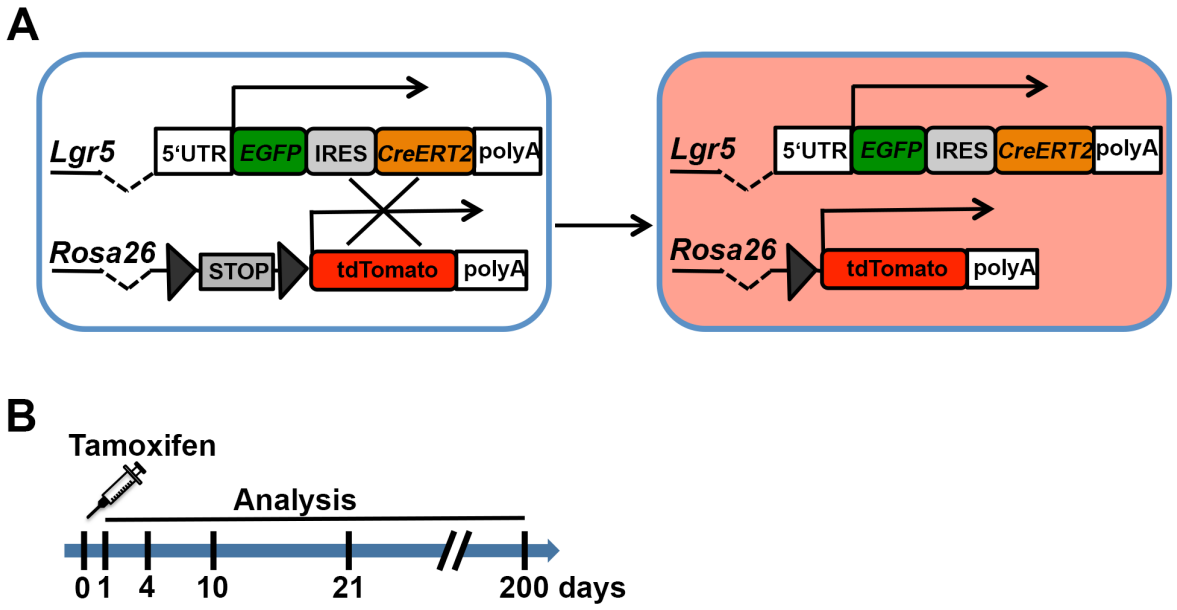

Figure 2.1. Lineage tracing of Lgr5^{+} stem cells in the mouse. (A) Experimental design of lineage tracing using *Lgr5*$^{eGFP\text{-}Ires\text{-}CreERT2}$Ai9 mice induced by tamoxifen administration. (B) Schedule for tamoxifen administration and material collection. See text for further details.

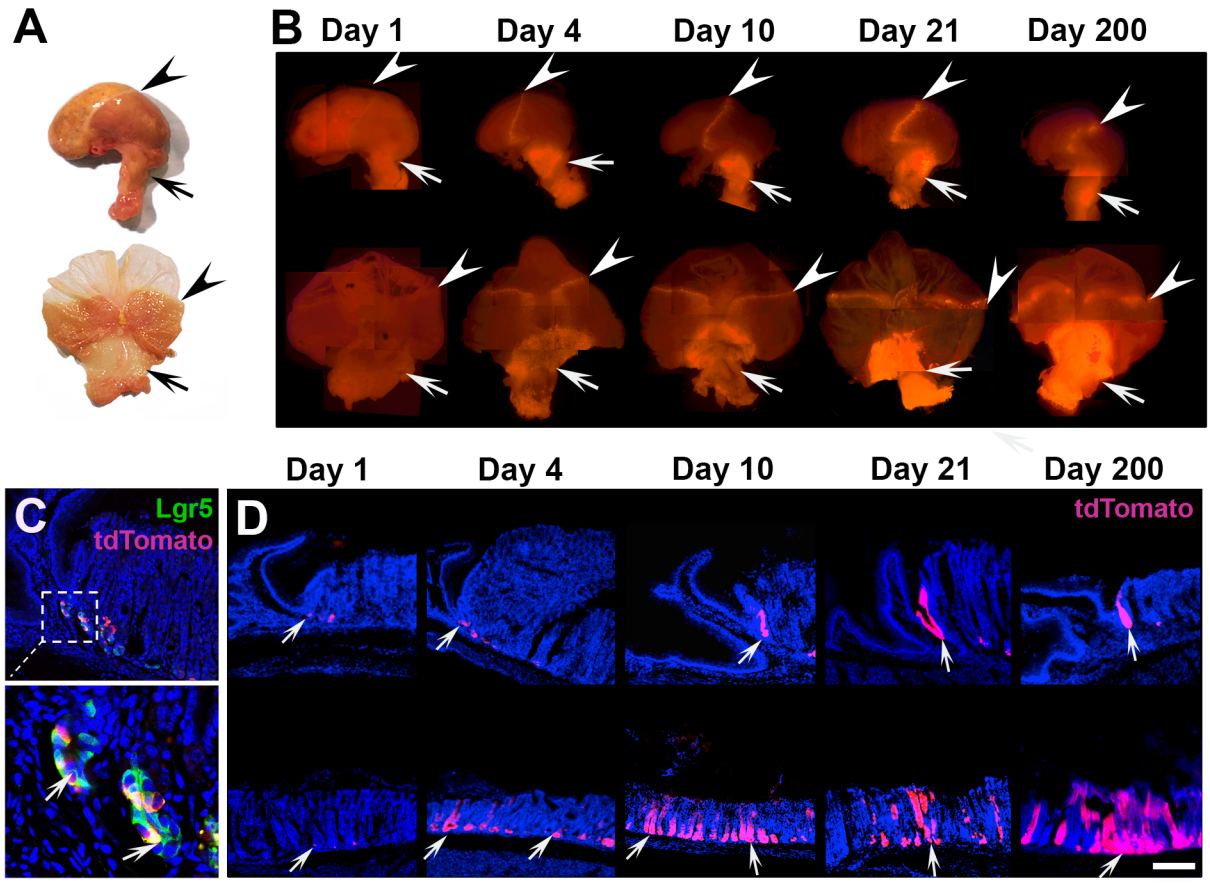
A
B
Day 1
Day 4
Day 10
Day 21
Day 200
C
Lgr5
tdTomato
D
Day 1
Day 4
Day 10
Day 21
Day 200
tdTomato

Figure 2.2 Epithelial homeostasis of the first pit of gastric squamous-columnar junction (SCJ) and the antral area is maintained by Lgr5^{+} stem cell. (A and B) Macroscopic light (A) and fluorescence (B) images of the intact (top) and dissected (bottom) stomachs of *Lgr5*$^{eGFP\text{-}Ires\text{-}CreERT2}$Ai9 mice collected at indicated days p.i. SCJ, arrowhead; Antrum, arrows. (C) Detection of co-localized expression of Lgr5-eGFP (green) and tdTomato (red) in Lgr5^{+} cells at SCJ (arrows in bottom image) 24 hours p.i. Rectangle in top image indicates area shown in bottom image. (D) Detection of tdTomato expression cells (red, arrows) in the longitudinal sections of SCJ (top) and antrum (bottom) of stomachs of *Lgr5*$^{eGFP\text{-}Ires\text{-}CreERT2}$Ai9 mice. Scale bars represent 3 mm (A and B), 100 μm (C, top panel), 25 μm (C, bottom panel), and 150 μm (D).

gastric pit of SCJ and the entire antral epithelium. Thus Lgr5^{+} cells represent long-term self-renewing stem/progenitor cells responsible for the normal epithelial homeostasis at the SCJ and antral regions. Only few individually scattered tdTomato^{+} cells can be found in the gastric corpus glands present until 200 days p.i. (Figure 2.3). These corpus Lgr5^{+} cells have been described as a subpopulation of quiescent, differentiated chief cells that actively proliferate and contribute to the corpus epithelial regeneration only following an injury (Leushacke et al., 2017). No tdTomato+ cells were observed in the forestomach squamous epithelium, suggesting that another stem/progenitor population is responsible for tissue homeostasis of this region (Figure 2.3). In addition, tdTomato expression was also observed in other organs, such as the ovary, skin, intestine and medulla of adrenal glands in our *Lgr5*-driven lineage tracing experiments (Figure 2.4).

Taken together, in the mouse stomach, the Lgr5^{+} cells are exclusively present in the glandular epithelium of mouse stomach. These cells are located at SCJ and antrum, and represent actively propagating stem/progenitor cells that account for the renewal of the entire epithelium of those regions under normal physiological conditions. Notably, the antral region has far larger number and wider distribution of Lgr5^{+} cells than the SCJ region.

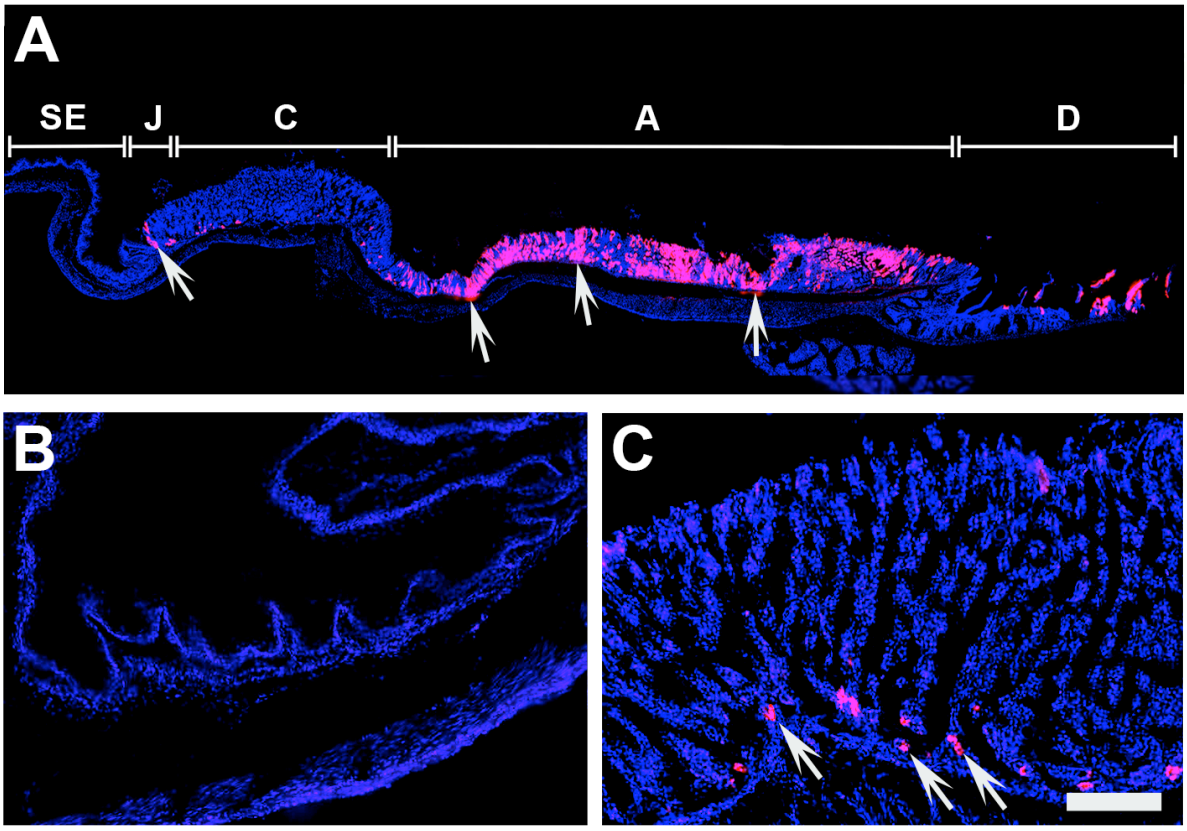

Figure 2.3 Detection of Lgr5^{+} cell lineage in the stomach. (A-C) Detection of tdTomato (red) in transverse section of whole gastric tissue (A), squamous forestomach (B) and corpus (C) of *Lgr5*$^{eGFP\text{-}Ires\text{-}CreERT2}$Ai9 mice with tamoxifen induction for 200 days. Arrows indicate the positive cells. SE, squamous epithelium, J, squamous-columnar junction (SCJ). C, corpus, A, antrum. D, duodenum. H, hilum. M, medulla. C, cortex. Counterstaining with DAPI (blue). Scale bars represent 1 mm (A), and 300 μm (B and C).

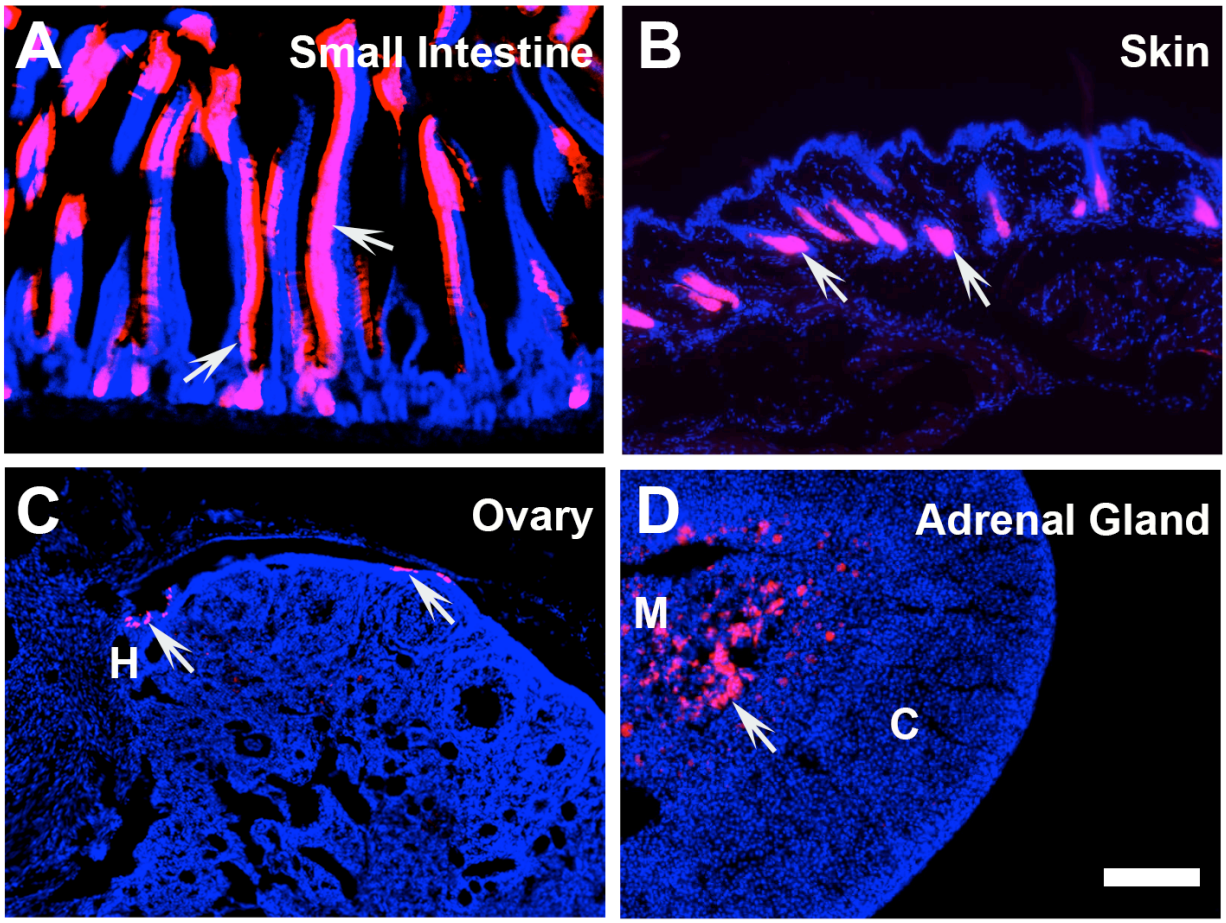
A
Small Intestine
B
Skin
C
Ovary
H
D
Adrenal Gland
M
C

Figure 2.4 Detection of Lgr5^{+} stem cell lineages in multiple organs. (A-D) Detection of tdTomato (red) in multiple organs of *Lgr5*$^{eGFP\text{-}Ires\text{-}CreERT2}$Ai9 mice 200 days post induction (p.i.) with tamoxifen. Positive cells (arrows) are present at in the small intestine (A), hair follicles (B), ovarian surface epithelium (C) of ovary, and medulla of adrenal gland (D). Counterstaining with DAPI (blue). Scale bars represent 300 µm (A, B and D) 230 µm (C).

2.4.2 Preferential susceptibility of the gastric squamous-columnar junction to malignant transformation after conditional inactivation of Trp53 and *Rb1 in Lgr5^{+} cells*

P53 and RB are the key factors of two main tumor suppressor pathways that operate cellular response to potential oncogenic stresses (Sherr and McCormick, 2002). Mutations in *Trp53* and *Rb1* (p53- and RB-edcoding genes) have been reported to be highly associated with carcinogenesis of various organs including prostate, ovary and lung (Flesken-Nikitin et al., 2013; Meuwissen et al., 2003; Zhou et al., 2007). Importantly, inactivation of *Trp53* and *Rb1* can lead to malignant transformation of the hilum cells, which are located at the epithelial junction between the ovarian surface epithelium, tubal epithelium and mesothelium (Flesken-Nikitin et al., 2013). It is noteworthy that the hilum area, which contains Lgr5^{+} stem cell niches, is more predisposed to malignant transformation than other regions of the ovarian surface epithelium.

To test if Lgr5^{+} stem cells located in the gastric SCJ areas are also more susceptible to the malignant transformation as compared to those in other areas of stomach, mice carrying floxed *Trp53* and *Rb1* alleles were crossed with *Lgr5$^{EGFP\text{-}Ires\text{-}CreERT2}$* mice to generate *Lgr5$^{EGFP\text{-}Ires\text{-}CreERT2}$Trp53$^{loxp/loxp}$* (*Trp53$^{-/-}$*) *Lgr5$^{EGFP\text{-}Ires\text{-}CreERT2}$Rb1$^{loxp/loxp}$*, (*Rb1$^{-/-}$*) and *Lgr5$^{EGFP\text{-}Ires\text{-}CreERT2}$Trp53$^{loxp/loxp}$Rb1$^{loxp/loxp}$* (*Trp53$^{-/-}$Rb1$^{-/-}$*) mice. To trace cells exposed to tamoxifen activated *Cre-ERT2* fusion protein, these mice were also crossed to Ai9 reporter mice strain (Figure 2.5A). In order to increase

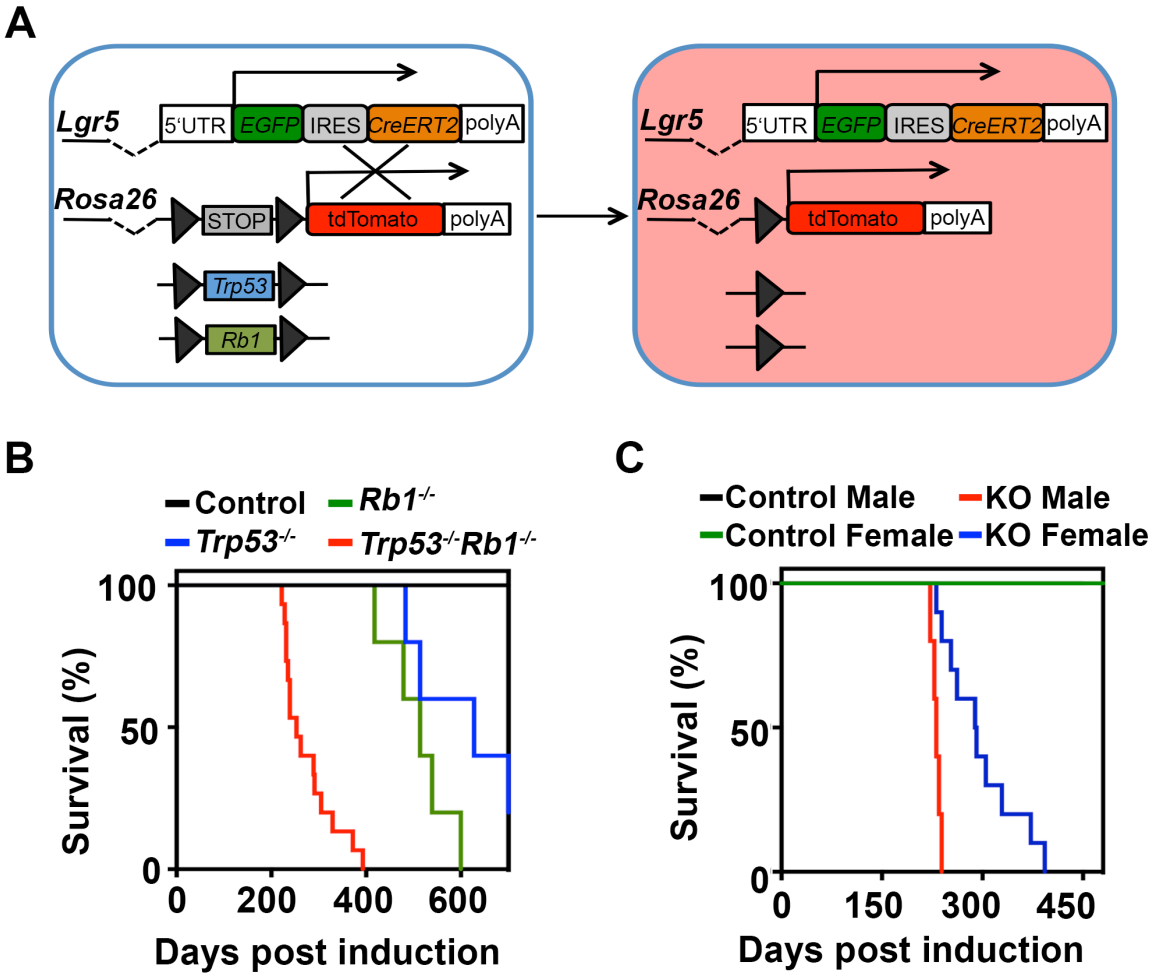
A
Lgr5
5'UTR
EGFP
IRES
CreERT2
polyA
Rosa26
STOP
tdTomato
polyA
Trp53
Rb1
Lgr5
5'UTR
EGFP
IRES
CreERT2
polyA
Rosa26
tdTomato
polyA
B
Control
Rb1-/-
Trp53-/-
Trp53-/-Rb1-/-
Survival (%)
100
50
0
0
200
400
600
Days post induction
C
Control Male
KO Male
Control Female
KO Female
Survival (%)
100
50
0
0
150
300
450
Days post induction

Figure 2.5 Inactivation of *Trp53* and/or *Rb1* in Lgr5^{+} cells. (A) Experimental strategy for conditional inactivation of *Trp53* and *Rb1* in Lgr5^{+} cells using *Lgr5*$^{eGFP\text{-}Ires\text{-}CreERT2}$*Trp53*$^{loxP/loxP}$*Rb1*$^{loxP/loxP}$Ai9 (B) Kaplan-Meier survival curve of *Lgr5*$^{eGFP\text{-}Ires\text{-}CreERT2}$*Trp53*$^{loxP/loxP}$*Rb1*$^{loxP/loxP}$Ai9 mice with tamoxifen induction (*Trp53*$^{-/-}$*Rb1*$^{-/-}$, n=15) compared with genetic background-matched control mice (*Lgr5*$^{eGFP\text{-}Ires\text{-}CreERT2}$*Trp53*$^{loxP/loxP}$*Rb1*$^{loxP/loxP}$Ai9 mice without tamoxifen induction, n=8, P<0.0001 by log-rank test), *Lgr5*$^{eGFP\text{-}Ires\text{-}CreERT2}$*Trp53*$^{loxP/loxP}$Ai9 mice with tamoxifen induction (*Trp53*$^{-/-}$, n=5, P<0.001), and *Lgr5*$^{eGFP\text{-}Ires\text{-}CreERT2}$*Rb1*$^{loxP/loxP}$Ai9 mice with tamoxifen induction (*Rb1*$^{-/-}$, n=5, P<0.001). (C) Kaplan-Meier survival curve. Male mice (n=5) with conditional knockout (KO) of *Trp53* and *Rb1* have significantly shorter survival span (median=231 days) compared to female mice (n=10) with the same KO (median=290 days). P<0.001. Male (n=5) and female (n=4) of *Lgr5*$^{eGFP\text{-}Ires\text{-}CreERT2}$*Trp53*$^{loxP/loxP}$*Rb1*$^{loxP/loxP}$Ai9 mice without tamoxifen induction were used as controls.

the activity of Cre-recombinase, tamoxifen was administrated every other day in a total of three injections to 6 to 10 week-old mice. *Trp53*$^{-/-}$*Rb1*$^{-/-}$ mice (n=15) had the shortest survival time (253 days after first injection of tamoxifen [p.i.]) as compared to *Trp53*$^{-/-}$ mice (n=5, median=628 days, P<0.001), *Rb1*$^{-/-}$ mice (n=5, median=514 days, P<0.001) and genetic background-matched control mice (*Lgr5*$^{eGFP\text{-}Ires\text{-}CreERT2}$*Trp53*$^{loxP/loxP}$*Rb1*$^{loxP/loxP}$Ai9 mice without tamoxifen induction, n=8, median> 700 days, P<0.0001) (Figure 2.5B). Additionally, among the *Trp53*$^{-/-}$*Rb1*$^{-/-}$ mice, male mice showed shorter survival time (median=231 days) than females (median=290 days) (Figure 2.5C).

Organs from all mice were collected and inspected both macro- and microscopically for evidence of neoplastic formation. Variable susceptibilities of tumor formation were observed among multiple organs of *Trp53*$^{-/-}$*Rb1*$^{-/-}$ mice (Figure 2.6A). All the mice succumbed to poorly differentiated, highly invasive and metastatic carcinomas in the stomach (Figure 2.6B and C). However, contrary to high incidence of cancer formation at SCJ, the antral region was less susceptible to neoplasia. Only 2 out of 20 (10%) *Tp53*$^{-/-}$*Rb1*$^{-/-}$ mice displayed adenomas in the antral regions without any tissue invasion (Figure 2.6C and D). Besides the stomach, all females also developed dysplastic lesions in the ovarian hilum, and some mice developed squamous cell carcinomas of the skin (2 out of 20, 10%) and adrenal pheochromocytomas (3 out of 15, 20%) (Figure 2.7). Intriguingly, up to 12 months of observation, no neoplastic lesions were observed in any other organ, including the intestine, where there are multiple Lgr5^{+} cells (Figure 2.6A) and (Barker et al., 2009).

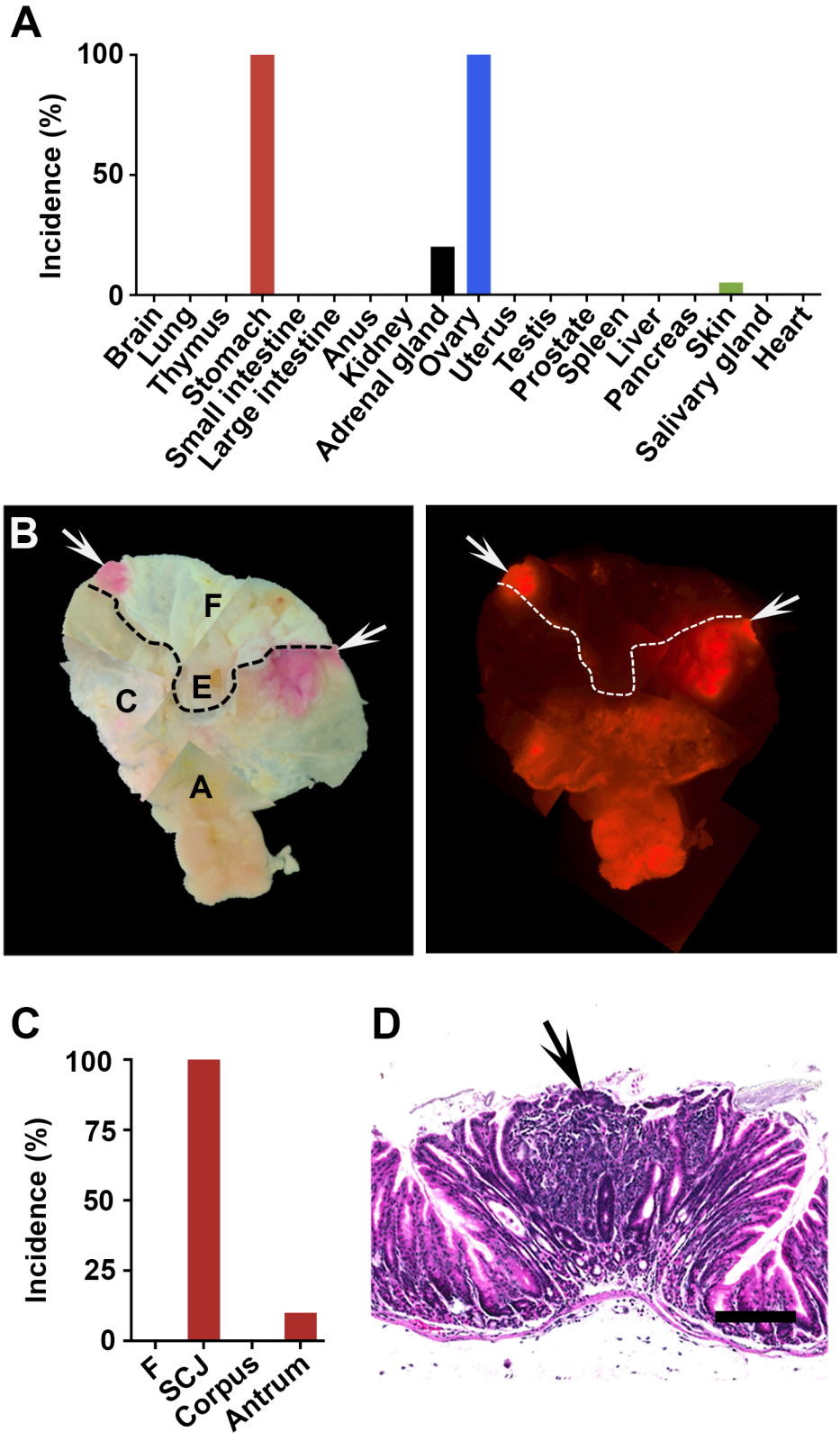
A
Incidence (%)
100
50
0
Brain
Lung
Thymus
Stomach
Small intestine
Large intestine
Anus
Kidney
Adrenal gland
Ovary
Uterus
Testis
Prostate
Spleen
Liver
Pancreas
Skin
Salivary gland
Heart
B
F
E
C
A
C
Incidence (%)
100
75
50
25
0
F
SCJ
Corpus
Antrum
D

Figure 2.6 Inactivation of *Trp53* and *Rb1* in Lgr5^{+} cells leads to preferential neoplasia formation at the gastric SCJ. (A) Incidence of neoplastic lesions in various organs of mice with conditional knockout (KO) of *Trp53* and *Rb1* (*Trp*$^{-/-}$*Rb1*$^{-/-}$; n=20). *Graph shows kidney instead of adreanl gland, please correct. Also, place anus after intestine, group all bars by organ sites and change "uterine" to "uterus".* (B) tdTomato-expressing (tdTomato^{+}) neoplastic masses (arrows) in the stomach of *Lgr5*$^{eGFP\text{-}Ires\text{-}CreERT2}$*Trp53*$^{loxP/loxP}$*Rb1*$^{loxP/loxP}$ Ai9 (*Trp53*$^{-/-}$*Rb1*$^{-/-}$Ai9) mouse 291 days post first injection with tamoxifen (p.i.). Bright field (left) and fluorescence (right). The punctate lines indicate SCJ line. F, foresotmach, E, esophagus, C, corpus, A, antrum. (C) Incidence of primary neoplasms in the stomach of *Trp53*$^{-/-}$*Rb1*$^{-/-}$Ai9 mice. (D) Representative image of adenoma (arrow) at the antrum of *Trp53*$^{-/-}$*Rb1*$^{-/-}$Ai9 mouse 309 days p.i. Hematoxylin and eosin staining. Scale bar represents 2.3 mm (B) and 250 μm (D).

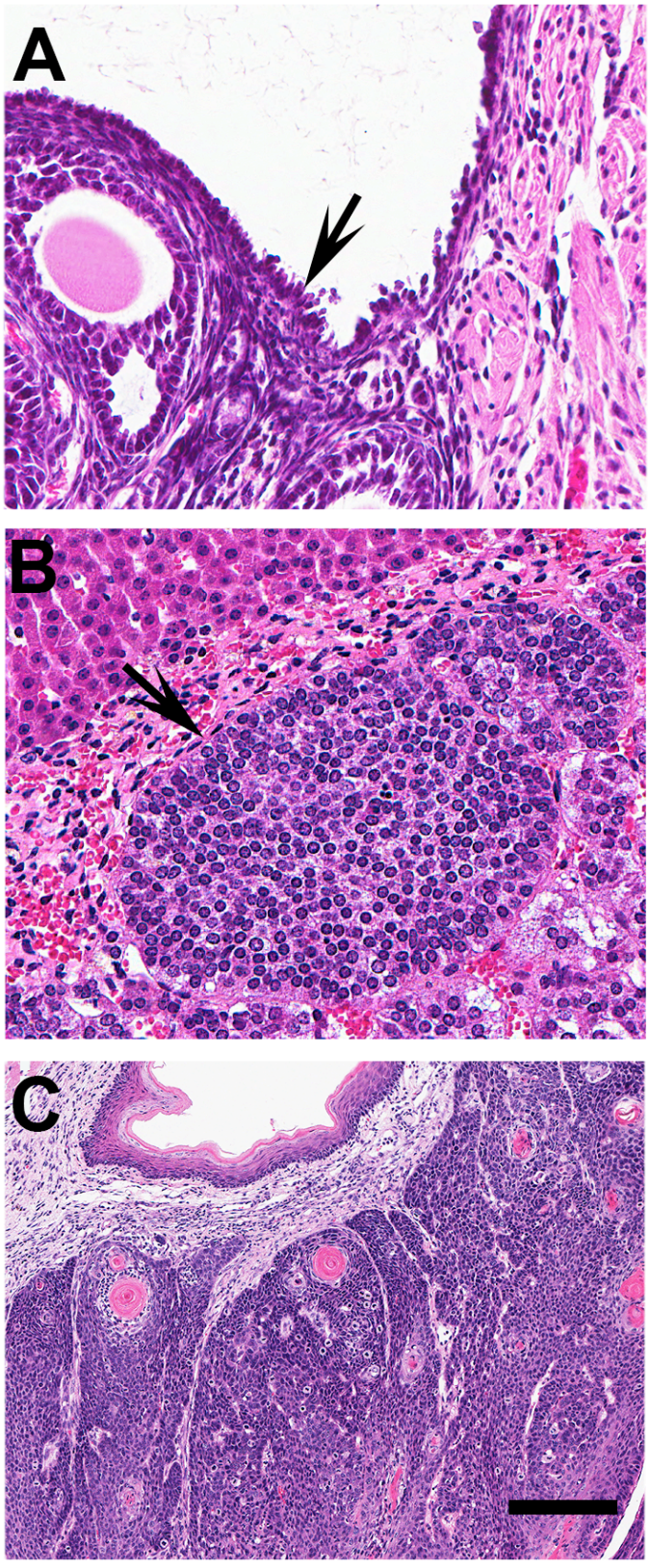
A
B
C

Figure 2.7 Dysplastic and neoplastic lesions in various organs of *Trp53*$^{-/-}$*Rb1*$^{-/-}$ mice. (A) Dysplasia (arrow) of the ovarian surface epithelium in the ovarian hilum region. 253 days p.i. (B) Pheochromocytoma (arrow) in the adrenal gland medulla. 231 days p.i. (g) Squamous cell carcinoma of the flank skin. 235 days p.i. Scale bar represents 60 μm (A and B), and 250 μm (C).

It suggests that either different initiating genetic alterations or longer time are needed for the carcinogenesis in these tissues.

2.4.3 Characterization of the gastric SCJ cancer in *Trp53*$^{-/-}$*Rb1*$^{-/-}$ mice

All neoplasms expressed tdTomato as indicator of tamoxifen induced Cre-recombinase activity (Figure 2.6B). To confirm that the gastric SCJ neoplasms were indeed initiated by the co-occurrence of Cre-*loxP* recombination-mediated mutations in *Trp53* and *Rb1*, neoplastic cells were isolated by laser microdissected from the gastric SCJ of and subjected to PCR genotyping for inactivating *Trp53* and *Rb1* mutations. Such mutations were consistently confirmed in the gastric SCJ neoplasms of *Trp53*$^{-/-}$*Rb1*$^{-/-}$ mice (Figure 2.8).

According to sequential analysis of carcinogenesis in the stomach of *Trp53*$^{-/-}$*Rb1*$^{-/-}$ Ai9 mice, early dysplastic epithelial lesions were observed at the bottom to middle part of the first gland at the SCJ by 60 to 120 days p.i. (Figure 2.9A-C). Such lesions were characterized by the cells with enlarged pleomorphic and hyperchromatic nuclei and irregular shapes. These lesions progressed to poorly differentiated carcinomas 177 days p.i. (Figure 2.9). Locally submucosal and muscular invasion (Figure 2.9) and distal metastasis to regional lymph nodes (4/20; 20%) and liver (7/20; 35%) were observed (Figure 2.10). This metastatic pattern of SCJ tumors, as well as their faster development in male mice (Figure 2.5), well correlated with similar features in human

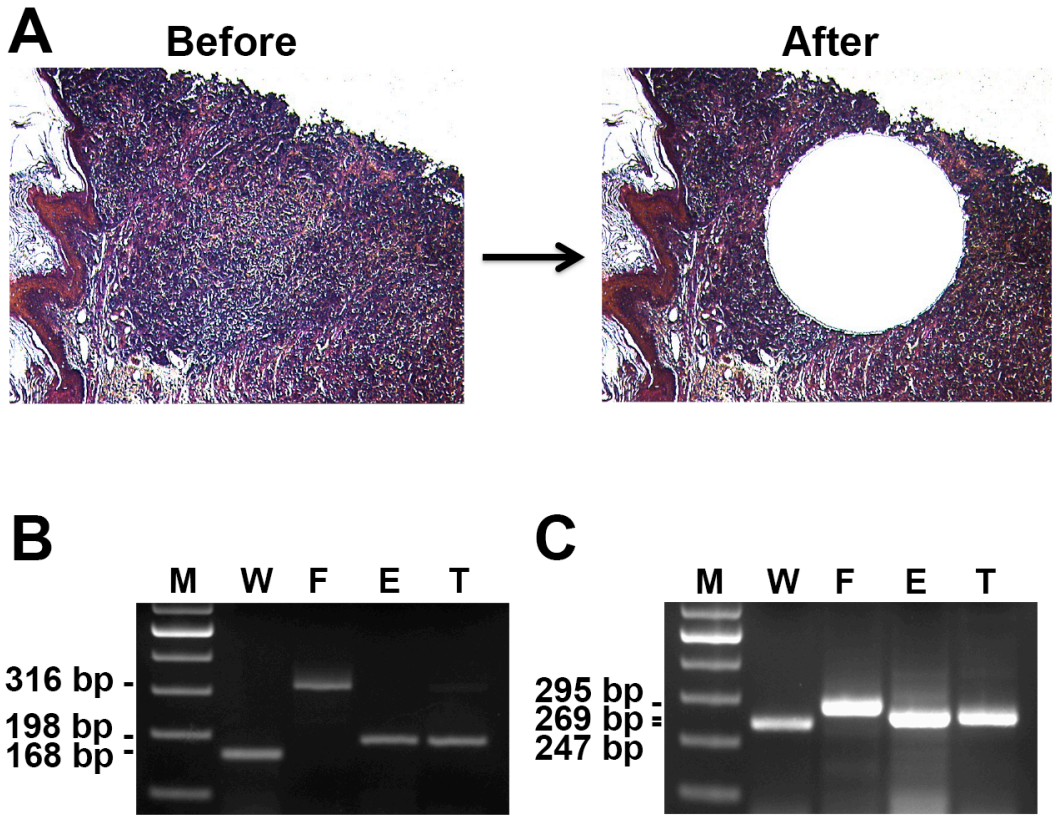
A
Before
After
B
M W F E T
316 bp
198 bp
168 bp
C
M W F E T
295 bp
269 bp
247 bp

Figure 2.8 Detection of Cre-*loxP* recombination in the gastric SCJ neoplastic cells of *Trp53*$^{-/-}$*Rb1*$^{-/-}$ Ai9 mice. (A) Before and after microdissection of neoplasm. (B and C) PCR analysis of *Trp53* (B) and *Rb1* (C) structures in samples collected from mouse cells with wild-type (W, lane 2), homozygous for floxed (F, lane 3) and excised (E, lane 4) genes, and from microdissected neoplastic cells (T, lane 4), respectively. M, marker.

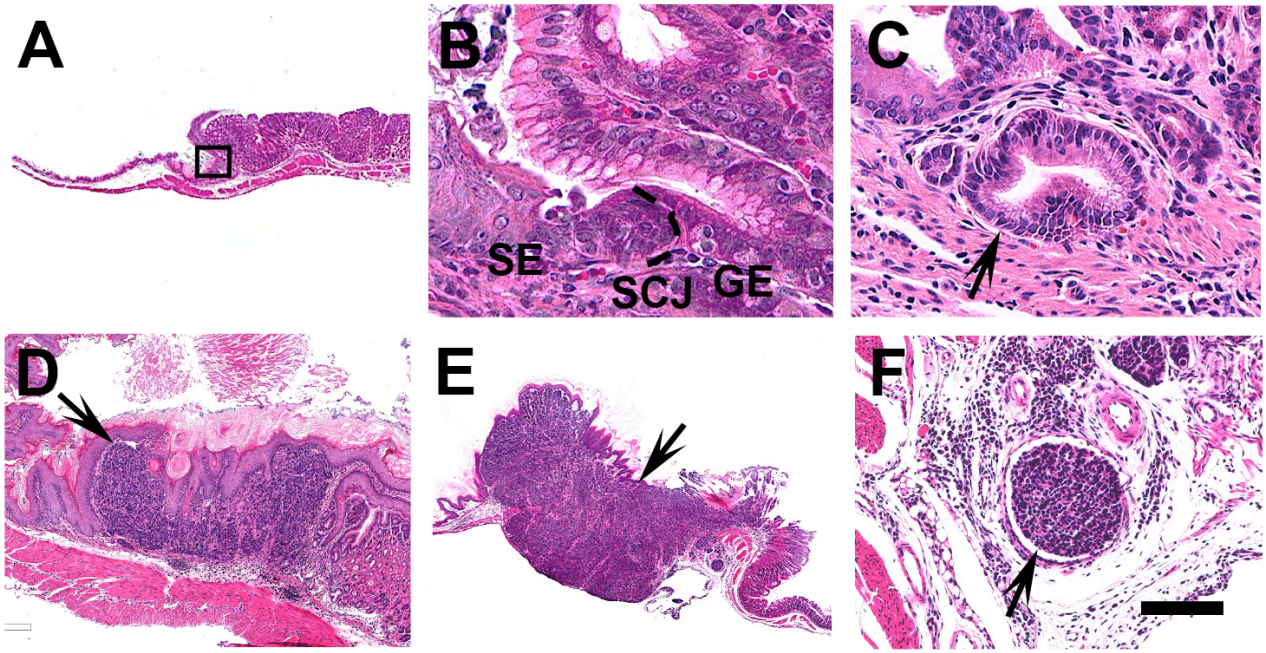

Figure 2.9 Primary neoplasms of the gastric SCJ in ***Trp53*$^{-/-}$*Rb1*$^{-/-}$Ai9 mice.** (A and B) SCJ between the gastric squamous (SE) and glandular (GE) epithelium in adult control mice (*Lgr5*$^{eGFP\text{-}Ires\text{-}CreERT2}$*Trp53*$^{loxP/loxP}$*Rb1*$^{loxP/loxP}$Ai9 mouse without tamoxifen induction). Rectangle in (A) indicates area shown in (B). (C-F) SCJ carcinogenesis in *Trp53*$^{-/-}$*Rb1*$^{-/-}$ Ai9 mice includes dysplastic glandular lesions (C, arrow, 120 days p.i.), early carcinoma (D, arrow, 177 days p.i.), and advanced carcinoma (E, arrow, 239 days p.i.) with vascular invasion (F). Hematoxylin and eosin staining. Scale bar represents 1 mm (A and E), 60 µm (B), 40 µm (C), 300 µm (D), 100 µm (F).

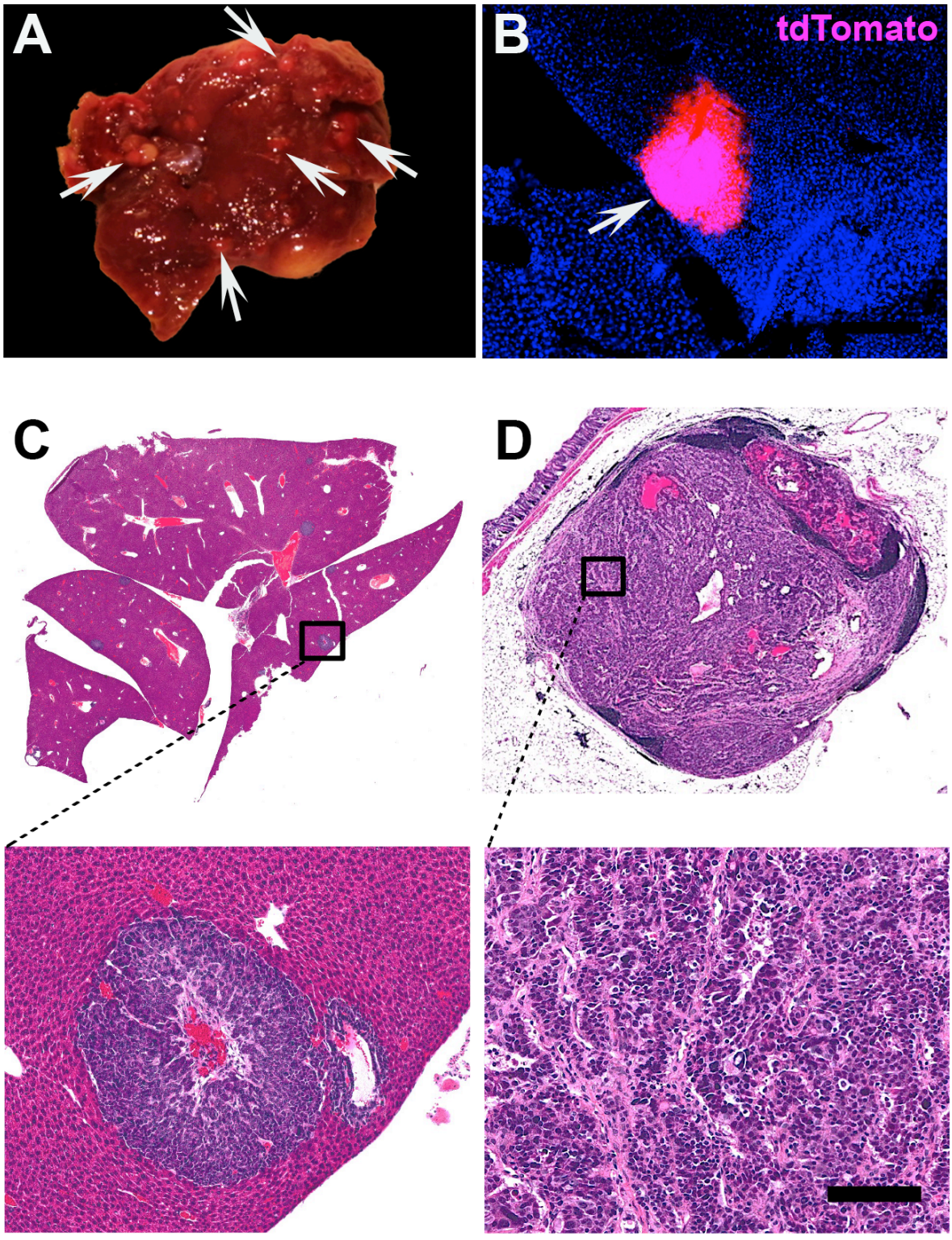
A
B
tdTomato
C
D

Figure 2.10 Metastatic neoplasms in *Trp53*$^{-/-}$*Rb1*$^{-/-}$ Ai9 mice. (A-B) Gross (A) and fluorescence microscopic (B) images of hepatic metastasis in *Trp53*$^{-/-}$*Rb1*$^{-/-}$ Ai9 mice. Arrows indicate metastatic neoplasms. The neoplastic cells (arrow in B) are tdTomato-positive. (C and D) Histopathological images of metastatic lesions in the liver (C, 35% of cases) and the lymph node (D, 20% of cases). Counterstained with DAPI (B). Hematoxylin and eosin staining (C and D). Rectangle in (C and D) top images indicates areas shown in bottom images. Scale bar represents 6 mm (A), 270 μm (B), 4.5 mm (top panel in C), and 175 μm (bottom panel in C), 600 μm (top panel in D), and 100 μm (bottom panel in D).

diseases (Blot et al., 1991; Sons and Borchard, 1986). Supporting the clinical relevance of our mouse model, p53 mutations and RB pathway aberrations are the most frequent alterations in human GEJ carcinomas (Dulak et al., 2013; Network, 2014, 2017). Furthermore, the gene set enrichment analyses (GSEA) of the RNA-seq transcriptional profile of the human GEJ carcinomas (Dulak et al., 2013; Network, 2014, 2017). Furthermore, the gene set enrichment analyses (GSEA) of the RNA-seq transcriptional profile of the RNA samples isolated from mouse proximal stomach carcinomas revealed strong concordance with the expression of signature gene set of human GEJ carcinomas (normalized enrichment score=1.38, $P<0.05$; Figure 2.11) (Isinger-Ekstrand et al., 2010).

2.4.4 Loss of Lgr5 expression in the gastric SCJ cancer cells arising from the Lgr5^{+} cells with deletions of *Trp53* and *Rb1*

Previous study has demonstrated that conditional knockout of the tumor suppressor *Apc* in Lgr5^{+} stem cells is able to initiate the intestinal adenoma formation (Barker et al. 2009). In these benign neoplasms, the stem cell marker, Lgr5, is expressed by a small subpopulation of neoplastic cells representing approximate 5-10% of all tumor cells. By lineage tracing using multicolor *Cre*-reporter R26R-Confetti mice, it was shown that these Lgr5^{+} neoplastic cells maintained the growth of intestinal adenoma in the *Apc*$^{-/-}$ mice (Schepers et al., 2012). Similarly, cellular expansions of Lgr5^{+} population were also observed in the antral microadenoma

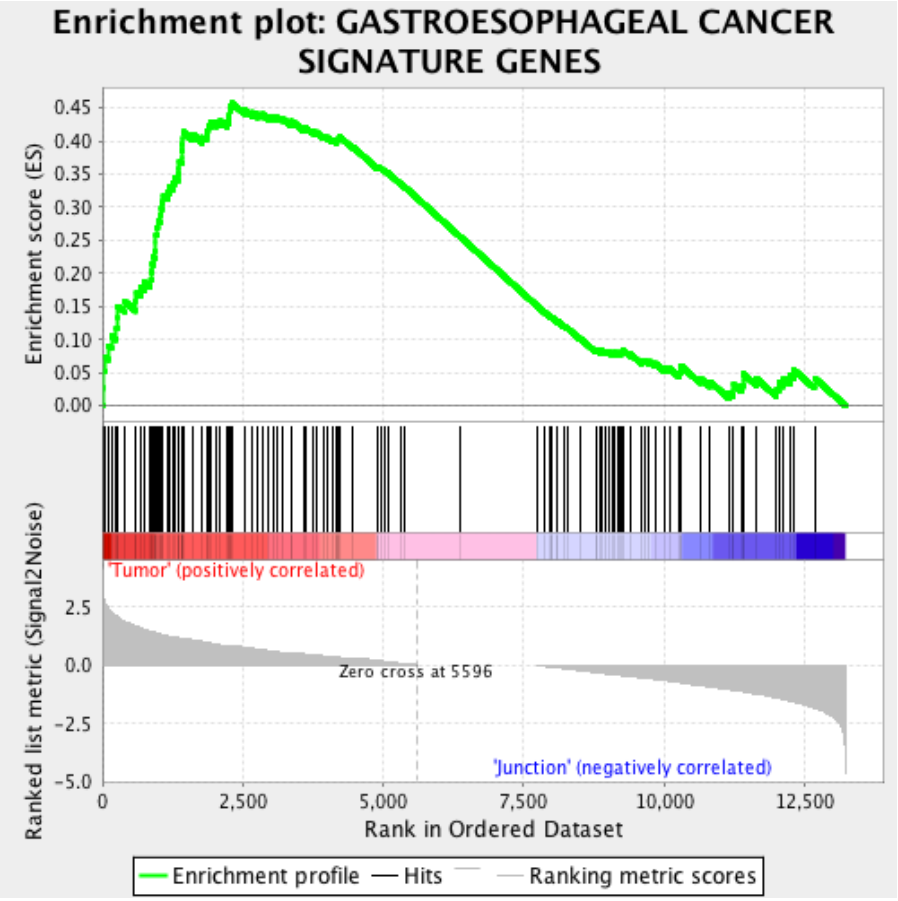

Figure 2.11 Comparison of gene expression profile of gastric SCJ cancer between mice and humans. Gene Set Enrichment Analysis (GSEA) of RNA-seq data of mouse gastric SCJ cancers using human GEJ cancer signature genes (Isinger-Ekstrand et al., 2010). Enrichment score (ES)=0.46, normalized enrichment score (NES) = 1.38, false discovery rate (FDR) *q* value=0.08. P<0.05.

induced by deletion of *Apc* targeted to Lgr5^{+} cells using *Lgr5*$^{eGFP\text{-}Ires\text{-}CreERT2}$*Apc*$^{loxp/loxp}$ mice (Barker et al., 2010). In contrary, in our *Trp53*$^{-/-}$*Rb1*$^{-/-}$Ai9 mouse model, Lgr5^{+} cells are absent in the gastric SCJ carcinomas (Figure 2.12A). This finding, however, is consistent with earlier studies reporting the absence of Lgr5 expression in human gastric premalignant lesions (Wang et al., 2012). This suggests that the expression of stem cell marker Lgr5 may vary depending on targeted regions of the gastrointestinal tract and/or initiating genetic alterations. We next sought to examine whether the gastric SCJ carcinomas of *Trp53*$^{-/-}$*Rb1*$^{-/-}$ Ai9 mice express DCLK1, CK5, KLF4, ALDH1, and CD44 (Figure 2.12B-F). These stem/progenitor markers were reported to identify putative cancer-propagating cells (aka cancer stem cells) in various types of tumors (Chandrakesan et al., 2017; Flesken-Nikitin et al., 2013; Giangreco et al., 2007; Ginestier et al., 2007; Morath et al., 2016; Nakanishi et al., 2013; Wei et al., 2016; Yan et al., 2015; Yu et al., 2011). Immunohistochemical staining revealed that CD44 is expressed by about 15-20% of neoplastic cells of gastric SCJ carcinomas of *Trp53*$^{-/-}$*Rb1*$^{-/-}$ Ai9 mice (Figure 2.12F). These findings are in agreement with the earlier observation of CD44 expression in the premalignant and malignant neoplasms at GEJ in human patients (Kim et al., 2005).

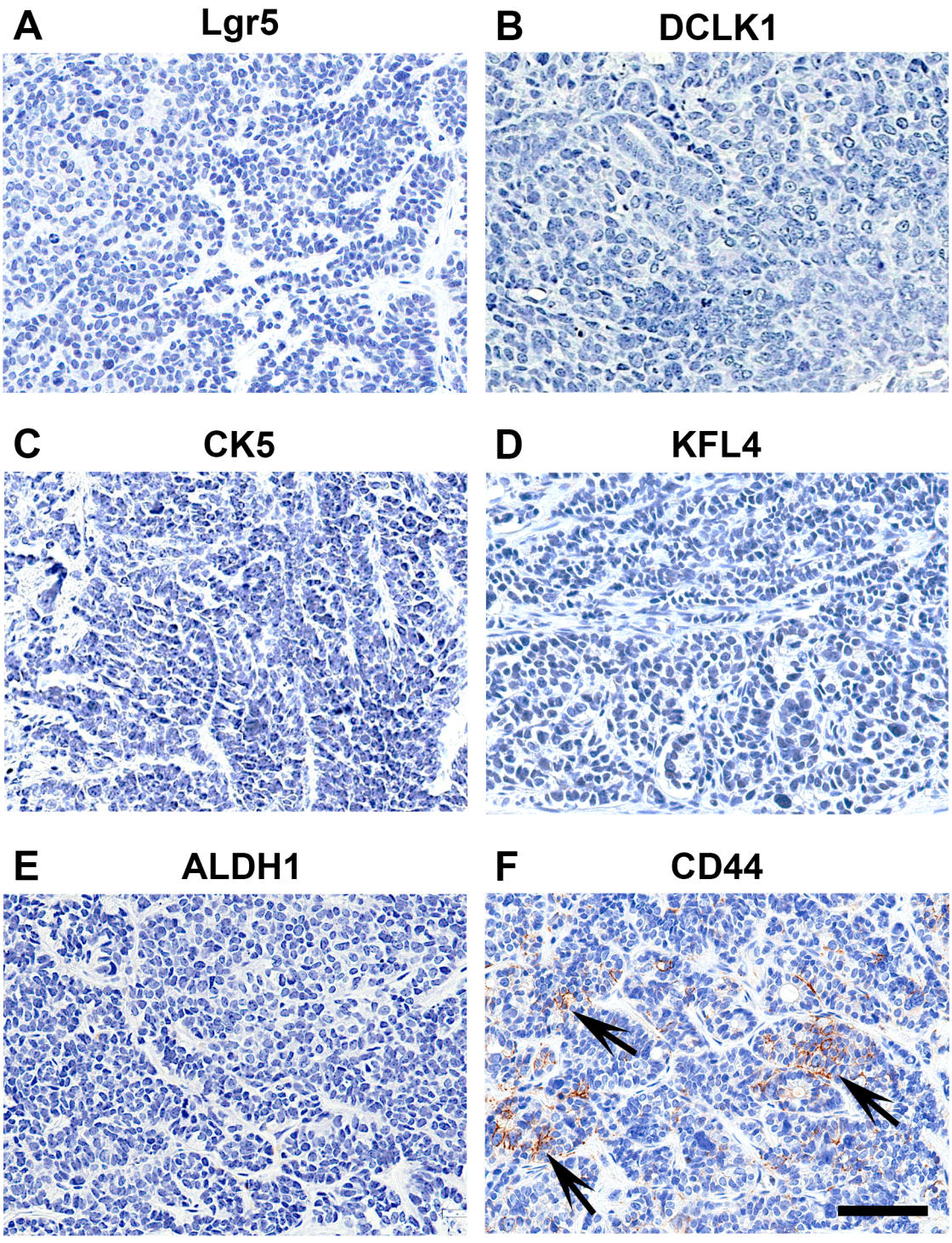
A
Lgr5
B
DCLK1
C
CK5
D
KFL4
E
ALDH1
F
CD44

Figure 2.12 Detection of stem/progenitor marker expression in the gastric SCJ cancer of *Trp53*$^{-/-}$*Rb1*$^{-/-}$Ai9 mice. (A-F) Immunostaining for Lgr5-eGFP (A), DCLK1 (B), CK5 (C), KLF4 (D), ALDH1 (E) and CD44 (F) of gastric SCJ neoplasm. Arrows indicate positive cells in F. All images, ABC Elite method with hematoxylin counterstaining. Scale bar represents 60 μm for all images.

2.5 Discussion

We established a mouse model gastric SCJ carcinoma that is based on conditional inactivation of both *Rb1* and *Trp5* in Lgr5^{+} cells. *Trp53* and *Rb1* mutations are common signaling aberrations in human GEJ cancer. In our model, the junction neoplasms were highly invasive, metastasized into lymph nodes and liver, and had comparable gene expression profiles, resembling human disease. Moreover, the GEJ cancer is approximately 5 times more frequent in men than women (Blot et al., 1991). In agreement with human disease, the male mice had shorter survival time as compared to female mice in our study. This gender predisposition to cancer may be explained by the variability of serum IL-6 concentration between male and female. IL-6 has been reported as a critical mediator in the pathogenesis of gastric SCJ cancer (Naugler et al., 2007; Quante et al., 2012). Thus it would be interesting to test if the same is true in our model.

As discussed in Chapter 1, the presence of cancer-prone stem/progenitor niches may predispose the epithelial transitional zone to cancer initiation and progression. Our results provide direct experimental evidence to this notion, which previously was comprehensively demonstrated only for the cancer-prone niche in the mouse hilum (Flesken-Nikitin et al, 2013). Thus, it is now more likely that identification of stem cell niches at the epithelial junction areas may contribute to predicting the cellular origin of cancer therein.

The first pit of gastric glandular epithelium has been seen as a unique anatomic structure with distinct cellular composition. It lacks secretory parietal cells, thereby more resembling the antral rather than the corpus glands (O'Neil et al., 2017). Consistently, Lgr5 marks the actively proliferating stem cells at the base of both the first pit and antral glands of mouse stomach. According to lineage tracing, these $Lgr5^+$ cells are responsible for the long-term epithelial homeostasis in these two areas. Importantly, the $Lgr5^+$ cells at the first pit of SCJ demonstrate significantly greater susceptibility to malignant transformation than those in the antrum, while no malignant neoplasms develop from the antral regions in our model. This preferential susceptibility of the junction $Lgr5^+$ cell to malignant transformation may be determined by unique mechanisms such as its uniquely cancer-prone properties, and/or by the extrinsic mechanisms such as responses to the tumorigenic signaling from the microenvironment (Bleuming et al., 2007; McNairn and Guasch, 2011; O'Neil et al., 2017; Plaks et al., 2015).

We have detected expression of cancer-propagating cell marker CD44 in our model. The concept of cancer-propagating cell (AKA cancer stem cell or tumor-initiating cell) has been proposed more than two decades ago to describe a restricted subpopulation of tumor cells fueling the whole process of tumor propagation and growth (Nassar and Blanpain, 2016). In acute myeloid leukemia, for instance, the putative cancer-propagating cells express the same makers ($CD34^+CD38^-$) as their hematopoietic stem cell origin, and possess the characteristics such as self-renewal and tumor-propagating potential that are distinct from their committed differentiated

lineage (Bonnet and Dick, 1997; Lapidot et al., 1994). Many solid tumors such as breast cancers, colon cancer, glioblastoma and melanoma have been reported to contain these cancer-propagating populations with greater ability to regrow the tumor mass after xenotransplantation (Chen et al., 2010; Eirew et al., 2015; Held et al., 2010; Ricci-Vitiani et al., 2007). In addition, by *in vivo* lineage tracing approaches, it is evident that cancer propagating cells in some organs can be identified by certain makers reflecting their stem cell origins, and these stem-like cells are able to propagate the tumor (Chen et al., 2012; Driessens et al., 2012; Schepers et al., 2012). Interestingly, our mouse model revealed an absence of Lgr5 expression in gastric SCJ cancers even though these neoplasms were initiated by inactivation of *Trp53* and *Rb1* in $Lgr5^+$ cells. This finding opens a possibility that in our model neoplastic cells may not be transformed directly from the mutant stem cell, but from the progeny cells, which inherit the mutations from $Lgr5^+$ stem cells. It will be interesting to test if CD44 cells represent cancer-propagating cells in gastric SCJ cancers.

Taken together, we demonstrate that *Trp53* and *Rb1* mutations, which are the consistent with common signaling aberrations in human GEJ cancer, lead to poorly differentiated carcinoma at mouse gastric SCJ. Our histopathological, immunohistochemistry and gene expression profile studies show that our newly established mouse model resembles human GEJ cancer, with similar aggressive behavior and distant metastatic potential, as well as expression of the cancer-propagating cell marker CD44. Interestingly, although the $Lgr5^+$ cells are present in

the epithelium at SCJ and antral regions, inactivation of *Trp53* and *Rb1* in those cells leads to preferential malignant transformation at the gastric SCJ. Our model should provide a valuable tool for future studies of the essential mechanisms by which the junction stem cell niches are more predisposed to cancer than their counterparts in other regions of the same organ.

References

Barker, N., Huch, M., Kujala, P., van de Wetering, M., Snippert, H.J., van Es, J.H., Sato, T., Stange, D.E., Begthel, H., van den Born, M.*, et al.* (2010). Lgr5(+ve) stem cells drive self-renewal in the stomach and build long-lived gastric units in vitro. Cell Stem Cell *6*, 25-36.

Barker, N., Ridgway, R.A., van Es, J.H., van de Wetering, M., Begthel, H., van den Born, M., Danenberg, E., Clarke, A.R., Sansom, O.J., and Clevers, H. (2009). Crypt stem cells as the cells-of-origin of intestinal cancer. Nature *457*, 608-611.

Barker, N., van Es, J.H., Kuipers, J., Kujala, P., van den Born, M., Cozijnsen, M., Haegebarth, A., Korving, J., Begthel, H., Peters, P.J.*, et al.* (2007). Identification of stem cells in small intestine and colon by marker gene Lgr5. Nature *449*, 1003-1007.

Blanpain, C. (2013). Tracing the cellular origin of cancer. Nature cell biology *15*, 126-134.

Bleuming, S.A., He, X.C., Kodach, L.L., Hardwick, J.C., Koopman, F.A., Fiebo, J., van Deventer, S.J., Hommes, D.W., Peppelenbosch, M.P., and Offerhaus, G.J. (2007). Bone morphogenetic protein signaling suppresses tumorigenesis at gastric epithelial transition zones in mice. Cancer research *67*, 8149-8155.

Blot, W.J., Devesa, S.S., Kneller, R.W., and Fraumeni, J.F. (1991). Rising incidence of adenocarcinoma of the esophagus and ngastric cardia. Jama *265*, 1287-1289.

Bonnet, D., and Dick, J.E. (1997). Human acute myeloid leukemia is organized as a hierarchy that originates from a primitive hematopoietic cell. Nature medicine *3*, 730.

Botterweck, A.A., Schouten, L.J., Volovics, A., Dorant, E., and van den Brandt, P.A. (2000). Trends in incidence of adenocarcinoma of the oesophagus and gastric cardia in ten European countries. International journal of epidemiology *29*, 645-654.

Buas, M.F., and Vaughan, T.L. (2013). Epidemiology and risk factors for gastroesophageal junction tumors: understanding the rising incidence of this disease. Seminars in radiation oncology *23*, 3-9.

Cavaleiro-Pinto, M., Peleteiro, B., Lunet, N., and Barros, H. (2011). Helicobacter pylori infection and gastric cardia cancer: systematic review and meta-analysis. Cancer causes & control : CCC *22*, 375-387.

Chandrakesan, P., Yao, J., Qu, D., May, R., Weygant, N., Ge, Y., Ali, N., Sureban, S.M., Gude, M., and Vega, K. (2017). Dclk1, a tumor stem cell marker, regulates pro-survival signaling and self-renewal of intestinal tumor cells. Molecular cancer *16*, 30.

Chen, J., Li, Y., Yu, T.-S., McKay, R.M., Burns, D.K., Kernie, S.G., and Parada, L.F. (2012). A restricted cell population propagates glioblastoma growth after chemotherapy. Nature *488*, 522.

Chen, R., Nishimura, M.C., Bumbaca, S.M., Kharbanda, S., Forrest, W.F., Kasman, I.M., Greve, J.M., Soriano, R.H., Gilmour, L.L., and Rivers, C.S. (2010). A hierarchy of self-renewing tumor-initiating cell types in glioblastoma. Cancer Cell *17*, 362-375.

Cheng, L., Ramesh, A.V., Flesken-Nikitin, A., Choi, J., and Nikitin, A.Y. (2010). Mouse models for cancer stem cell research. Toxicologic pathology *38*, 62-71.

Contino, G., Eldridge, M.D., Secrier, M., Bower, L., Elliott, R.F., Weaver, J., Lynch, A.G., Edwards, P.A., and Fitzgerald, R.C. (2016). Whole-genome sequencing of nine esophageal adenocarcinoma cell lines. F1000Research *5*, 1336.

Driessens, G., Beck, B., Caauwe, A., Simons, B.D., and Blanpain, C. (2012). Defining the mode of tumour growth by clonal analysis. Nature *488*, 527.

Dulak, A.M., Stojanov, P., Peng, S., Lawrence, M.S., Fox, C., Stewart, C., Bandla, S., Imamura, Y., Schumacher, S.E., Shefler, E*., et al.* (2013). Exome and whole-genome sequencing of esophageal adenocarcinoma identifies recurrent driver events and mutational complexity. Nature genetics *45*, 478-486.

Dulak, A.M., Schumacher, S.E., van Lieshout, J., Imamura, Y., Fox, C., Shim, B., Ramos, A.H., Saksena, G., Baca, S.C., Baselga, J*., et al.* (2012). Gastrointestinal adenocarcinomas of the esophagus, stomach, and colon exhibit distinct patterns of genome instability and oncogenesis. Cancer research *72*, 4383-4393.

Eirew, P., Steif, A., Khattra, J., Ha, G., Yap, D., Farahani, H., Gelmon, K., Chia, S., Mar, C., and Wan, A. (2015). Dynamics of genomic clones in breast cancer patient xenografts at single-cell resolution. Nature *518*, 422.

Flesken-Nikitin, A., Choi, K.-C., Eng, J.P., Shmidt, E.N., and Nikitin, A.Y. (2003). Induction of carcinogenesis by concurrent inactivation of p53 and Rb1 in the mouse ovarian surface epithelium. Cancer research *63*, 3459-3463.

Flesken-Nikitin, A., Hwang, C.I., Cheng, C.Y., Michurina, T.V., Enikolopov, G., and Nikitin, A.Y. (2013). Ovarian surface epithelium at the junction area contains a cancer-prone stem cell niche. Nature *495*, 241-245.

Flesken-Nikitin, A., Odai-Afotey, A.A., and Nikitin, A.Y. (2014). Role of the stem cell niche in the pathogenesis of epithelial ovarian cancers. Molecular & cellular oncology *1*, e963435.

Fox, J.G., and Wang, T.C. (2014). Dietary factors modulate Helicobacter-associated gastric cancer in rodent models. Toxicologic pathology *42*, 162-181.

Fu, D.-J., Miller, A.D., Southard, T.L., Flesken-Nikitin, A., Ellenson, L.H., and Nikitin, A.Y. (2018). Stem Cell Pathology. Annual Review of Pathology: Mechanisms of Disease.

Giangreco, A., Groot, K.R., and Janes, S.M. (2007). Lung cancer and lung stem cells: strange bedfellows? American journal of respiratory and critical care medicine *175*, 547-553.

Ginestier, C., Hur, M.H., Charafe-Jauffret, E., Monville, F., Dutcher, J., Brown, M., Jacquemier, J., Viens, P., Kleer, C.G., and Liu, S. (2007). ALDH1 is a marker of normal and malignant human mammary stem cells and a predictor of poor clinical outcome. Cell Stem Cell *1*, 555-567.

Hardie, L.J., Darnton, S.J., Wallis, Y.L., Chauhan, A., Hainaut, P., Wild, C.P., and Casson, A.G. (2005). p16 expression in Barrett's esophagus and esophageal adenocarcinoma: association with genetic and epigenetic alterations. Cancer letters *217*, 221-230.

Hayakawa, Y., Sethi, N., Sepulveda, A.R., Bass, A.J., and Wang, T.C. (2016). Oesophageal adenocarcinoma and gastric cancer: should we mind the gap? Nature reviews Cancer *16*, 305-318.

Held, M.A., Curley, D.P., Dankort, D., McMahon, M., Muthusamy, V., and Bosenberg, M.W. (2010). Characterization of melanoma cells capable of propagating tumors from a single cell. Cancer research *70*, 388-397.

Herfs, M., Yamamoto, Y., Laury, A., Wang, X., Nucci, M.R., McLaughlin-Drubin, M.E., Münger, K., Feldman, S., McKeon, F.D., and Xian, W. (2012). A discrete population of squamocolumnar junction cells implicated in the pathogenesis of cervical cancer. Proceedings of the National Academy of Sciences *109*, 10516-10521.

Isinger-Ekstrand, A., Johansson, J., Ohlsson, M., Francis, P., Staaf, J., Jonsson, M., Borg, A., and Nilbert, M. (2010). Genetic profiles of gastroesophageal cancer: combined analysis using expression array and tiling array--

comparative genomic hybridization. Cancer genetics and cytogenetics *200*, 120-126.

Jaks, V., Barker, N., Kasper, M., Van Es, J.H., Snippert, H.J., Clevers, H., and Toftgård, R. (2008). Lgr5 marks cycling, yet long-lived, hair follicle stem cells. Nature genetics *40*, 1291.

Jemal, A., Bray, F., Center, M.M., Ferlay, J., Ward, E., and Forman, D. (2011). Global cancer statistics. CA: a cancer journal for clinicians *61*, 69-90.

Jiang, M., Li, H., Zhang, Y., Yang, Y., Lu, R., Liu, K., Lin, S., Lan, X., Wang, H., and Wu, H. (2017). Transitional basal cells at the squamous–columnar junction generate Barrett's oesophagus. Nature *550*, 529.

Karimi, P., Islami, F., Anandasabapathy, S., Freedman, N.D., and Kamangar, F. (2014). Gastric cancer: descriptive epidemiology, risk factors, screening, and prevention. Cancer epidemiology, biomarkers & prevention : a publication of the American Association for Cancer Research, cosponsored by the American Society of Preventive Oncology *23*, 700-713.

Kim, M.A., Lee, H.S., Yang, H.K., and Kim, W.H. (2005). Clinicopathologic and protein expression differences between cardia carcinoma and noncardia carcinoma of the stomach. Cancer *103*, 1439-1446.

Ksander, B.R., Kolovou, P.E., Wilson, B.J., Saab, K.R., Guo, Q., Ma, J., McGuire, S.P., Gregory, M.S., Vincent, W.J., Perez, V.L.*, et al.* (2014). ABCB5 is a limbal stem cell gene required for corneal development and repair. Nature *511*, 353-357.

Kusano, C., Gotoda, T., Khor, C.J., Katai, H., Kato, H., Taniguchi, H., and Shimoda, T. (2008). Changing trends in the proportion of adenocarcinoma of the esophagogastric junction in a large tertiary referral center in Japan. Journal of gastroenterology and hepatology *23*, 1662-1665.

Lapidot, T., Sirard, C., Vormoor, J., Murdoch, B., Hoang, T., Caceres-Cortes, J., Minden, M., Paterson, B., Caligiuri, M.A., and Dick, J.E. (1994). A cell initiating human acute myeloid leukaemia after transplantation into SCID mice. Nature *367*, 645.

Leushacke, M., Tan, S.H., Wong, A., Swathi, Y., Hajamohideen, A., Tan, L.T., Goh, J., Wong, E., Denil, S., Murakami, K.*, et al.* (2017). Lgr5-expressing chief cells drive epithelial regeneration and cancer in the oxyntic stomach. Nature cell biology *19*, 774-786.

McKelvie, P.A., Daniell, M., McNab, A., Loughnan, M., and Santamaria, J.D. (2002). Squamous cell carcinoma of the conjunctiva: a series of 26 cases. British Journal of Ophthalmology *86*, 168-173.

McLean, M.H., and El-Omar, E.M. (2014). Genetics of gastric cancer. Nature reviews Gastroenterology & hepatology *11*, 664-674.

McNairn, A.J., and Guasch, G. (2011). Epithelial transition zones: merging microenvironments, niches, and cellular transformation. European journal of dermatology : EJD *21 Suppl 2*, 21-28.

Meuwissen, R., Linn, S.C., Linnoila, R.I., Zevenhoven, J., Mooi, W.J., and Berns, A. (2003). Induction of small cell lung cancer by somatic inactivation of both Trp53 and Rb1 in a conditional mouse model. Cancer Cell *4*, 181-189.

Morath, I., Hartmann, T., and Orian-Rousseau, V. (2016). CD44: More than a mere stem cell marker. The international journal of biochemistry & cell biology *81*, 166-173.

Nakanishi, Y., Seno, H., Fukuoka, A., Ueo, T., Yamaga, Y., Maruno, T., Nakanishi, N., Kanda, K., Komekado, H., and Kawada, M. (2013). Dclk1 distinguishes between tumor and normal stem cells in the intestine. Nature genetics *45*, 98.

Nassar, D., and Blanpain, C. (2016). Cancer stem cells: basic concepts and therapeutic implications. Annual Review of Pathology: Mechanisms of Disease *11*, 47-76.

Naugler, W.E., Sakurai, T., Kim, S., Maeda, S., Kim, K., Elsharkawy, A.M., and Karin, M. (2007). Gender disparity in liver cancer due to sex differences in MyD88-dependent IL-6 production. Science *317*, 121-124.

Network, C.G.A.R. (2014). Comprehensive molecular characterization of gastric adenocarcinoma. Nature *513*, 202-209.

Network, C.G.A.R. (2017). Integrated genomic characterization of oesophageal carcinoma. Nature *541*, 169-175.

Ng, A., Tan, S., Singh, G., Rizk, P., Swathi, Y., Tan, T.Z., Huang, R.Y., Leushacke, M., and Barker, N. (2014). Lgr5 marks stem/progenitor cells in ovary and tubal epithelia. Nature cell biology *16*, 745-757.

Nikitin, A., and Lee, W.-H. (1996). Early loss of the retinoblastoma gene is associated with impaired growth inhibitory innervation during melanotroph carcinogenesis in Rb+/-mice. Genes & development *10*, 1870-1879.

O'Neil, A., Petersen, C.P., Choi, E., Engevik, A.C., and Goldenring, J.R. (2017). Unique cellular lineage composition of the first gland of the mouse gastric corpus. Journal of Histochemistry & Cytochemistry *65*, 47-58.

Plaks, V., Kong, N., and Werb, Z. (2015). The cancer stem cell niche: how essential is the niche in regulating stemness of tumor cells? Cell stem cell *16*, 225-238.

Quante, M., Bhagat, G., Abrams, J.A., Marache, F., Good, P., Lee, M.D., Lee, Y., Friedman, R., Asfaha, S., Dubeykovskaya, Z*., et al.* (2012). Bile acid and inflammation activate gastric cardia stem cells in a mouse model of Barrett-like metaplasia. Cancer cell *21*, 36-51.

Rayess, H., Wang, M.B., and Srivatsan, E.S. (2012). Cellular senescence and tumor suppressor gene p16. International journal of cancer *130*, 1715-1725.

Ricci-Vitiani, L., Lombardi, D.G., Pilozzi, E., Biffoni, M., Todaro, M., Peschle, C., and De Maria, R. (2007). Identification and expansion of human colon-cancer-initiating cells. Nature *445*, 111.

Ross-Innes, C.S., Becq, J., Warren, A., Cheetham, R.K., Northen, H., O'Donovan, M., Malhotra, S., di Pietro, M., Ivakhno, S., He, M*., et al.* (2015). Whole-genome sequencing provides new insights into the clonal architecture of Barrett's esophagus and esophageal adenocarcinoma. Nature genetics *47*, 1038-1046.

Runck, L.A., Kramer, M., Ciraolo, G., Lewis, A.G., and Guasch, G. (2010). Identification of epithelial label-retaining cells at the transition between the anal canal and the rectum in mice. Cell Cycle *9*, 3039-3045.

Schepers, A.G., Snippert, H.J., Stange, D.E., van den Born, M., van Es, J.H., van de Wetering, M., and Clevers, H. (2012). Lineage tracing reveals Lgr5+ stem cell activity in mouse intestinal adenomas. Science *337*, 730-735.

Schmoeckel, E., Odai-Afotey, A.A., Schleißheimer, M., Rottmann, M., Flesken-Nikitin, A., Ellenson, L.H., Kirchner, T., Mayr, D., and Nikitin, A.Y. (2017). LEF1 is preferentially expressed in the tubal-peritoneal junctions and is a reliable marker of tubal intraepithelial lesions. Nature Publishing Group *30*, 1241-1250.

Serra, S., and Chetty, R. (2006). Tumours of the anal canal. Current Diagnostic Pathology *12*, 136-151.

Sherr, C.J., and McCormick, F. (2002). The RB and p53 pathways in cancer. Cancer Cell *2*, 103-112.

Snippert, H.J., and Clevers, H. (2011). Tracking adult stem cells. EMBO reports *12*, 113-122.

Sons, H., and Borchard, F. (1986). Cancer of the distal esophagus and cardia. Incidence, tumorous infiltration, and metastatic spread. Annals of surgery *203*, 188.

Stachler, M.D., Taylor-Weiner, A., Peng, S., McKenna, A., Agoston, A.T., Odze, R.D., Davison, J.M., Nason, K.S., Loda, M., and Leshchiner, I. (2015). Paired exome analysis of Barrett's esophagus and adenocarcinoma. Nature genetics *47*, 1047.

Visvader, J.E. (2011). Cells of origin in cancer. Nature *469*, 314-322.

Vorhagen, S., Jackow, J., Mohor, S.G., Tanghe, G., Tanrikulu, L., Skazik-Vogt, C., and Tellkamp, F. (2015). Lineage tracing mediated by cre-recombinase activity. The Journal of investigative dermatology *135*, e28.

Wang, T., Yeoh, K.G., and Salto-Tellez, M. (2012). Lgr5 expression is absent in human premalignant lesions of the stomach. Gut *61*, 1777.

Wang, X., Ouyang, H., Yamamoto, Y., Kumar, P.A., Wei, T.S., Dagher, R., Vincent, M., Lu, X., Bellizzi, A.M., Ho, K.Y.*, et al.* (2011). Residual embryonic cells as precursors of a Barrett's-like metaplasia. Cell *145*, 1023-1035.

Wei, D., Wang, L., Yan, Y., Jia, Z., Gagea, M., Li, Z., Zuo, X., Kong, X., Huang, S., and Xie, K. (2016). KLF4 is essential for induction of cellular identity change and acinar-to-ductal reprogramming during early pancreatic carcinogenesis. Cancer Cell *29*, 324-338.

White, A.C., and Lowry, W.E. (2015). Refining the role for adult stem cells as cancer cells of origin. Trends in cell biology *25*, 11-20.

White, A.C., Tran, K., Khuu, J., Dang, C., Cui, Y., Binder, S.W., and Lowry, W.E. (2011). Defining the origins of Ras/p53-mediated squamous cell carcinoma. Proceedings of the National Academy of Sciences of the United States of America *108*, 7425-7430.

Wong, D.J., Paulson, T.G., Prevo, L.J., Galipeau, P.C., Longton, G., Blount, P.L., and Reid, B.J. (2001). p16INK4a lesions are common, early abnormalities that undergo clonal expansion in Barrett's metaplastic epithelium. Cancer research *61*, 8284-8289.

Yan, Y., Zuo, X., and Wei, D. (2015). Concise review: emerging role of CD44 in cancer stem cells: a promising biomarker and therapeutic target. Stem cells translational medicine *4*, 1033-1043.

Yu, F., Li, J., Chen, H., Fu, J., Ray, S., Huang, S., Zheng, H., and Ai, W. (2011). Kruppel-like factor 4 (KLF4) is required for maintenance of breast cancer stem cells and for cell migration and invasion. Oncogene *30*, 2161.

Zhou, Z., Flesken-Nikitin, A., and Nikitin, A.Y. (2007). Prostate cancer associated with p53 and Rb deficiency arises from the stem/progenitor cell–enriched proximal region of prostatic ducts. Cancer research *67*, 5683-5690.

CHAPTER 3

IDENTIFYING THE CELL-OF-ORIGIN OF GASTRIC SQUAMOUS-COLUMNAR JUNCTION CANCER*

3.1 Abstract

The junction area between the esophagus and stomach (AKA squamous-columnar junction; SCJ) is known to be predisposed to precancerous metaplasia and cancer. However, the cells of SCJ cancer origin remain insufficiently established. Previously we reported that cells in the first pit of gastric glandular epithelium, which locates at the SCJ area of the stomach, are highly susceptible to malignant transformation following conditional inactivation of *Tpr53* and *Rb1* in the $Lgr5^+$ stem cells. Here we describe a distinct population of $Lgr5^-CD44^+$ cells originating from and residing above the $Lgr5^+$ stem cells in the first gland of SCJ region. These $Lgr5^-CD44^+$ cells are highly proliferative and lack gastric differentiation markers. Of note, the $Lgr5^-CD44^+$ cells show a higher potential to malignant transformation compared to other populations in the first gland. In addition, inactivation of *Cd44* gene using the CRISPR/Cas9 approach attenuates the gastric epithelium regeneration as wells as the malignant transformation induced by *Trp53* and *Rb1* knockout. Our findings reveal a previously uncharacterized subpopulation of immature $Lgr5^-CD44^+$ cells in the first gland of SCJ region and provide evidence that these cells serve as the

cellular origin of the SCJ cancer. They also point to the important role of CD44 signaling in gastric carcinogenesis and suggest that targeting of CD44 signaling may have clinical relevance for preventing SCJ cancer initiation and progression.

*In part submitted as Fu, D.-J., Wang, L., Chouairi, F.K., Rose, I.M., Miller, A.D., Yamulla, R.J., Schimenti, J.C., Flesken-Nikitin, A., Nikitin, A.Y., Osteopontin-CD44 signaling keeps progeny of Lgr5^{+} cells in immature cancer-prone state at the gastric squamous-columnar junction (2018).

Author contributions: Dah-Jiun Fu and Alexander Yu. Nikitin designed the study, interpreted data and wrote the manuscript. Dah-Jiun Fu and Fouad Chouairi performed experiments and analyzed data. Robert J. Yamulla and John C. Schimenti contributed new reagents and technology. Alexander Yu. Nikitin supervised the project.

3.2 Introduction

The “cell-of-origin” of cancer is defined as the first normal cell that acquires the full-set of oncogenic mutations and is subject to malignant transformation at the beginning of tumorigenesis (Visvader, 2011). Identification of these crucial target cell populations has been seen as a critical step for exploring the mechanism underlying cancer initiation and progression (Blanpain, 2013). A better understanding of why some cells are more susceptible to malignant transformation following oncogenic events, whereas some cells are relatively resistant is crucial for the development of more effective diagnostic, preventive, and therapeutic approaches (Rycaj and Tang, 2015).

As discussed in Chapters 1 and 2, the cellular origin of the cancer arising from the junction area between esophagus and stomach (aka squamous-columnar junction; SCJ) has been debated over several decades. The proposed cell types include the squamous epithelial cells of the esophagus, which can transdifferentiate into intestinal-like columnar premalignant cells by the activation of bone morphogenetic protein 4 (BMP-4) signaling pathway (Milano et al., 2007; Yu et al., 2005) and overexpression of transcription factor CDX2 (Kong et al., 2011), the metaplastic esophageal gland, which show similar oncogenic mutations with premalignant lesion (Leedham et al., 2008), the circulating bone marrow progenitor cells, which migrate to the SCJ area following gastroesophageal reflux (Sarosi et al., 2008), the cardiac glandular epithelial cell, which give rise to Barrett’s-like metaplastic lesion upon the

bile acid- and cytokine-induced inflammation (Quante et al., 2012). Unfortunately, these experimental models merely recapitulate the precancerous lesion at the SCJ region, while none of them undergo further progression to advanced malignancy. As discussed in Chapter 2, we have established a new genetically modified mouse model, which features metastatic SCJ carcinomas resembling human gastroesophageal cancer. These carcinomas develop from the cells in the first gland laying at the gastric SCJ after conditional inactivation of tumor suppressor genes *Trp53* and *Rb1* in the $Lgr5^{+}$ stem cells.

Here, we further investigated the cellular components in the first gland and identified a subpopulation of actively proliferating immature $Lgr5^{-}CD44^{+}$ cells deriving from and located above the $Lgr5^{+}$ stem cell niches in the first gland. By sequential analysis of SCJ carcinogenesis and *ex vivo* organoid culture approach, we show that these $Lgr5^{-}CD44^{+}$ cells represent the most likely cell of SCJ carcinoma origin.

3.3 Materials and Methods

Experimental animals. The *Lgr5*$^{tm1(cre/ERT2)Cle}$*/J* (*Lgr5*$^{eGFP\text{-}Ires\text{-}CreERT2}$) knock in mice were crossbred with *Gt(ROSA)26Sor*$^{tm9(CAG\text{-}tdTomato)Hze}$ (*Rosa-loxp-stop-loxp-*tdTomato/Ai9) mice as well as the mice with floxed copies of *Trp53* and *Rb1* (*Trp53*$^{loxP/loxP}$*Rb1*$^{loxP/loxP}$) as described in the Material and Methods in Chapter 2. NOD.Cg-*Prkdc*^{scid} *Il2rg*^{tm1wjl}/SzJ (NSG) mice (Stock number 005557 were purchased from The Jackson Laboratory (Bar Harbor, ME, USA). The *Lgr5-DTR* mice were a generous gift from Dr. Frederic J. de Sauvage (Tian et al., 2011). All experiments involving animals were carried out under the approval of the Institutional Laboratory Animal Use and Care Committee of Cornell University.

Immunostaining and analysis. All tissues were fixed, processed, and, sectioned as described in the Materials and Methods in Chapter 2. For peroxidase-based immunohistochemistry, antigen retrieval was carried out with incubation of rehydrated tissue sections in boiling 10 mM sodium citrate buffer (pH 6.0) for 10 minutes. The sections were then incubated with the primary antibodies against GFP (NOVUS biological, Littleton, CO, USA; NB600-303), CD44 (Santa Cruz Biotechnologies, Dallas, TX, USA; sc-18849), Mucin5AC (Abcam, Cambridge, UK; ab3649), H^+K^+-ATPase (MBL international corp., Woburn, MA, USA; D032-3H), chromogranin A (Santa Cruz, sc-1488), pepsinogen C (Abbexa, Cambridge, UK; abx002093), and RFP (Rockland Immunochemical Inc, Pottstown, PA, USA; 600-401-379S) at room

temperature (RT) for 1 hour. Subsequently, the sections were incubated with biotinylated secondary antibodies for 30 minutes at RT followed by incubation with Modified Elite avidin-biotin peroxidase (ABC) (Vector Laboratories, Burlingame, CA, USA; pk-6100) for another 30 minutes at RT. Diaminobenzidine (DAB; Sigma-Aldrich, St. Louis, MO, USA; D4418-50SET) was used as the chromogen, and the sections were counterstained with Mayer's hematoxylin. All antibody conditions used for immunostaining are listed in Table 3.1. For bright field tissue section imaging, all slides were mounted by Canada Balsam medium (Polysciences Inc., Warrington, PA), and scanned by ScanScope CS2 (Leica Biosystems, Vista, CA, USA) with 40X objective lens. All images were then analyzed using HALO Image Analysis Software (PerkinElmer Inc., Shelton, CT, USA) or Aperio ImageScope Software (Leica).

For immunofluorescence staining, antigen retrieval was carried out as described above followed by incubation with primary antibodies against GFP (Novus biological; NB600-303), CD44 (Santa Cruz Biotechnologies; sc-18849) at RT for 30 minutes. Subsequently, the sections were incubated with Fluorescent protein-conjugated secondary antibodies for 1 hour at RT followed by nuclear counterstaining with DAPI. All sections were mounted by Fluoro-Gel (Electron Microscopy Sciences, Hatfield, PA, USA; 17985-10) and scanned with Aperio ScanScope FL (Leica). All image stacks were merged and analyzed with ImageJ software (National Institutes of Health, Bethesda, MD, USA).

Table 3.1 List of antibodies used for immunohistochemistry and immunofluorescence staining

Antigen	Antibody source, catalogue number	Clone	Dilution	Detection system
GFP	Novus biological, NB600-303	PC*	1:8000	Vectastain Elite ABC-HRP Kit
CD44	Santa Cruz, sc-18849	IM7	1:1000	Vectastain Elite ABC-HRP Kit
Mucin5AC	Abcam, ab3649	45M1	1:500	Vectastain Elite ABC-HRP Kit
H^+K^+-ATPase	MBL international corp., D032-3H	2B6	1:500	Vectastain Elite ABC-HRP Kit
Chromogranin A	Santa Cruz, sc-1488	PC*	1:2000	Vectastain Elite ABC-HRP Kit
Pepsinogen C	Abbexa, abx002093	PC*	1:400	Vectastain Elite ABC-HRP Kit
RFP	Rockland Immunochemicals Inc., 600-401-379S	PC*	1:400	Vectastain Elite ABC-HRP Kit
BrdU	Abcam, ab2284	PC*	1:100	Immunofluorescence
GFP	Novus biological, NB600-303	PC*	1:1000	Immunofluorescence
CD44	Santa Cruz, sc-18849	IM7	1:100	Immunofluorescence

PC*: Polyclonal.

BrdU incorporation assay. A single dose (20 µl/g body weight) of BrdU (2.5 mg/ml, Sigma; B5002) was administered to mice by intraperitoneal injection. Mice were euthanized using CO_2 two hours after BrdU injection, and the tissues were collected and fixed with 4% paraformaldehyde overnight at 4°C, followed by standard tissue processing. Deparaffinized 4 µm tissue sections were exposed to 10-minute boiling in 10 mM citrate buffer followed by incubation with 4N hydrogen chloride (HCl, RT, 10 minutes). The anti-BrdU primary antibody (Abcam, Cambridge, UK; ab2284) was incubated at RT for 1 hour, followed by incubation with Alexa 594-conjugated secondary antibody (Invitrogen, Carlsbad, CA, USA; A11016) for 30 minutes at RT. DAPI (Sigma; 32670-5MG-F) was used for nuclear counterstaining.

Isolation of primary gastric epithelial cells. Individual stomachs were isolated from 6-10 week-old *Lgr5*$^{eGFP\text{-}Ires\text{-}CreERT2}$*Trp53*$^{loxp/loxp}$*Rb1*$^{loxp/loxp}$, *Trp53*$^{loxp/loxp}$*Rb1*$^{loxp/loxp}$Ai9 or *Lgr5-DTR* mice, washed with ice-cold PBS buffer several times, dissected into small pieces (<2 mm in length), and incubated in gentle dissociation buffer (Stem Cell Technologies, Vancouver, Canada; 07174) at RT for 15 minutes. After removal of the dissociation buffer, the tissue fragments were vigorously pipetted for 10-20 times with ice-cold 0.1% BSA/PBS solution using 10 ml pipette, and transferred to 50 ml conical tubes. The gastric epithelial cells were collected and counted after centrifugation followed by re-suspension in DMEM F12 50/50 medium (Corning Inc., Corning, NY, USA; 10-092-CV).

Gastric organoid culture. The primary gastric organoid culture was modified from previously described method (Cheng et al., 2014). Briefly, 10^4 primary murine gastric epithelial cells were suspended in 0.1 ml of DMEM F12 50/50 medium, mixed 1:1 with liquid growth factor-reduced Matrigel (Corning, 354230), and plated around the rim of the well of a 24-well tissue culture plate. Matrigel was allowed to solidify in the 37°C incubator for 20 minutes, and overlaid by stem cell culture medium (IntestiCult^{TM} Organoid Growth Medium [Stemcell Technologies; 6005] supplemented with 10 nM gastrin [Sigma; G9020]) and penicillin/streptomycin (Corning; 30-002-CI) for the first 3 days. Each well was washed with PBS twice followed by addition of differentiation medium (Advanced DMEM/F12 50/50 medium supplemented with 1 µg/ml R-spondin1 [PeproTech Inc., Rocky Hill, NJ, USA; 120-38] and 50 ng/ml EGF [PeproTech, 315-09]) during subsequent 4 days. For culturing $Lgr5^+$ organoids, small molecules CHIR99021 (2 µM, Stemcell Technologies, 72052) and valproic acid (2 mM, Stemcell Technologies, 72292) were added to stem cell culture medium. For culturing $Lgr5^-CD44^+$ organoids, diphtheria toxin (2 ng/mL, Sigma, D0564) was added to stem cell culture medium to abolish the $Lgr5^+$ cells. For culture of $Lgr5^-$ $CD44^-$ organoids, diphtheria toxin (2 ng/mL, Sigma; D0564) was also added to differentiation medium as described above.

For passaging, 1 ml of Accumax cell dissociation solution (Innovative Cell Technologies, San Diego, CA, USA; AM105-500), was added to each well followed by incubation at 37°C for 10 minutes. The organoids were separated into single cells

upon vigorous pipetting, and transferred into 15 ml conical tube. After double washing with 10 ml DMEM/F12 50/50 medium, the cells were counted and cultured as described above. In experiments with adenovirus-mediated Cre (Ad-*Cre*) recombination, organoids were treated with Cre-expressing adenovirus ($2X10^7$ pfu in stem cell culture medium) at 37°C for 2 hours on the second day of culture. Blank adenovirus was used as control under same conditions. In the lentiviral CRISPR/Cas9-mediated experiments, the recombinant lentivirus was added to the stem cell culture medium during the first 3 days after plating.

Whole mount analysis of organoid. The whole mount staining and imaging of organoids was carried out following previously described procedures (Mahe et al., 2013). Briefly, the organoids were embedded in Matrigel and cultured in 8-well Chambered Coverglass (Thermo Fisher Scientific; 155411) at 37°C. After few days, the Matrigel-embedded organoids were fixed with 4% paraformaldehyde at RT for 30 minutes, and then incubated with ammonium chloride (NH_4Cl, 50 mM in PBS) for 30 minutes, followed by incubation with Triton-X100 (0.1% in PBS) for 30 minutes, 5% BSA in PBS for 1 hours and primary antibodies such as GFP (Novus Biologicals; NB600-303) and CD44 (Santa Cruz Biotechnologies; sc-18849) for 1 hours. After wash with PBS 5 times, the incubation with fluorescence-conjugated secondary antibodies and nuclear counterstaining with DAPI were performed. The whole mount images were taken using Leica TCS SP5 confocal laser-scanning microscope (Leica) and all image stacks were then merged and analyzed with ImageJ software (National

Institutes of Health, Bethesda, MD, USA).

Organoid preparation for paraffin embedding. The Matrigel-embedded organoids were incubated with 1 ml of gentle dissociation buffer (Stemcell Technologies; 07174) at RT for 10 minutes, and gently collected into 15 mL conical tube. Subsequently, the suspended organoids were incubated with 4% paraformaldehyde at 4°C for 1 hour, and followed by centrifugation at 300g for 5 minutes at 4°C. After double wash with PBS, the organoids were re-suspended with 65°C HistoGel (Thermo Fischer Scientific; HG-4000-012) in Falcon™ Round-Bottom Polystyrene Tubes (Fisher scientific; 14-959-6), and followed by centrifugation at 3000 rpm at RT for 10 minutes. Solidified HistoGel samples were collected and processed for paraffin embedding using standard procedures.

Transplantation. The organoids were collected by centrifugation at 300 g for 5 minutes, resuspended with 50% of complete culture medium and 50% of high concentration Matrigel (Corning; 354263) in total volume of 100 µl, and subcutaneously injected (1,500 organoids) in the flanks of NSG mice.

Construction of CRISPR plasmids. The lentiCRISPR v2 was obtained from Addgene (Cambridge, MA, US; 52961). The *Cd44*-sgRNA (CRISPR-*Cd44*) sequences

(CTGGAGAACGTGGGCGCACG) were designed using web tools Optimized CRISPR Design (http://crispr.mit.edu) and CHOPCHOP (https://chopchop.rc.fas.harvard.edu). Insertion of sgRNA was performed as previous described (Sanjana et al., 2014). Briefly, the lentiCRISPR v2 plasmid was digested by FastDigest *BsmBI* (Thermo Fischer Scientific; FD0454). The sgRNA dimers were phosphorylated by T4 polynucleotide Kinase (NEB) and ligated into plasmid using Rapid DNA Ligation Kit (Thermo Fischer Scientific; K1423s). For CRISPR-Trp53 and CRISPR-Rb1 experiments three sets of *Trp53*-sgRNAs (CRISPR-*Trp53a:* AGTGAAGCCCTCCGAGTGTC, CRISPR-*Trp53b:* GAAGTCACAGCACATGACGG, CRISPR-*Trp53c:* AAATTTGTATCCCGAGTATC) and three sets of *Rb1*-sgRNAs (CRISPR-*Rb1a:* TGTAGCTCAGTAAAAGTGAA, CRISPR-*Rb1b:* TTGGGAGAAAGTTTCATCCG, CRISPR-*Rb1c:* AGAAATCGATACCAGTACCA) were separately inserted into the lentiCRISPR v2 plasmid following manufacture's recommendation.

Statistical analyses. Statistical comparisons were carried out using a two-tailed unpaired *t* test with InStat 3 and Prism 6 software (GraphPad Software Inc., La Jolla, CA, USA). Significance was determined as $P<0.05$.

3.4 Results

3.4.1 The first pit of gastric glandular epithelium contains larger fraction of highly proliferating immature cells as compared to antral glands

The squamous-columnar junction (SCJ) of the stomach is an anatomic structure where the squamous epithelium transit into the glandular epithelium. The first pit of glandular epithelium at the gastric SCJ area has characteristics that are distinct from those of the glandular units in the corpus and antral (O'Neil et al., 2017; Wang et al., 2011). By *in vivo* lineage tracing, we (Chapter 2) and others (Barker 2010) have shown that $Lgr5^+$ cells are located at the base of both in the first pit of SCJ and in the glands in antrum. These cells represent the active stem cell population responsible for the maintenance of the epithelial homeostasis at these regions (Fu et al., 2018). The antrum contains far more of $Lgr5^+$ stem cells than SCJ. However, SCJ $Lgr5^+$ stem cells are far more susceptible to malignant transformation initiated by conditional inactivation of *Trp53* and *Rb1* than antral $Lgr5^+$ stem cells, (Chapter 2). To investigate if this difference in cancer susceptibility can be explained by variations in cellular compositions of the first pit of SCJ and antral glands, we employed serial immunohistochemistry stainings of markers for stem/progenitor and committed differentiated cell types on the mouse gastric epithelium, such as Lgr5-eGFP for stem cells, CD44 for stem/progenitor cells, Mucin5AC for pit cells, H^+K^+-ATPase for parietal cells, chromogranin A for neuroendocrine cells and pepsinogen C for chief

cells (Figure 3.1A). The first gland of SCJ revealed remarkably larger fraction of cells expressing the stem/progenitor marker CD44, compared to antral glands (49.6 ± 2.4% vs 23.3 ± 2.4% of cells per single gland, respectively) (Figure 3.1B). Notably, a large fraction of first pit $CD44^+$ cells (35.2 ± 2.3%) did not express Lgr5 and were distributed from the bottom to middle length of the first pit (Figure 3.2). $Lgr5^-$ $CD44^+$ SCJ cells were actively proliferating (Figure 3.3) and remained immature according to the lack of differentiation markers typical for pit, parietal cells and chief cells (Figure 3.1). On the contrary, all antral $CD44^+$ cells were located at the base of the pit, contained smaller fraction of $Lgr5^-CD44^+$ population (8.75 ± 1.1%) of cells per single gland (Figure 3.2) and showed limited proliferative activity (Figure 3.3). According to lineage tracing analysis all $Lgr5^-CD44^+$ cells derived from $Lgr5^+$ cells (Figure 3.4). Taken together, we identified a uniquely large fraction of immature $Lgr5^-$ $CD44^+$population in the first pit of gastric SCJ (Figure 3.5),

3.4.2 CD44 expression is associated with the capacities to gastric epithelial regeneration and malignant transformation

CD44 is a well-known marker of stem/progenitor cells and cancer-propagating cells

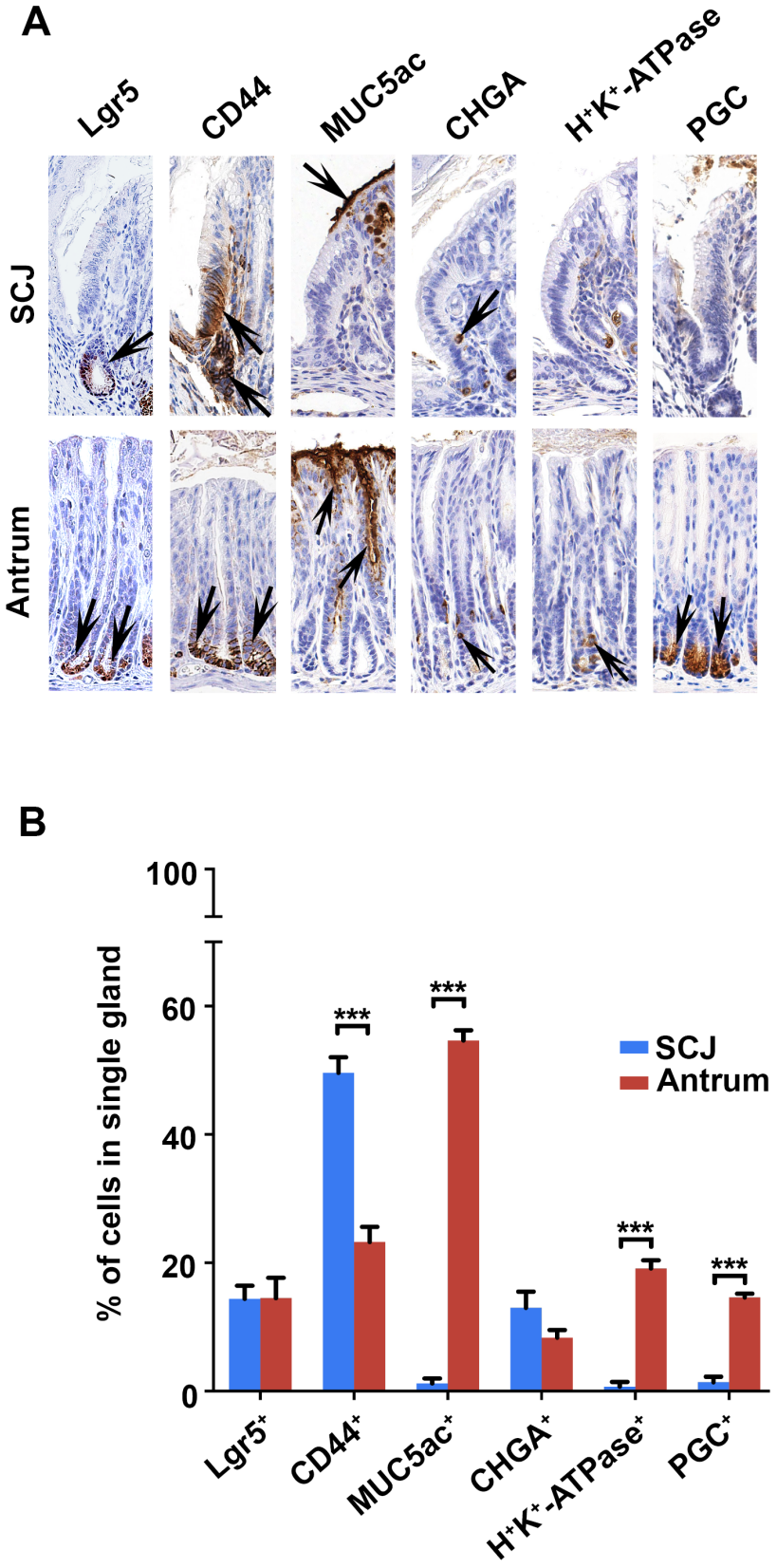
A
Lgr5
CD44
MUC5ac
CHGA
H+K+-ATPase
PGC
SCJ
Antrum
B
% of cells in single gland
100
60
40
20
0
***
***
***
***
SCJ
Antrum
Lgr5+
CD44+
MUC5ac+
CHGA+
H+K+-ATPase+
PGC+

Figure 3.1 Comparison of cellular components between the gastric SCJ and antrum in adult mice. (A and B) Detection (A, brown color, arrows) and quantification (B) of cells expressing Lgr5 (Lgr5-eGFP), CD44 and differentiation markers of pit cells (Mucin5AC), neuroendocrine cells (chromogranin A, CHGA), parietal cells (H^+K^+-ATPase) and chief cells (pepsinogen C. PGC). All images, counterstaining with hematoxylin. *P<0.05. **P<0.01. ***P<0.001.

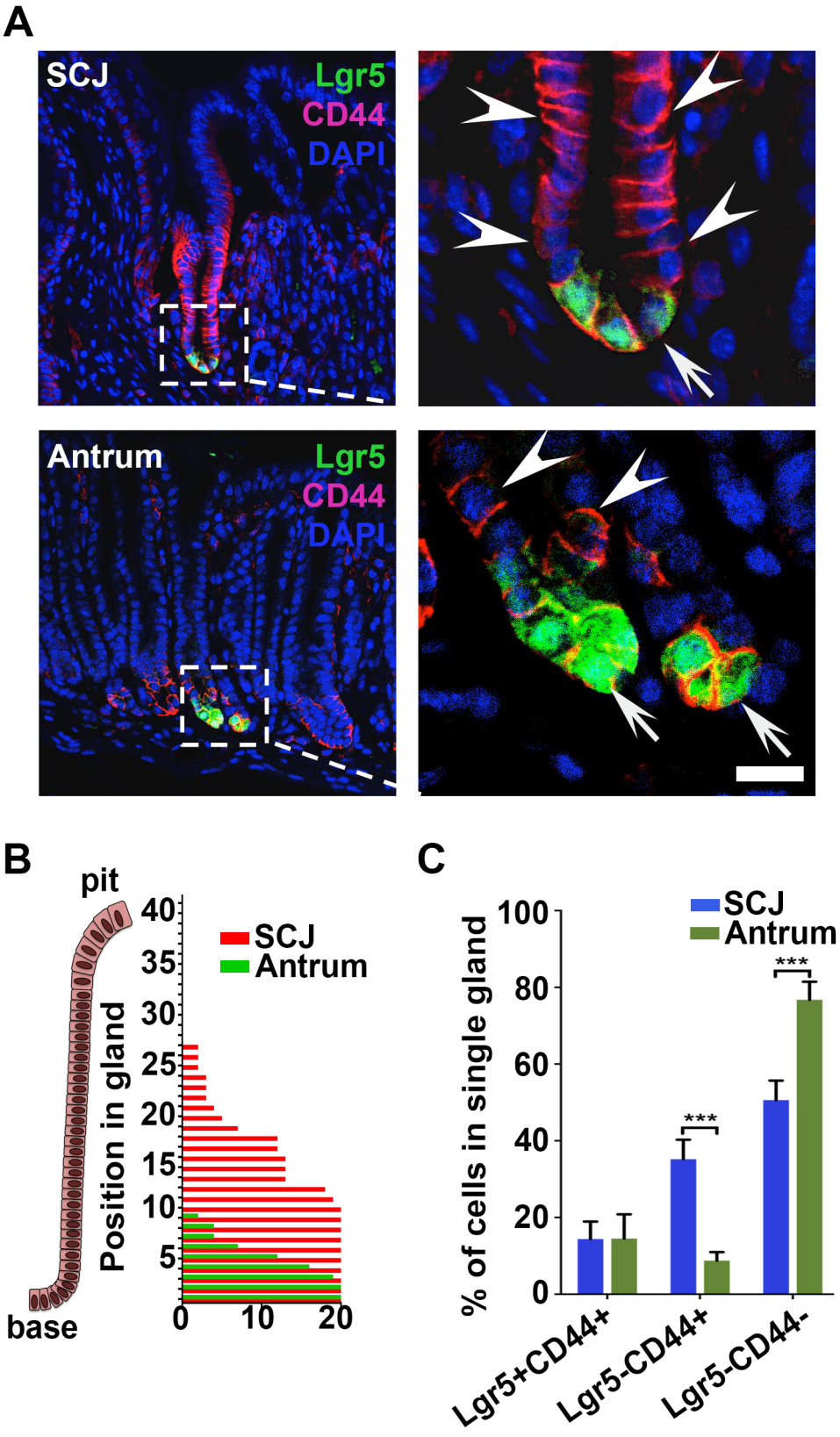
A
SCJ
Lgr5
CD44
DAPI
Antrum
Lgr5
CD44
DAPI
B
pit
base
Position in gland
40
35
30
25
20
15
10
5
0
10
20
SCJ
Antrum
C
% of cells in single gland
100
80
60
40
20
0
SCJ
Antrum
***
***
Lgr5+CD44+
Lgr5-CD44+
Lgr5-CD44-

Figure 3.2 Detection of CD44 and Lgr5 expression in the SCJ and antrum of adult mice. (A) Immunostaining of Lgr5-eGFP and CD44 in the SCJ and antral epithelium of adult mice (B) Number of $CD44^+$ cells located at specific positions in the glands of the SCJ and antrum. (C) Quantitative analysis of $Lgr5^+CD44^+$, $Lgr5^-CD44^+$, $Lgr5^-CD44^-$ cells at the SCJ and antrum. Counterstaining with DAPI (A). Scale bar represents 50 μm (left panels of A), 15 μm (upper right panel in A), 10 μm (lower right panel of A). *P<0.05. **P<0.01. ***P<0.001.

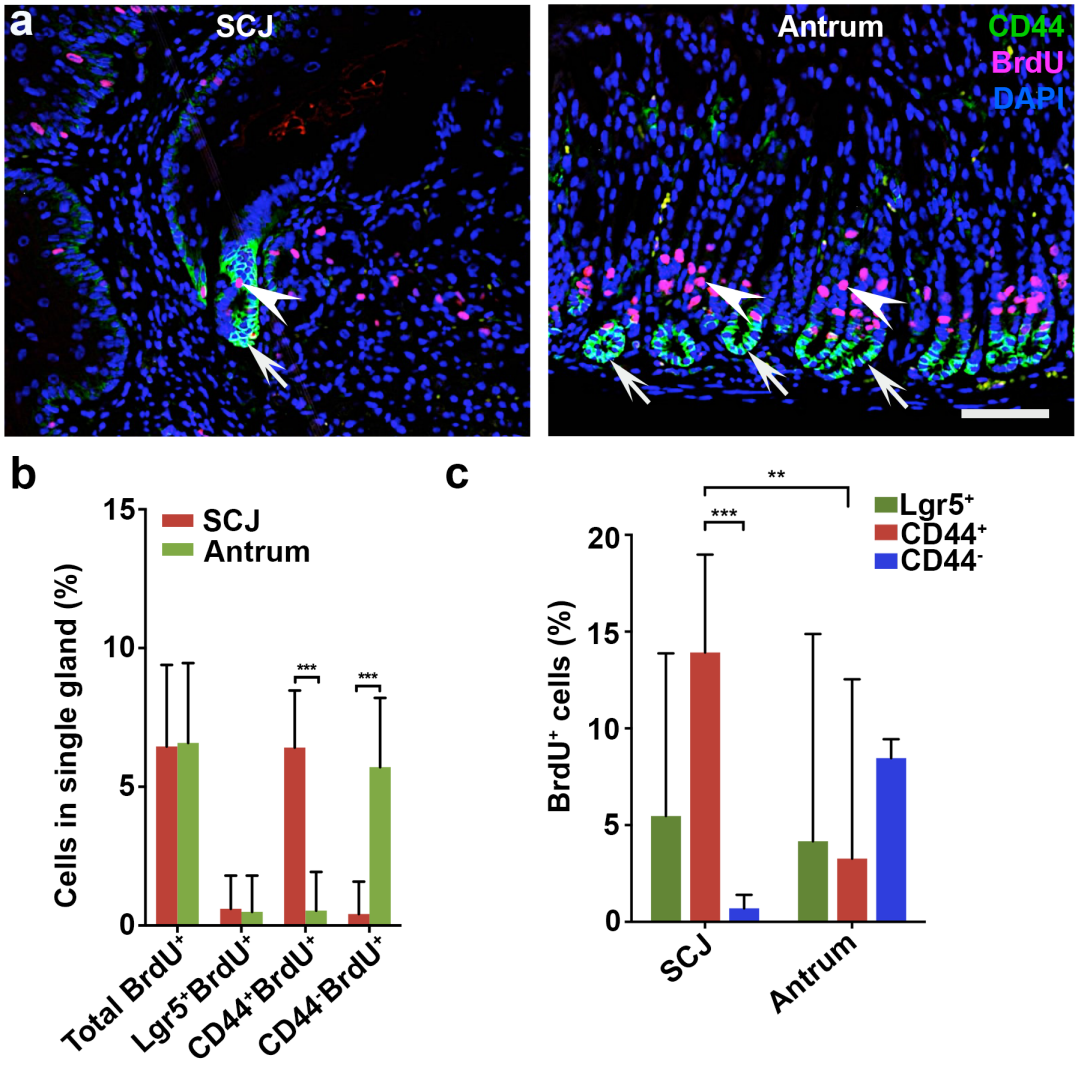

Figure 3.3 Cell proliferation in the SCJ and antrum of adult wild-type mice. (A) Detection of cells expressing CD44 (green) and incorporating BrdU (red) in the SCJ (top) and antrum (bottom). (B) Quantification of $Lgr5^+$ and $CD44^+$ cells incorporating BrdU. (C) Percentage of $BrdU^+$ cells in $Lgr5^+$, $CD44^+$, and $CD44^-$ fractions (n=8 in each group).

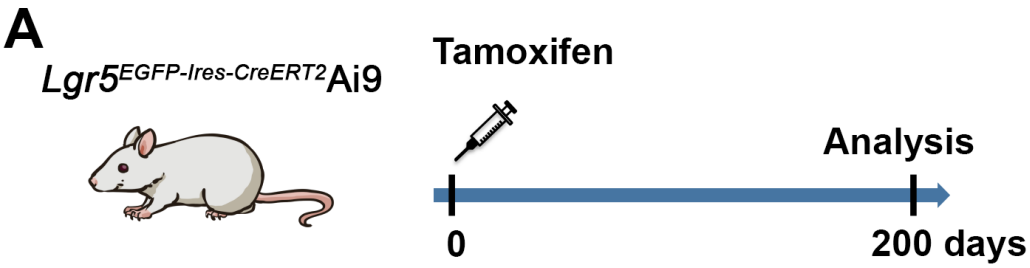
A
Lgr5EGFP-Ires-CreERT2Ai9
Tamoxifen
Analysis
0
200 days

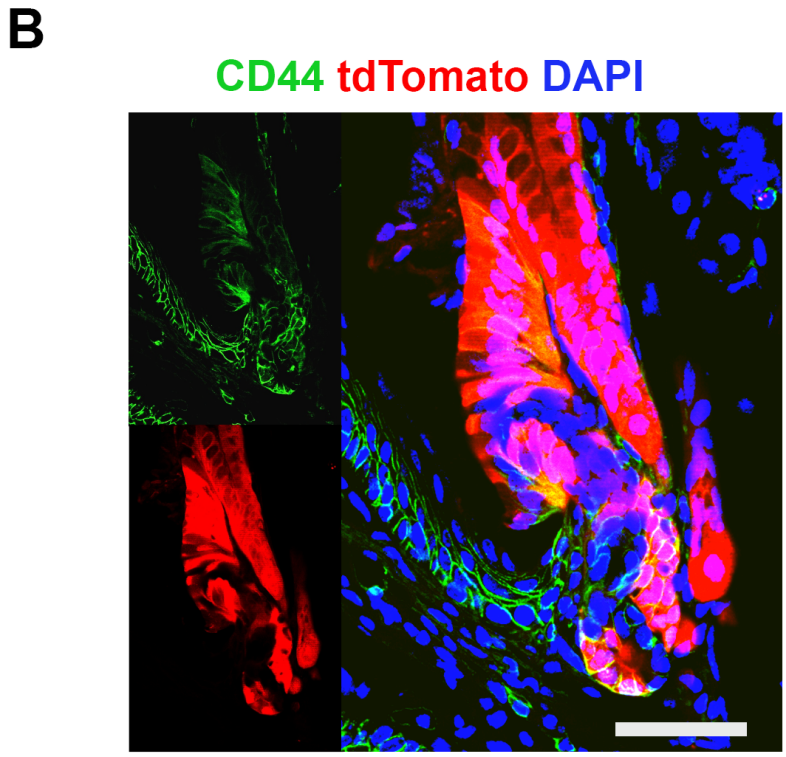
B
CD44 tdTomato DAPI

Figure 3.4 Lineage tracing of Lgr5^{+} cells using *Lgr5*$^{eGFP\text{-}Ires\text{-}CreERT2}$Ai9 mice. (A) Design of experiment. (B) Detection of CD44 expression in Lgr5^{+} cell progeny in the first gland of the SCJ. Counterstaining with DAPI in (B). Scale bars represent 50 μm (left panels of B) and 25 μm (right panel of B). *P<0.05. **P<0.01. ***P<0.001.

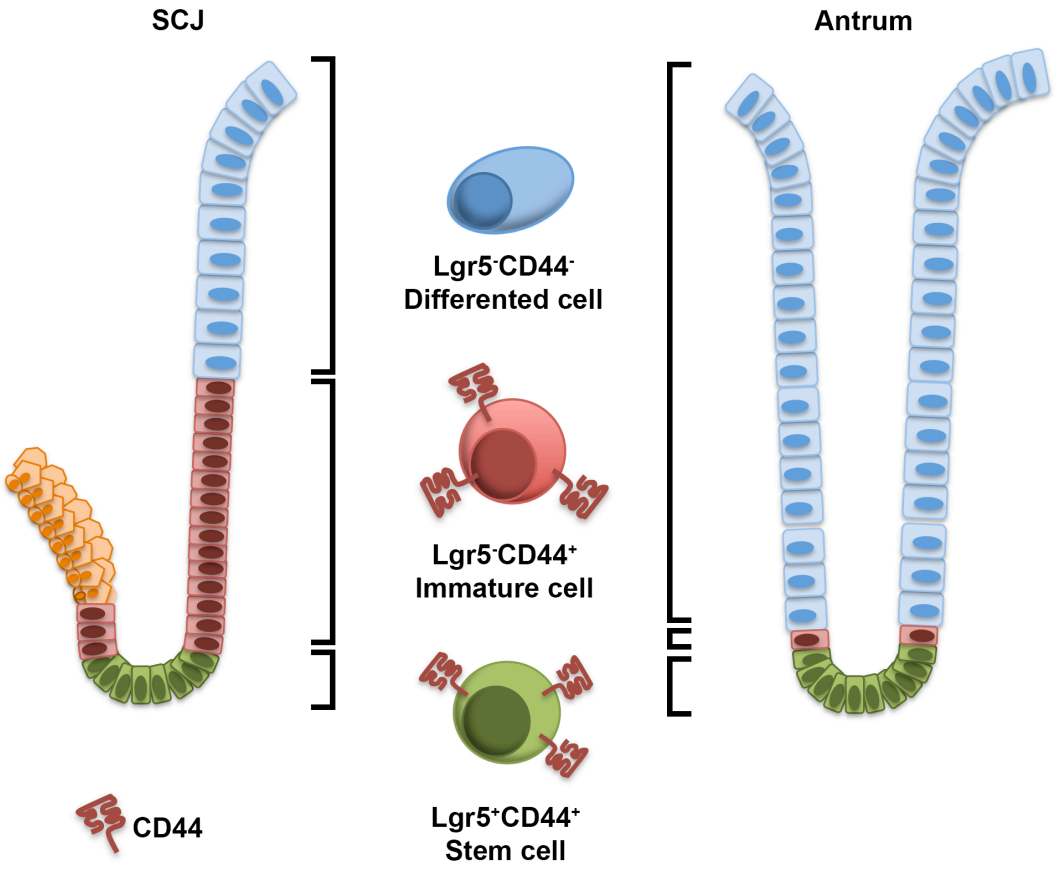

Figure 3.5 Proposed model to illustrate differences in cell composition between the gastric SCJ and antrum of adult mice. The first gland of SCJ contain larger fraction of immature cells that express CD44 but not Lgr5.

that contribute to the maintenance of stemness and regulation of cell proliferation and differentiation in these cell types (Morath et al., 2016). To test the functional role of CD44 in the regeneration and malignant transformation of the stomach epithelium, we silenced *Cd44* gene expression using Clustered Regularly Interspaced Palindromic Repeats (CRISPR)/Cas9-mediated genome editing, which targeted the promoter of *Cd44* gene in the primary gastric epithelial cells derived from *Lgr5*$^{eGFP\text{-}Ires\text{-}CreERT2}$*Trp53*$^{loxP/loxP}$*Rb1*$^{loxP/loxP}$Ai9 mice (Figure 3.6A). Loss of CD44 expression resulted in decreased formation frequency and size of organoids (Figure 3.6B and C). Besides, *ex vivo* inactivation of *Trp53* and *Rb1* was conducted using adenovirus-mediated Cre (AdCre) recombination (Figure 3.6A to C). Mutations of these genes led to increase in the frequency and size of organoids (Figure 3.6B and C), and resulted in marked change of their morphology from a single layer of cuboidal cells to multilayered dysplastic cell structures (Figure 3.6D). These effects were abrogated by *Cd44*-silencing indicating critical role of CD44 in the malignant transformation.

3.4.3 Lgr5^{-}CD44^{+} immature cell is the cell-of-origin of gastric SCJ cancer

To identify the most likely cellular origin of gastric SCJ cancer, we have evaluated expression of Lgr5 and CD44 during gastric carcinogenesis in our *Lgr5*$^{EGFP\text{-}Ires\text{-}CreERT2}$*p53*$^{loxP/loxP}$*Rb*$^{loxP/loxP}$Ai9 mouse model. The early lesions were observed at the

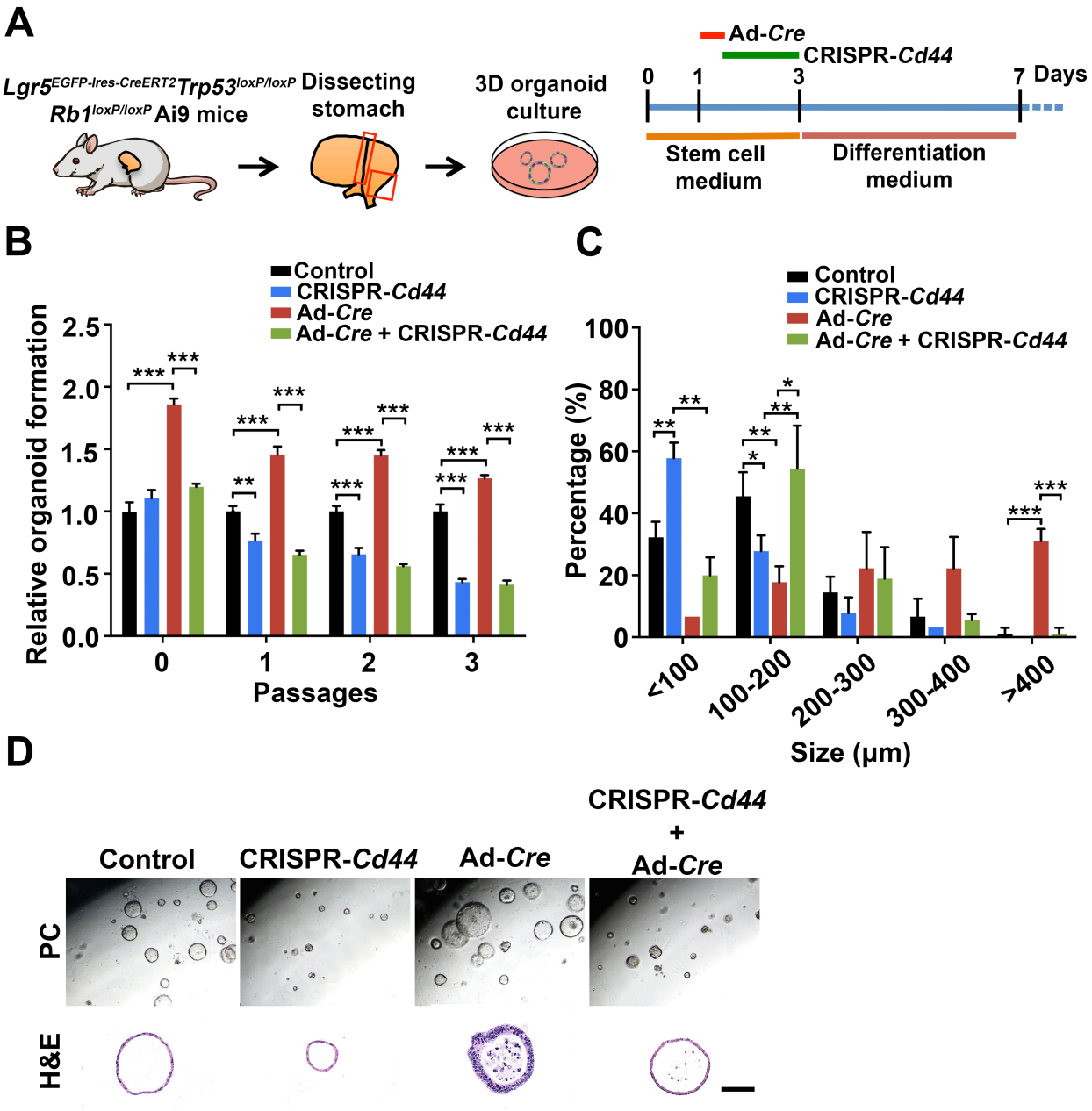
A
Lgr5EGFP-Ires-CreERT2 Trp53loxP/loxP Rb1loxP/loxP Ai9 mice
Dissecting stomach
3D organoid culture
Ad-Cre
CRISPR-Cd44
0
1
3
7 Days
Stem cell medium
Differentiation medium
B
Control
CRISPR-Cd44
Ad-Cre
Ad-Cre + CRISPR-Cd44
Relative organoid formation
Passages
C
Percentage (%)
<100
100-200
200-300
300-400
>400
Size (μm)
D
Control
CRISPR-Cd44
Ad-Cre
CRISPR-Cd44 + Ad-Cre
PC
H&E

Figure 3.6 The role of CD44 in the growth and transformation of gastric organoids. (A) Experimental design. The rectangles indicate regions used for organoid preparation. (B and C) The relative numbers (B) and sizes (C) of gastric organoids before and after inactivation of *Trp53* and *Rb1* (Ad-*Cre*) and/or CD44 (CRISPR-*Cd44*). The organoid numbers were normalized to control organoids at the same passage. (D) Organoids formed by gastric epithelial cells derived from *Lgr5*$^{eGFP\text{-}Ires\text{-}CreERT2}$*Trp53*$^{loxP/loxP}$*Rb1*$^{loxP/loxP}$Ai9 mice before (control) and after deletion of CD44 (CRISPR-*Cd44*), *Trp53* and *Rb1* (Ad-*Cre*) or all three genes (CRISPR-*Cd44*+Ad-*Cre*). The scale bar represents 500 μm (top panels of D) and 70 μm (bottom panels of D). *P<0.05. **P<0.01. ***P<0.001.

gastric SCJ region 60 days after exposure to tamoxifen (Figure 3.7). The affected cells represented dysplastic characteristics such as enlarged pleomorphic and hyperchromatic nuclei with irregular shapes (Figure 3.7). The $Lgr5^{+}$ stem cell niches were found at the base of morphologically normal first pit of SCJ but no Lgr5 expression was observed in dysplastic lesions (Figure 3.7). At the same time, dysplastic cells showed prominent CD44 expression. Consistently, approximately 20-30% of neoplastic cells in the advanced SCJ tumor showed CD44 expression, while none of them expressed Lgr5. We also transplanted the wild-type control and the *Trp53*$^{-/-}$*Rb1*$^{-/-}$ gastric organoids into the flanks of NSG mice. Over 223 days post grafting, the *Trp53*$^{-/-}$*Rb1*$^{-/-}$ organoids gave rise to a high graded, invasive, poorly differentiated tumor (Figure 3.8). Marked expression of tdTomato in the neoplasm indicated its allograft origin (Figure 3.8). The neoplastic cells had predominant CD44 expression but absence of Lgr5 expression (Figure 3.8). Taken together, these findings suggest that either the $Lgr5^{+}$ stem cells do not take part in the initiation of malignant transformation or were outcompeted by $Lgr5^{-}$ neoplastic cells. At the same time they indicate that $Lgr5^{-}CD44^{+}$ cells may be preferentially susceptible to malignant transformation and may play an important role as cancer-propagating cells during SCJ carcinogenesis. .

To compare the transformation potential among various cell populations in gastric epithelium, we isolated the gastric epithelium cells from the gastric TZ of *LGR5*$^{DTR\text{-}eGFP}$ (*Lgr5-DTR*) mice, and cultured them under conditions that promote

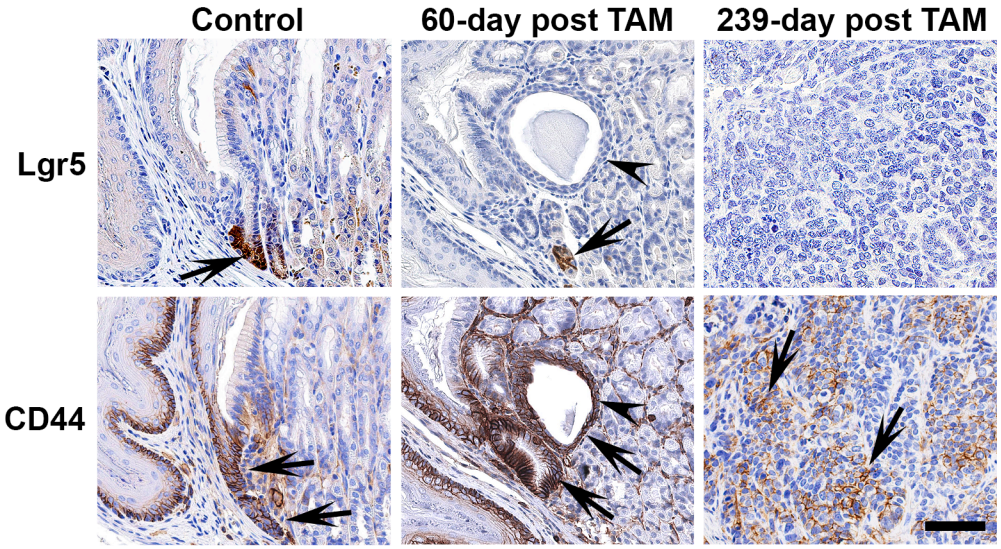

Figure 3.7 Lgr5^{-}CD44^{+} cells show preferential transformation after conditional inactivation of *Trp53* and *Rb1* genes. Detection of Lgr5-eGFP (arrows in top panels) and CD44 (arrows in bottom panels) in the gastric SCJ before (TAM-) and after (TAM+ 60 days and TAM+ 239 days) after tamoxifen administration to *Lgr5*$^{eGFP\text{-}Ires\text{-}CreERT2}$*Trp53*$^{loxP/loxP}$*Rb1*$^{loxP/loxP}$Ai9 mice. Early stage dysplastic lesions (arrowheads, TAM^{+} 60 days) and advanced carcinoma (TAM^{+} 239 days) are shown at the SCJ region. ABC Elite, counterstaining with hematoxylin. Scale bar represents 50 μm.

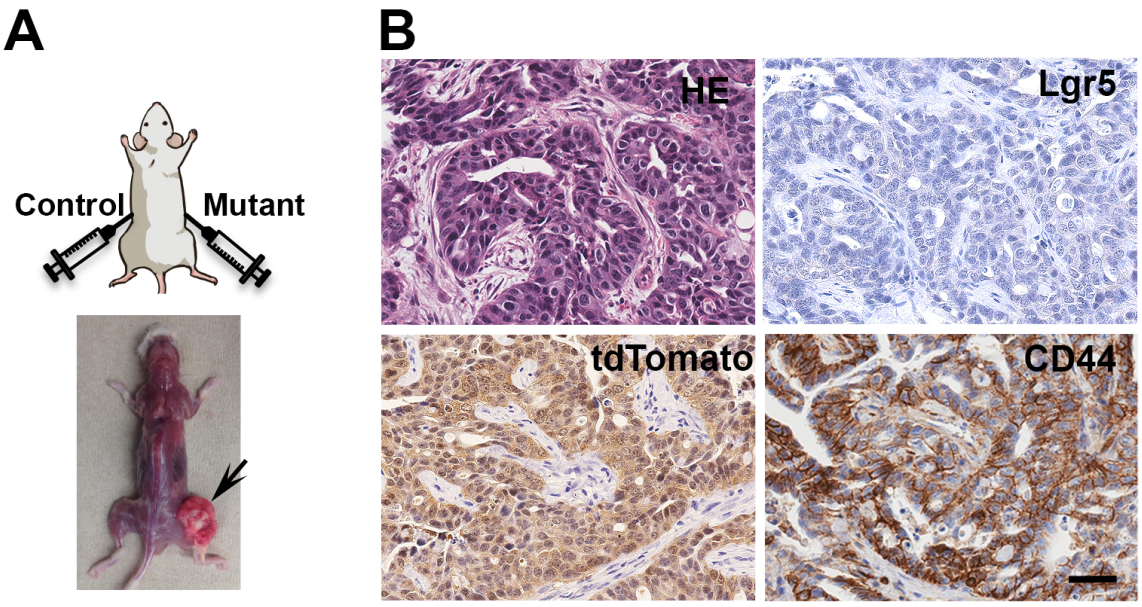

Figure 3.8 Characterization of neoplasms formed from gastric SCJ organoids deficient for *Trp53* and *Rb1*. (A and B) Gross (A) and histological (B) images of neoplasm (arrow in a) formed from *Lgr5*$^{eGFP\text{-}Ires\text{-}CreERT2}$*Trp53*$^{loxP/loxP}$*Rb1*$^{loxP/loxP}$Ai9 mouse derived, Ad-*Cre* pre-exposed organoids 223 days after s.c. transplantation into NSG mouse. Control, transplanted organoids pre-exposed to Ad-blank. Neoplastic cells express tdTomato and CD44 (brown color) but not Lgr5-eGFP. Hematoxylin and eosin (HE; B, upper left image). ABC Elite, Counterstaining with hematoxylin (B, other images). Scale bar represents 50 μm.

preferential organoid composition as $Lgr5^+$ cells (addition of CHIR99021, which is a GSK3β inhibitor, and valproic acid, which is an inhibitor for histone deacetylase), $Lgr5^-CD44^+$ cells (ablation of $Lgr5^+$ cells by diphtheria toxin treatment), or $Lgr5^-CD44^-$ cells (Wnt3a-, FGF-, noggin-, and gastrin- media accompanied with diphtheria toxin treatment) (Flesken-Nikitin et al., 2014; Sato and Clevers, 2015) (Figure 3.9). Following CRISPR/Cas9-mediated *Trp53* and *Rb1* inactivation, the most pronounced increase in organoid formation number, size, and dysplastic morphologic changes was observed in $Lgr5^-CD44^+$ organoids (Figure 3.10). These findings support the notion that Lgr5-CD44+ cells are the most likely cells of gastric SCJ carcinoma origin.

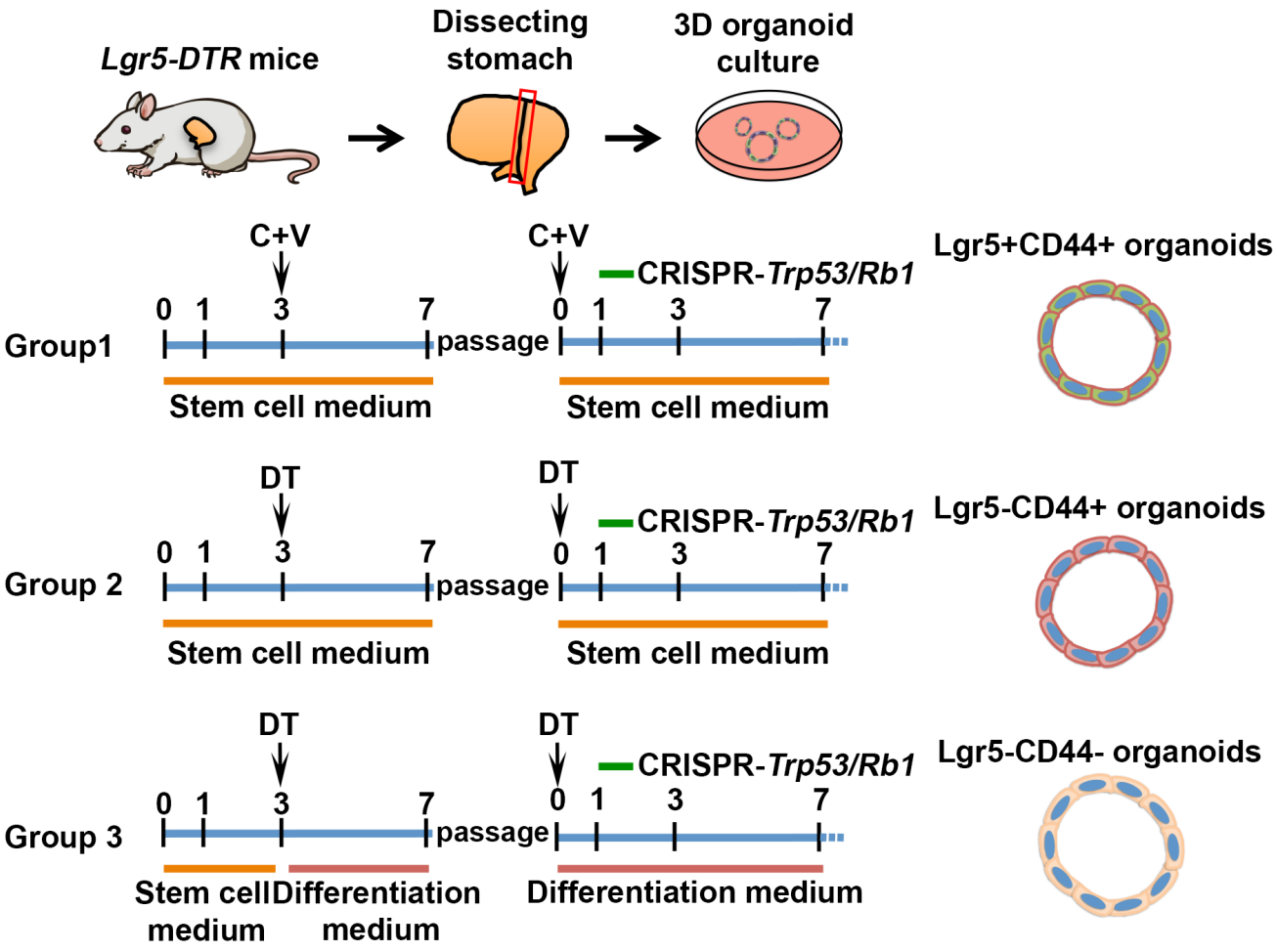

Figure 3.9 Experimental design for comparing the transformation potential among the gastric SCJ organoids maintained at various differentiation stages. The rectangle indicates the regions used for cell isolation. C, CHIR99021. V, valproic acid. DT, diphtheria toxin.

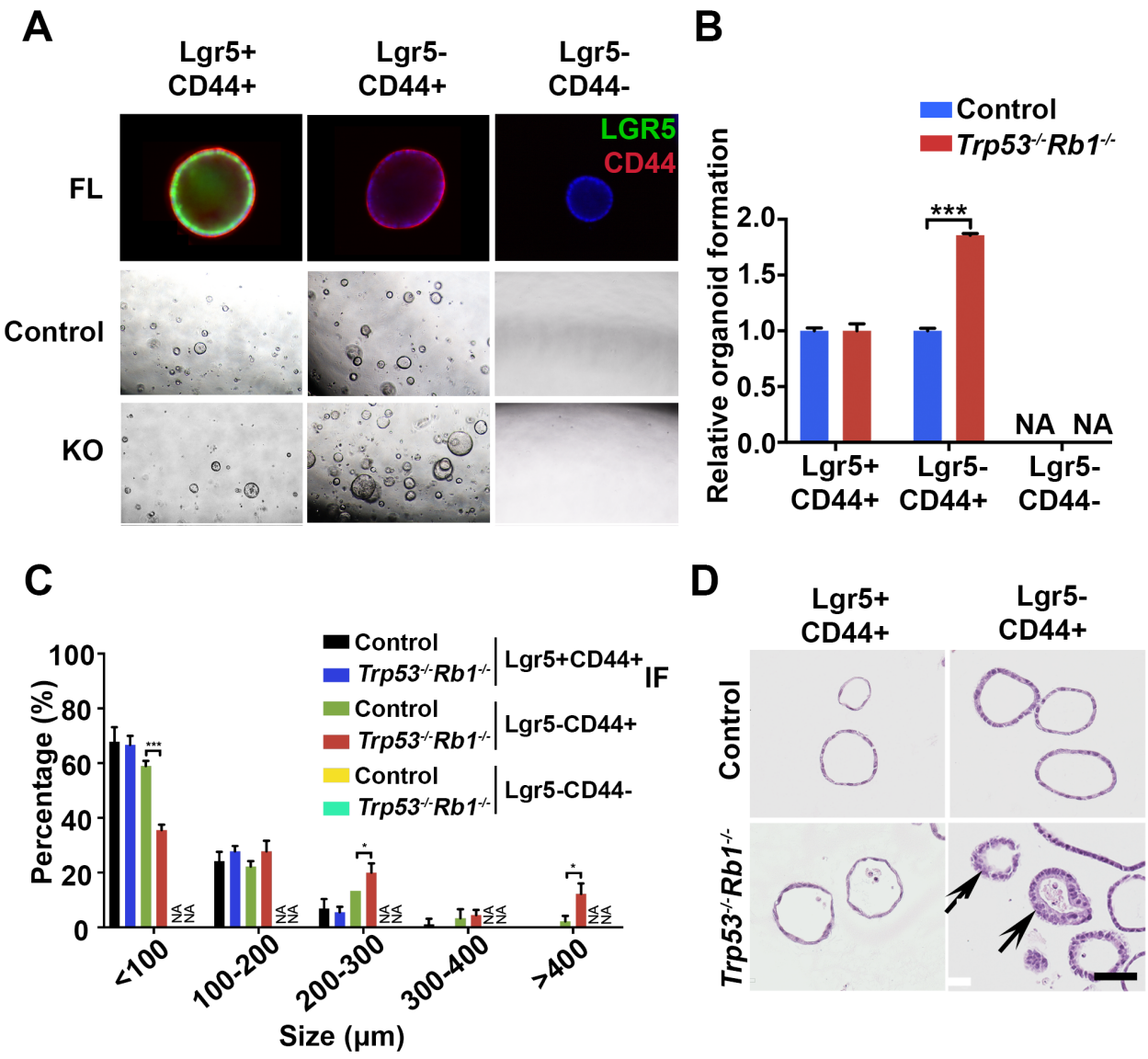
A
Lgr5+ CD44+
Lgr5- CD44+
Lgr5- CD44-
LGR5
CD44
FL
Control
KO
B
Control
Trp53-/-Rb1-/-
Relative organoid formation
2.0
1.5
1.0
0.5
0.0
***
NA NA
Lgr5+ CD44+
Lgr5- CD44+
Lgr5- CD44-
C
Control
Trp53-/-Rb1-/-
Lgr5+CD44+
IF
Control
Trp53-/-Rb1-/-
Lgr5-CD44+
Control
Trp53-/-Rb1-/-
Lgr5-CD44-
Percentage (%)
100
80
60
40
20
0
***
*
*
<100
100-200
200-300
300-400
>400
Size (μm)
D
Lgr5+ CD44+
Lgr5- CD44+
Control
Trp53-/-Rb1-/-

Figure 3.10 Lgr5^{-}CD44^{+} cells show preferential transformation after conditional inactivation of *Trp53* and *Rb1* genes. (A) Representative fluorescence and phase contrast images of SCJ organoids derived from *Lgr5-DTR* mice and cultured under conditions promoting the presence of Lgr5^{+}CD44^{+} cells (CHIR99021 and valproic acid), Lgr5^{-}CD44^{+} cells (diphtheria toxin), or mature Lgr5^{-}CD44^{-} cells (Wnt3a-, FGF-, noggin-, and gastrin- media). Detection of Lgr5-eGFP (green) and CD44 (red) with immunostaining (FL). (B and C) The number (B) and size (C) of various types of the SCJ organoids derived from *Lgr5-DTR* mice and maintained at various differentiation conditions with or without CRISPR-mediated *Trp53* and *Rb1* deletion. Normalized to control groups. NA, not available. (D) Gastric SCJ organoids cultures formed before and after CRISPR-mediated *Trp53* and *Rb1* inactivation in the cells derived from *Lgr5-DTR* mice. The arrows indicate the dysplastic changes in the transformed organoids. Immunostaining and counterstaining with DAPI (top panels in A), and hematoxylin and eosin staining (D). Scale bars represent 100 μm (A, top panel), 500 μm (A, middle and bottom panels), and 55 μm (D). *P<0.05. **P<0.01. ***P<0.001.

3.5 Discussion

In this study, we identified a distinct cancer-prone immature $Lgr5^{-}CD44^{+}$ population in the first gland of gastric SCJ area. The cells of the first gland prominently express both MUC4 and EpCAM, which are the biomarkers found in the premalignant Barrett's esophagus and advanced gastric cancer correlating with poor survival (Anders et al., 2008; O'Neil et al., 2017; Shi et al., 2013). Moreover, the first gland also express the spasmolytic polypeptide-expressing metaplasia (SPEM) marker Clusterin, which have proven upregulated in the process of premalignant metaplastic progression, suggesting that the first gland may be the source of precancerous lineage (O'Neil et al., 2017; Weis et al., 2012). A recent study has suggested that the preferential transformation of the first gland may be attributable to the retention of a distinct embryonic epithelial lineage at the gastric SCJ (Wang et al., 2011). These unique embryonic epithelial cells, which express both cytokeratin 7 (CK7) and MUC4, cover the entire luminal surface of the stomach at the earlier embryogenesis and persistently remain at the gastric SCJ junction of adult mice and humans (Wang et al., 2011). Upon programmed injury via diphtheria toxin A (DTA) expression in the cytokeratin 14 (CK14)-positive squamous epithelium, these residual embryonic cells shift toward the squamous forestomach and recapitulate early Barrett's-like epithelium at the junction region (Wang et al., 2011). Another study reported that the Barrett's-like metaplasia induced by overexpression of cytokine IL-1 may develop from the proximal expansion of $Lgr5^{+}$ stem cell progeny (Quante et al., 2012). Consistently, the location of these $Lgr5^{+}$ cell progeny appeared to overlap with $CK7^{+}$ residual embryonic cells at the first pit of SCJ region (Quante et al., 2012; Wang et al.,

2011). These findings suggest that the first pit of gastric glands may have a potential to develop premalignant metaplasia. In our study, we further characterized the cellular lineage of the first gland and identified immature progeny of $Lgr5^{+}CD44^{+}$ cells as $Lgr5^{-}CD44^{+}$ cells. By using organoid culture experiments we have shown that $Lgr5^{-}CD44^{+}$ cells, but not $Lgr5^{+}CD44^{+}$ or $Lgr5^{-}CD44^{-}$ cells, can be easily transformed by inactivation of *Trp53* and *Rb1*. These findings point to $Lgr5^{-}CD44^{+}$ cells, as the most likely cell of SCJ carcinoma origin.

Our findings suggest that the presence of extensive pools of immature cells predisposes the transitional zones/epithelial junctions to cancer. This brings an additional focus on the role of the stem cells in the cancer initiation. This issue remains debatable for several reasons. First, many recent studies have experimentally induced carcinogenesis in various organs by exploiting certain oncogenic alterations selectively targeting the adult stem cells (Hayakawa et al., 2015; Li et al., 2016; Matsuo et al., 2017; Powell et al., 2012; Zhu et al., 2009). However, even though the oncogenic mutations selectively occur in the stem cells, their progeny obtains these mutations from the affected stem cells. In actively renewing tissues, like gastrointestinal epithelium, proliferating stem cells will rapidly transmit their mutational load to their progeny during the routine renewing process. Thus these animal models are not sufficient to prove that all cancers directly arise from the stem cells and not their progeny. Second, it has been previously reported that the differentiated progeny may acquire the capacity to dedifferentiate to stem-like state during the carcinogenesis (Friedmann-Morvinski et al., 2012; Schwitalla et al.,

2013). Upon obtaining certain genetic alterations, the differentiated glial cells can undergo reprograming to neural precursor cell and subsequently give rise to malignant glioma (Friedmann-Morvinski et al., 2012). Similar mechanism has been proposed in the intestinal neoplasia, where it has been shown that the mature intestinal cells dedifferentiate to intestinal stem-like cells following oncogenic mutations and eventually form to adenoma (Schwitalla et al., 2013). Third, in some cases the stem cells show tumor-suppressive property, thereby becoming less susceptible to tumorigenesis (Wu et al., 2014; Zhou et al., 2017). Through the binding with ligand R-spondin 1 and 2, the stem cell marker Lgr5 may function as a tumor suppressor to attenuate tumor progression and metastasis by activating TGFβ-mediated signaling as well as interfering with WNT signaling (Wu et al., 2014; Zhou et al., 2017). In our study, we traced the carcinogenesis in the gastric SCJ region of *Lgr5*$^{EGFP\text{-}Ires\text{-}CreERT2}$*Trp53*$^{loxP/loxP}$*Rb1*$^{loxP/loxP}$Ai9 mice and found that Lgr5^{+} stem cells were not involved in the neoplastic initiation, while dysplastic lesions most likely developed from the Lgr5^{-}CD44^{+} immature subpopulation, which arise from the Lgr5^{+} stem cells. Furthermore, we also found the tumors arising from the transplantation of mutant gastric organoids showed absence of Lgr5 expression. These studies are consistent with our observations of preferential transformation of Lgr5^{-}CD44^{+} organoids by inactivation of *Trp53* and *Rb1* and support dispensable role of Lgr5 in the process of tumor initiation and progression. The detailed molecular analysis of Lgr5 function in the normal and neoplastic SCJ epithelium warrants further investigations.

As discussed in Chapter 1, Cd44 is a major cell surface receptor that interacts with extracellular matrix, cytokines, and growth factors (Ahmed et al., 2016; Avigdor et al., 2004; Weber et al., 1996; Yan et al., 2015). Through binding to various ligands, CD44 is involved in a wide variety of physiological processes such as cell-cell and cell-matrix adhesion, cell proliferation, differentiation, apoptosis, and trafficking (Baaten et al., 2010; Bourguignon et al., 2008; Mylona et al., 2006; Okamoto et al., 1999; Orian-Rousseau, 2010). Being the direct target of WNT signaling, CD44 variant isoform (CD44v) is expressed by the intestinal stem cells, which highly express WNT-signaling associated receptor Lgr5 (Zeilstra et al., 2014). In agreement with these observation, we found that all gastric $Lgr5^{+}$ stem cells at the base of SCJ and antral glands strongly express CD44. A subpopulation of $CD44^{+}$ SCJ and antral cells lacks Lgr5 expression. However, unlike antral cells, $Lgr5^{-}CD44^{+}$ cells constitute a large part of the gland and have the attributes of immature progenitors such as active proliferation and lack of differentiation. We have also found that deletion of *Cd44* gene in the gastric organoids using CRISPR/cas9 mediated technology attenuates their capacity for self-renewal and growth. Thus, the CD44 expression is likely to be critical for the gastric epithelium regeneration. Besides the normal physiology functions, CD44 is known to be involved tumor initiation, progression, and metastasis in a wide variety of organs including intestine, brain, stomach, breast, ovary, and prostate (Bourguignon et al., 2000; D'Arena et al., 2014; Hirata et al., 2013; Liu et al., 2011; Pietras et al., 2014; Rodríguez-Rodríguez et al., 2003; Todaro et al., 2014; Wielenga et al., 1999). It was also previously reported that the CD44 is preferentially expressed in the cancers arising from the gastroesophageal junction area rather than

those from other regions of the stomach (Kim et al., 2005). Consistent with human disease, CD44 expression was detected in a considerable number of gastric SCJ cancer cells in our *Lgr5*$^{EGFP\text{-}Ires\text{-}CreERT2}$*Trp53*$^{loxP/loxP}$*Rb1*$^{loxP/loxP}$Ai9 mouse model, as well as in tumor arising from transplanted mutant gastric SCJ organoids. Furthermore, we have shown that inactivation of *Cd44* may inhibit the malignant transformation of gastric organoids following oncogenic mutations, supporting the pivotal role of CD44 in the process of SCJ cancer initiation.

To sum up, we identified a subpopulation of immature Lgr5^{-}CD44^{+} progenitors that acts as the most likely target for malignant transformation during the carcinogenesis. We have also found that Lgr5^{+} cells do not represent essential component of SCJ carcinomas. In addition, inhibition of the critical marker CD44 expression and intervention of its signaling pathway may have important implications for preventing tumor initiation and progression. These finding have the clinical relevance for the earlier detection of malignancy and the development of new targeting therapeutics against the disease.

References

Ahmed, M., Sottnik, J.L., Dancik, G.M., Sahu, D., Hansel, D.E., Theodorescu, D., and Schwartz, M.A. (2016). An Osteopontin/CD44 Axis in RhoGDI2-Mediated Metastasis Suppression. Cancer cell *30*, 432-443.

Anders, M., Sarbia, M., Grotzinger, C., Meining, A., Hofler, H., Wiedenmann, B., and Rosch, T. (2008). Expression of EpCam and villin in Barrett's esophagus and in gastric cardia. Dis Markers *24*, 287-292.

Avigdor, A., Goichberg, P., Shivtiel, S., Dar, A., Peled, A., Samira, S., Kollet, O., Hershkoviz, R., Alon, R., and Hardan, I. (2004). CD44 and hyaluronic acid cooperate with SDF-1 in the trafficking of human CD34+ stem/progenitor cells to bone marrow. Blood *103*, 2981-2989.

Baaten, B.J., Li, C.-R., Deiro, M.F., Lin, M.M., Linton, P.J., and Bradley, L.M. (2010). CD44 regulates survival and memory development in Th1 cells. Immunity *32*, 104-115.

Barker, N., Huch, M., Kujala, P., van de Wetering, M., Snippert, H.J., van Es, J.H., Sato, T., Stange, D.E., Begthel, H., van den Born, M*., et al.* (2010). Lgr5(+ve) stem cells drive self-renewal in the stomach and build long-lived gastric units in vitro. Cell stem cell *6*, 25-36.

Barker, N., van Es, J.H., Kuipers, J., Kujala, P., van den Born, M., Cozijnsen, M., Haegebarth, A., Korving, J., Begthel, H., Peters, P.J*., et al.* (2007). Identification of stem cells in small intestine and colon by marker gene Lgr5. Nature … *449*, 1003-1007.

Blanpain, C. (2013). Tracing the cellular origin of cancer. Nat Cell Bio 15, 126-134.

Bourguignon, L.Y., Zhu, H., Shao, L., and Chen, Y.W. (2000). CD44 interaction with tiam1 promotes Rac1 signaling and hyaluronic acid-mediated breast tumor cell migration. J Biol Chem *275*, 1829-1838.

Bourguignon, L.Y.W., Peyrollier, K., Xia, W., and Gilad, E. (2008). Hyaluronan-CD44 interaction activates stem cell marker Nanog, Stat-3-mediated MDR1 gene expression, and ankyrin-regulated multidrug efflux in breast and ovarian tumor cells. J Biol Chem *283*, 17635-17651.

Cheng, C.Y., Hwang, C.I., Corney, D.C., Flesken-Nikitin, A., Jiang, L., Oner, G.M., Munroe, R.J., Schimenti, J.C., Hermeking, H., and Nikitin, A.Y. (2014). miR-34 cooperates with p53 in suppression of prostate cancer by joint regulation of stem cell compartment. Cell reports *6*, 1000-1007.

D'Arena, G., Calapai, G., and Deaglio, S. (2014). Anti-CD44 mAb for the treatment of B-cell chronic lymphocytic leukemia and other hematological malignancies: evaluation of WO2013063498. Expert Opin Ther Pat *24*, 821-828.

Flesken-Nikitin, A., Odai-Afotey, A.A., and Nikitin, A.Y. (2014). Role of the stem cell niche in the pathogenesis of epithelial ovarian cancers. Molecular & cellular oncology *1*, e963435.

Friedmann-Morvinski, D., Bushong, E.A., Ke, E., Soda, Y., Marumoto, T., Singer, O., Ellisman, M.H., and Verma, I.M. (2012). Dedifferentiation of neurons and astrocytes by oncogenes can induce gliomas in mice. Science (New York, NY) *338*, 1080-1084.

Fu, D.-J., Miller, A.D., Southard, T.L., Flesken-Nikitin, A., Ellenson, L.H., and Nikitin, A.Y. (2018). Stem Cell Pathology. Annu Rev Pathol *13*, 71-92.

Hayakawa, Y., Ariyama, H., Stancikova, J., Sakitani, K., Asfaha, S., Renz, B.W., Dubeykovskaya, Z.A., Shibata, W., Wang, H., Westphalen, C.B.*, et al.* (2015). Mist1 Expressing Gastric Stem Cells Maintain the Normal and Neoplastic Gastric Epithelium and Are Supported by a Perivascular Stem Cell Niche. Cancer Cell *28*, 800-814.

Hirata, K., Suzuki, H., Imaeda, H., Matsuzaki, J., Tsugawa, H., Nagano, O., Asakura, K., Saya, H., and Hibi, T. (2013). CD44 variant 9 expression in primary early gastric cancer as a predictive marker for recurrence. British journal of cancer *109*, 379.

Jiang, M., Li, H., Zhang, Y., Yang, Y., Lu, R., Liu, K., Lin, S., Lan, X., Wang, H., Wu, H.*, et al.* (2017). Transitional basal cells at the squamous-columnar junction generate Barrett's oesophagus. Nature *550*, 529-533

Kim, M.A., Lee, H.S., Yang, H.-K., and Kim, W.H. (2005). Clinicopathologic and protein expression differences between cardia carcinoma and noncardia carcinoma of the stomach. Cancer *103*, 1439-1446.

Kong, J., Crissey, M.A., Funakoshi, S., Kreindler, J.L., and Lynch, J.P. (2011). Ectopic Cdx2 expression in murine esophagus models an intermediate stage in the emergence of Barrett's esophagus. PLoS ONE *6*, e18280.

Leedham, S.J., Preston, S.L., McDonald, S.A., Elia, G., Bhandari, P., Poller, D., Harrison, R., Novelli, M.R., Jankowski, J.A., and Wright, N.A. (2008). Individual crypt genetic heterogeneity and the origin of metaplastic glandular epithelium in human Barrett's oesophagus. Gut *57*, 1041-1048.

Li, X.-B., Yang, G., Zhu, L., Tang, Y.-L., Zhang, C., Ju, Z., Yang, X., and Teng, Y. (2016). Gastric Lgr5(+) stem cells are the cellular origin of invasive intestinal-type gastric cancer in mice. Cell Res *26*, 838-849.

Liu, C., Kelnar, K., Liu, B., Chen, X., Calhoun-Davis, T., Li, H., Patrawala, L., Yan, H., Jeter, C., Honorio, S.*, et al.* (2011). The microRNA miR-34a inhibits prostate cancer stem cells and metastasis by directly repressing CD44. Nature medicine *17*, 211-215.

Mahe, M.M., Aihara, E., Schumacher, M.A., Zavros, Y., Montrose, M.H., Helmrath, M.A., Sato, T., and Shroyer, N.F. (2013). Establishment of gastrointestinal epithelial organoids. Current protocols in mouse biology, 217-240.

Matsuo, J., Kimura, S., Yamamura, A., Koh, C.P., Hossain, M.Z., Heng, D.L., Kohu, K., Voon, D.C.-C., Hiai, H., Unno, M.*, et al.* (2017). Identification of Stem Cells in the Epithelium of the Stomach Corpus and Antrum of Mice. Gastroenterology *152*, 218-231.e214.

Milano, F., van Baal, J.W.P.M., Buttar, N.S., Rygiel, A.M., de Kort, F., DeMars, C.J., Rosmolen, W.D., Bergman, J.J.G.H.M., van Marle, J., Wang, K.K.*, et al.* (2007). Bone morphogenetic protein 4 expressed in esophagitis induces a columnar phenotype in esophageal squamous cells. YGAST *132*, 2412-2421.

Morath, I., Hartmann, T.N., and Orian-Rousseau, V. (2016). CD44: more than a mere stem cell marker. The international journal of biochemistry & cell biology.

Mylona, E., Jones, K.A., Mills, S.T., and Pavlath, G.K. (2006). CD44 regulates myoblast migration and differentiation. J Cell Physiol *209*, 314-321.

O'Neil, A., Petersen, C.P., Choi, E., Engevik, A.C., and Goldenring, J.R. (2017). Unique Cellular Lineage Composition of the First Gland of the Mouse Gastric Corpus. Journal of Histochemistry & Cytochemistry *65*, 47-58.

Odze, R.D. (2005). Unraveling the mystery of the gastroesophageal junction: a pathologist's perspective. The American journal of gastroenterology *100*, 1853.

Okamoto, I., Kawano, Y., Tsuiki, H., Sasaki, J.-i., Nakao, M., Matsumoto, M., Suga, M., Ando, M., Nakajima, M., and Saya, H. (1999). CD44 cleavage induced by a membrane-associated metalloprotease plays a critical role in tumor cell migration. Oncogene *18*, 1435.

Orian-Rousseau, V. (2010). CD44, a therapeutic target for metastasising tumours. Eur J Cancer *46*, 1271-1277.

Pietras, A., Katz, A.M., Ekstrom, E.J., Wee, B., Halliday, J.J., Pitter, K.L., Werbeck, J.L., Amankulor, N.M., Huse, J.T., and Holland, E.C. (2014). Osteopontin-CD44 signaling in the glioma perivascular niche enhances cancer stem cell phenotypes and promotes aggressive tumor growth. Cell stem cell *14*, 357-369.

Powell, A.E., Wang, Y., Li, Y., Poulin, E.J., Means, A.L., Washington, M.K., Higginbotham, J.N., Juchheim, A., Prasad, N., Levy, S.E.*, et al.* (2012). The pan-ErbB negative regulator Lrig1 is an intestinal stem cell marker that functions as a tumor suppressor. Cell *149*, 146-158.

Quante, M., Bhagat, G., Abrams, J.A., Marache, F., Good, P., Lee, M.D., Lee, Y., Friedman, R., Asfaha, S., Dubeykovskaya, Z.*, et al.* (2012). Bile acid and inflammation activate gastric cardia stem cells in a mouse model of Barrett-like metaplasia. Cancer cell *21*, 36-51.

Rodríguez-Rodríguez, L., Sancho-Torres, I., Mesonero, C., Gibbon, D.G., Shih, W.J., and Zotalis, G. (2003). The CD44 receptor is a molecular predictor of survival in ovarian cancer. Med Oncol *20*, 255-263.

Sangiorgi, E., and Capecchi, M.R. (2008). Bmi1 is expressed in vivo in intestinal stem cells. Nature genetics *40*, 915-920.

Sanjana, N.E., Shalem, O., and Zhang, F. (2014). Improved vectors and genome-wide libraries for CRISPR screening. Nature methods *11*, 783-784.

Sarosi, G., Brown, G., Jaiswal, K., Feagins, L., Lee, E., Crook, T., Souza, R., Zou, Y., Shay, J., and Spechler, S.J. (2008). Bone marrow progenitor cells contribute to esophageal regeneration and metaplasia in a rat model of Barrett's esophagus. Diseases of the Esophagus *21*, 43-50.

Sato, T., and Clevers, H. (2015). SnapShot: growing organoids from stem cells. Cell *161*, 1700-1700. e1701.

Schwitalla, S., Fingerle, A.A., Cammareri, P., Nebelsiek, T., Göktuna, S.I., Ziegler, P.K., Canli, O., Heijmans, J., Huels, D.J., Moreaux, G.*, et al.* (2013). Intestinal tumorigenesis initiated by dedifferentiation and acquisition of stem-cell-like properties. Cell *152*, 25-38.

Shi, M., Yang, Z., Hu, M., Liu, D., Hu, Y., Qian, L., Zhang, W., Chen, H., Guo, L., and Yu, M. (2013). Catecholamine-Induced β2-adrenergic receptor activation mediates desensitization of gastric cancer cells to trastuzumab by upregulating MUC4 expression. The Journal of Immunology *190*, 5600-5608.

Todaro, M., Gaggianesi, M., Catalano, V., Benfante, A., Iovino, F., Biffoni, M., Apuzzo, T., Sperduti, I., Volpe, S., Cocorullo, G.*, et al.* (2014). CD44v6 Is a Marker of Constitutive and Reprogrammed Cancer Stem Cells Driving Colon Cancer Metastasis. Stem Cell *14*, 342-356.

Visvader, J.E. (2011). Cells of origin in cancer. Nature *469*, 314-322.

Wang, X., Ouyang, H., Yamamoto, Y., Kumar, P.A., Wei, T.S., Dagher, R., Vincent, M., Lu, X., Bellizzi, A.M., Ho, K.Y.*, et al.* (2011). Residual embryonic cells as precursors of a Barrett's-like metaplasia. Cell *145*, 1023-1035.

Weber, G.F., Ashkar, S., Glimcher, M.J., and Cantor, H. (1996). Receptor-ligand interaction between CD44 and osteopontin (Eta-1). Science (New York, NY) *271*, 509-512.

Weis, V.G., Sousa, J.F., LaFleur, B.J., Nam, K.T., Weis, J.A., Finke, P.E., Ameen, N.A., Fox, J.G., and Goldenring, J.R. (2012). Heterogeneity in mouse spasmolytic polypeptide-expressing metaplasia lineages identifies markers of metaplastic progression. Gut, gutjnl-2012-302401.

Wielenga, V.J., Smits, R., Korinek, V., Smit, L., Kielman, M., Fodde, R., Clevers, H., and Pals, S.T. (1999). Expression of CD44 in Apc and Tcfmutant mice implies regulation by the WNT pathway. The American journal of pathology *154*, 515-523.

Wu, C., Qiu, S., Lu, L., Zou, J., Li, W.-f., Wang, O., Zhao, H., Wang, H., Tang, J., Chen, L.*, et al.* (2014). RSPO2-LGR5 signaling has tumour-suppressive activity in colorectal cancer. Nat Commun *5*, 3149.

Yan, Y., Zuo, X., and Wei, D. (2015). Concise Review: Emerging Role of CD44 in Cancer Stem Cells: A Promising Biomarker and Therapeutic Target. Stem cells translational medicine *4*, 1033-1043.

Yu, W.-Y., Slack, J.M., and Tosh, D. (2005). Conversion of columnar to stratified squamous epithelium in the developing mouse oesophagus. Developmental biology *284*, 157-170.

Zeilstra, J., Joosten, S.P.J., van Andel, H., Tolg, C., Berns, A., Snoek, M., van de Wetering, M., Spaargaren, M., Clevers, H., and Pals, S.T. (2014). Stem cell CD44v isoforms promote intestinal cancer formation in Apc(min) mice downstream of Wnt signaling. Oncogene *33*, 665-670.

Zhou, X., Geng, L., Wang, D., Yi, H., Talmon, G., and Wang, J. (2017). R-Spondin1/LGR5 Activates TGFβ Signaling and Suppresses Colon Cancer Metastasis. Cancer research *77*, 6589-6602.

Zhu, L., Gibson, P., Currle, D.S., Tong, Y., Richardson, R.J., Bayazitov, I.T., Poppleton, H., Zakharenko, S., Ellison, D.W., and Gilbertson, R.J. (2009). Prominin 1 marks intestinal stem cells that are susceptible to neoplastic transformation. Nature *457*, 603-607.

CHAPTER 4*

DEFINING THE ROLE OF OSTEOPONTIN-CD44 SIGNALING IN THE PATHOGENESIS OF GASTRIC SQUAMOUS-COLUMNAR JUNCTION CANCER*

4.1 Abstract

The incidence of the gastric squamous-columnar junction (SCJ) cancer is steadily rising over the past decades, thus understanding the cellular and molecular basis for this cancer initiation and progression is critical. Here we show that OPN shares a similar expression pattern with its receptor CD44 in the first gland of gastric SCJ region. The OPN-CD44 signaling induces of the stem/progenitor cell characteristics, promotes the cell growth, and potentiates the malignant transformation of the targeted cells following *Trp53* and *Rb1* inactivation. Importantly, OPN and CD44 expression in human gastric SCJ cancer are associated with less favorable prognosis. Furthermore, we report that LGR5 acts as a tumor suppressor by reducing the growth and tumorigenicity of human SCJ cancer cells through downregulation of the OPN expression. Taken together, these findings supports the notion that OPN-CD44 signaling plays an important role in the carcinogenesis of gastric SCJ area and provides a new direction for development of new strategies to intervene and prevent the SCJ cancer development and progression.

*In part submitted as Fu, D.-J., Wang, L., Chouairi, F.K., Rose, I.M., Miller, A.D., Yamulla, R.J., Schimenti, J.C., Flesken-Nikitin, A., Nikitin, A.Y., Osteopontin-CD44 signaling keeps progeny of Lgr5^{+} cells in immature cancer-prone state at the gastric squamous-columnar junction (2018).

Author contributions: Dah-Jiun Fu and Alexander Yu. Nikitin designed the study, interpreted data and wrote the manuscript. Dah-Jiun Fu and Lianghai Wang performed experiments and analyzed data. Alexander Yu. Nikitin supervised the project.

4.2 Introduction

The cancer arising around the junction between the stomach and esophagus (aka squamous-columnar junction; SCJ) has gained increasing attentions over the past decades due to its rising incidence and poor prognosis (Botterweck et al., 2000; Buas and Vaughan, 2013; Fu et al., 2018; Jiang et al., 2017; Kim et al., 2005; Kusano et al., 2008; Quante et al., 2012). However, the underlying mechanism by which this region is susceptible to malignant transformation remains poorly understood. Recently, we identified the $Lgr5^{-}CD44^{+}$ immature progenitor cells residing in the first gland of gastric SCJ as the most likely cells of SCJ cancer origin (Chapter 3). We also found that CD44 is not only a cell surface marker for identification of immature progenitor cells but also is directly implicated in the gastric epithelial regeneration and malignant transformation. These findings have provided valuable clues for further exploration of the pathogenesis of this disease.

The stem/progenitor cells in adult tissue reside in anatomically distinct microenvironments (aka niches), the cellular and molecular components of which regulate the fate of the stem/progenitor cells by determining the self-renewal activities and differentiation potentials (Festa et al., 2011; Ordonez and Di Girolamo, 2012; Sato et al., 2011). Interestingly, aberration of niche factor signaling has been shown to play a crucial role in tumor initiation and progression (Flesken-Nikitin et al., 2014; Hsu and Fuchs, 2012; Lau et al., 2017; Quante et al., 2012; Quante et al., 2011; White and Lowry, 2015). As discussed in Chapter 1, Osteopontin (OPN), which is a

secreted, sialic acid-rich, glycosylated phosphoprotein, has been identified as a multifunctional niche factor in many organs participating in various physiological processes such as tissue remodeling, wound healing, regeneration, and angiogenesis (Guidi et al., 2017; Reinholt et al., 1990; Singh et al., 1995; Wang et al., 2015; Wang et al., 2017; Xie et al., 2003). In addition to normal biological function, OPN has also been implicated in cancer development, invasion, and metastasis due to its oncogenic potentials (Ahmed et al., 2016; Mi et al., 2011; Rabenstein et al., 2015; Rangaswami et al., 2006; Sun et al., 2013; Tilli et al., 2011; Wei et al., 2017). Importantly, OPN expression correlates with poor prognosis of cancers in wide range of organs including esophagus (Lin et al., 2015), stomach (Gu et al., 2016), colon (Zhao et al., 2015), ovary (Hu et al., 2015), brain (Pietras et al., 2014), and lung (Sun et al., 2013). Through binding to cell surface receptor CD44, perivascular niche-derived OPN promotes the stemness and tumorigenicity of cancer cells via cleavage and translocation of the C-terminal intracellular domain (ICD) of CD44 into the nucleus (Pietras et al., 2014). The CD44ICD functions as a critical transcriptional factor to induce the stem-like properties in targeted cells by enhancing the hypoxic inducible factor-2α (HIF-2α) in a CBP/p300-dependent manner (Li et al., 2009; Okamoto et al., 2001). Moreover, OPN-CD44 interactions have been shown to activate downstream signaling pathways, such as phosphatidylinositiol 3-kinase (PI3K)/Akt cascade (Bellahcène et al., 2008; Lin and Yang-Yen, 2001) and TIAM1-Rac1 signaling (Ahmed et al., 2016), that are highly associated with cancer progression and metastasis via enhancing cell proliferation, survival, and mobility

(Haga and Ridley, 2016; Mertens et al., 2003). It is therefore likely that targeting OPN-CD44 signaling may have clinical applications for cancer therapy.

In this study, we explore the association between the OPN-CD44 signaling and the tumorigenic potentials in the gastric SCJ cancer. By utilizing mouse models and human cell cultures, we provide direct evidence that the OPN-CD44 signaling indeed promotes the stemness, growth, and tumorigenicity of gastric SCJ cancer. Furthermore, our findings identify LGR5 as a modulator of OPN-CD44 signaling that functions as an inhibitor in gastric SCJ carcinogenesis.

4.3 Materials and Methods

Experimental animals. The *Lgr5*$^{eGFP\text{-}Ires\text{-}CreERT2}$ mice were crossed with *Trp53*$^{loxP/loxP}$ mice, *Rb1*$^{loxP/loxP}$ mice, and Ai9 mice as described in Materials and Methods in Chapter 2. NOD.Cg-*Prkdc*^{scid} *Il2rg*^{tm1wjl}/SzJ (NSG) mice (Stock number 005557), *Lgr5*$^{tm1(cre/ERT2)Cle}$*/J* (*Lgr5*$^{eGFP\text{-}Ires\text{-}CreERT2}$) knock in mice (Stock number 008875) were purchased from The Jackson Laboratory (Bar Harbor, ME, USA). All experimental animals were maintained in accordance to the guidelines of the Institutional Laboratory Animal Use and Care Committee of Cornell University.

Human materials. All tissue specimens from anonymous patients with gastroesophageal junction (GEJ) cancers were collected, fixed, and processed at Department of Pathology and Key Laboratories for Xinjiang Endemic and Ethnic Diseases, Shihezi University School of Medicine, China. Four μm-thick paraffin sections were prepared and transported to Cornell University by Dr. Lianghai Wang. The ESO26 human GEJ cancer cell line (ECACC 11012009) was purchased from Sigma-Aldrich (11012009) and cultured following the manufacture's recommendation.

Immunostaining and analysis. Tissue sections were performed as described in

Materials and Methods in Chapter 2. For immunofluorescence staining, rehydrated tissue sections were incubated with boiling 10 mM sodium citrate buffer (pH 6.0) for 10 minutes for antigen retrieval, followed by incubation with blocking solution (1% bovine serum albumin [Sigma-Aldrich, St. Louis, MO, USA; A9418] in PBS buffer supplemented with 1:50 diluted horse serum [Jackson Immunoresearch Lab, West Grove, PA, USA; 008-000-121], Triton X-100 [Sigma-Aldrich; T8787] and TWEEN 20 [Sigma-Aldrich; P9416]) at room temperature (RT) for 30 minutes. The tissue sections were then incubated with primary antibody against GFP (Novus Biologicals, Littilton, CO, USA; NB600-303), CD44 (Santa Cruz Biotechnologies, Dallas, TX, USA; sc-18849), and OPN (R & D Systems, Minneapolis, MN; AF808) at RT for 1 hour, followed by incubation with fluorescence-conjugated secondary antibodies for another 1 hour at RT and nuclear counterstaining with DAPI. The stained sections were mounted by Fluoro-Gel (Electron Microscopy Sciences, Hatfield, PA, USA; 17985-10), and then scanned using Aperio ScanScope FL (Leica Biosystems, Vista, CA, USA). Image merging and analysis were performed with ImageJ software (National Institutes of Health, Bethesda, MD, USA).

For immunochemistry, antigen retrieval and blocking were carried out as described above. The tissue sections were incubated with primary antibodies against CD44

(Santa Cruz Biotechnologies; sc-18849) and SPP1 (Sigma-Aldrich; HPA027541) for 1 hour at RT, followed by incubation with biotinylated secondary antibodies for 30 minutes at RT and Modified Elite avidin-biotin peroxidase (ABC) (Vector Laboratories, Burlingame, CA, USA; pk-6100) for another 30 minutes at RT. Diaminobenzidine (DAB; Sigma-Aldrich, St. Louis, MO, USA; D4418-50SET) and Mayer's hematoxylin were used as the chromogen and nuclear counterstain, respectively. All immunostaining conditions are listed in the table 4.1. The immunostained sections were scanned using ScanScope CS2 (Leica Biosystems, Vista, CA, USA) with 40X objective lens, and subsequently analyzed using Aperio ImageScope Software (Leica) and HALO Image Analysis Software (PerkinElmer Inc., Shelton, CT, USA).

Mouse gastric organoid culture. The preparation and culture of mouse gastric organoid were performed as described in Materials and Methods in Chapter 3. Briefly, the SCJ and antrum tissues were dissected from the stomach of 6-10 week-old *Lgr5*$^{eGFP\text{-}Ires\text{-}CreERT2}$*Trp53*$^{loxp/loxp}$*Rb1*$^{loxp/loxp}$Ai9 mice, followed by washes with ice-cold PBS buffer several times, and further cut into small fragments (<2 mm in length), and incubated with gentle dissociation solution (Stemcell technologies, Vancouver, Canada; 07174) for 15 minutes at RT on the shaker. Subsequently, the gentle dissociation solution was removed, the tissue fragments were vigorously suspended 10 to 20 times with ice-cold 0.1% BSA/PBS solution using 10 ml pipette, and then transferred to 50 ml conical tube. After centrifugation at 500 g for 5 minutes,

Table 4.1 List of antibodies used for immunohistochemistry and immunofluorescence staining

Antigen	Antibody source, catalogue number	Clone	Dilution	Detection system
GFP	Novus Biologicals, NB600-303	PC*	1:1000	immunofluorescence
CD44	Santa Cruz, sc-18849	IM7	1:100	immunofluorescence
OPN	R & D systems, AF808	PC*	1:100	immunofluorescence
SPP1	Sigma, HPA027541	PC*	1:400	Vectastain Elite ABC-HRP Kit
CD44	Santa Cruz, sc-18849	IM7	1:400	Vectastain Elite ABC-HRP Kit

PC*: Polyclonal.

the isolated cells were resuspended with DMEM F12 50/50 medium (Corning Inc., Corning, NY, USA; 10-092-CV) and liquid growth factor-reduced Matrigel (Corning, 354230), and seeded around the rim of the well of a 24-well tissue culture plate. After polymerization of Matrigel in the 37°C incubator for 20 minutes, the 500 µl of the stem cell culture medium was added into each well (IntestiCult^{TM} Organoid Growth Medium [Stemcell Technologies; 6005] supplemented with 10 nM gastrin [Sigma; G9020]) and penicillin/streptomycin (Corning; 30-002-CI) in the first 3 days. After removal of old culture medium, each well was washed with PBS twice and the Matrigel was then overlaid with the differentiation medium (Advanced DMEM/F12 50/50 medium supplemented with 1 µg/ml R-spondin1 [PeproTech Inc., Rocky Hill, NJ, USA; 120-38] and 50 ng/ml EGF [PeproTech, 315-09]) for the following 4 days.

Xenograft transplantation. Cells were collected by centrifugation at 500 g for 5 minutes, resuspended with 50 µl of complete culture medium, mixed at 1:1 ratio with 50 µl of high concentration Matrigel (Corning Inc., Corning, NY, USA; 354263), and subcutaneously injected into the flank of anesthetized NSG mice (Jackson Laboratory; 005557) using 1 ml sterile syringe with 23 G needle.

OPN treatment. 1 µg/ml recombinant OPN (Sigma; SRP3131) was used for the cultures of mouse primary organoids and ESO26 cells as previously described (Todaro et al., 2014). The medium was freshly replaced every 4 days.

Quantitative reverse transcription real-time PCR (qRT-PCR). All the qRT-PCR experiments were carried out as previously described (Hwang et al., 2011). All primer sequences for genes of interest are listed in Table 2. β-actin and GAPDH mRNAs were used as the reference control for mouse and human genes, respectively.

Fluorescence activated cell sorting (FACS). The cells were isolated and dissociated with 0.05% trypsin/0.53 mM EDTA (Corning; 25-052-CI), and then washed with cold PBS. For sorting of $CD44^+$ and $CD44^-$ fractions, the isolated cells were stained with fluorescence conjugated primary antibody against CD44 (eBioscience, San Diego, CA, USA; 12-0441) and IgG2b kappa isotype control (eBioscience; 12-4031-82) on ice for 30 minutes. Cell sorting and analysis were performed on BD FACSaria fusion sorter equipped with BD FACSDiva software (BD Bioscience, San Jose, CA, USA).

Table 4.2 List of primers used for gene expression analysis in mouse gastric organoids and ESO26 cells

Gene name	Species	Sequence (5' → 3')	
		Forward Primer	**Reverse primer**
Cd44	Mouse	CCACGACCCTTTTCCAGAG	CGGCAGGTTACATTCAAATCG
Lgr5	Mouse	TCTTCTAGGAAGCAGAGGCG	CAACCTCAGCGTCTTCACCT
Sox2	Mouse	AAAGCGTTAATTTGGATGGG	ACAAGAGAA TTGGGAGGGGT
Sox9	Mouse	CAAGACTCTGGGCAAGCTC	GGGCTGGTACTTGTAATCGG
Oct4	Mouse	AGTGGAAAGCAACTCAGAGG	AACTGTTCTAGCTCCTTCTGC
Mist1	Mouse	AAAGCTACGTGTCCTTGTCC	CCGGTTTTTGGTCTTCATAGC
Ata4a	Mouse	CTATCTGCCTCATTGCCTTTG	TTGTGCTCTTGAACTCCTGG
Muc5ac	Mouse	CTGATGTTCCTCACCCTCAAG	TCTTGTAGTGGAAGTTGCCC
Muc6	Mouse	GCCTCCAGATCACACCATAC	CTCTTGCTTCAATGTTCCAGG
Chga	Mouse	GAACAGCCCCATGACAAAAG	GATCCTCTCGTCTCCTTGGA
β-actin	Mouse	GATTACTGCTCTGGCTCCTAGC	GACTCATCGTACTCCTGCTTGC
Spp1	Mouse	GTGATTTGCTTTTGCCTGTTTG	GAGATTCTGCTTCTGAGATGGG
CD44	Human	GGACACCATGGACAAGTTTTG	GCGGCAGGTTATATTCAAATCG
SOX2	Human	CACACTGCCCCTCTCAC	TCCATGCTGTTTCTTACTCTCC
SOX9	Human	CACAGCTCACTCGACCTTG	ACACAAATGTCCAAAGGGAATTC
SPP1	Human	AGAATGCTGTGTCCTCTGAAG	GTTCGAGTCAATGGAGTCCTG
GAPDH	Human	GTCTCCTCTGACTTCAACAGCG	ACCACCCTGTTGCTGTAGCCAA

Statistical analysis. Statistical comparisons were carried out with Prism 7 and InStat 3 software after figures were generated (GraphPad Software Inc., La Jolla, CA, USA). Two-tailed unpaired *t* test, Chi-square test and log-rank Mantel-Cox test were used as appropriate. The survival curves were computed using the Kaplan-Meier method with Prism 7 software as well. Statistical significance was determined as P value <0.05 in each test.

4.4 Results

4.4.1 Osteopontin (OPN) is highly expressed in the first gland of the mouse gastric SCJ region

By immunofluorescence staining, we found the first gland of the SCJ region in mouse stomach contained a large fraction of OPN+ cells that mainly presented at the lower half of the glands (Figure 4.1A and B). Of note, 97.5% of the OPN^+ cells co-expressed the OPN-receptor CD44 and only 0.56% of OPN^+ cells were co-localized with the $Lgr5^+$ stem cell niches at the bottom of the glands (Figure 4.1C). Contrary to the SCJ regions, the antral glands showed far smaller number of OPN^+ cells that were restrictedly present above the $Lgr5^+$ stem cell niches and less frequently extend to the middle of the glands (Figure 4.1B and C). These findings suggest that the OPN expression varies between the SCJ and antral regions in the mouse stomach. Compared to antrum, the SCJ region contained larger fraction of OPN^+ cells, and their distribution mostly overlaps with $Lgr5^-CD44^+$ immature population in the glands.

4.4.2 OPN-CD44 signaling plays an important role in the mouse gastric epithelial regeneration and malignant transformation

To investigate the functional role of OPN in gastric epithelial homeostasis and carcinogenesis, we generated organoid cultures using the primary gastric epithelial

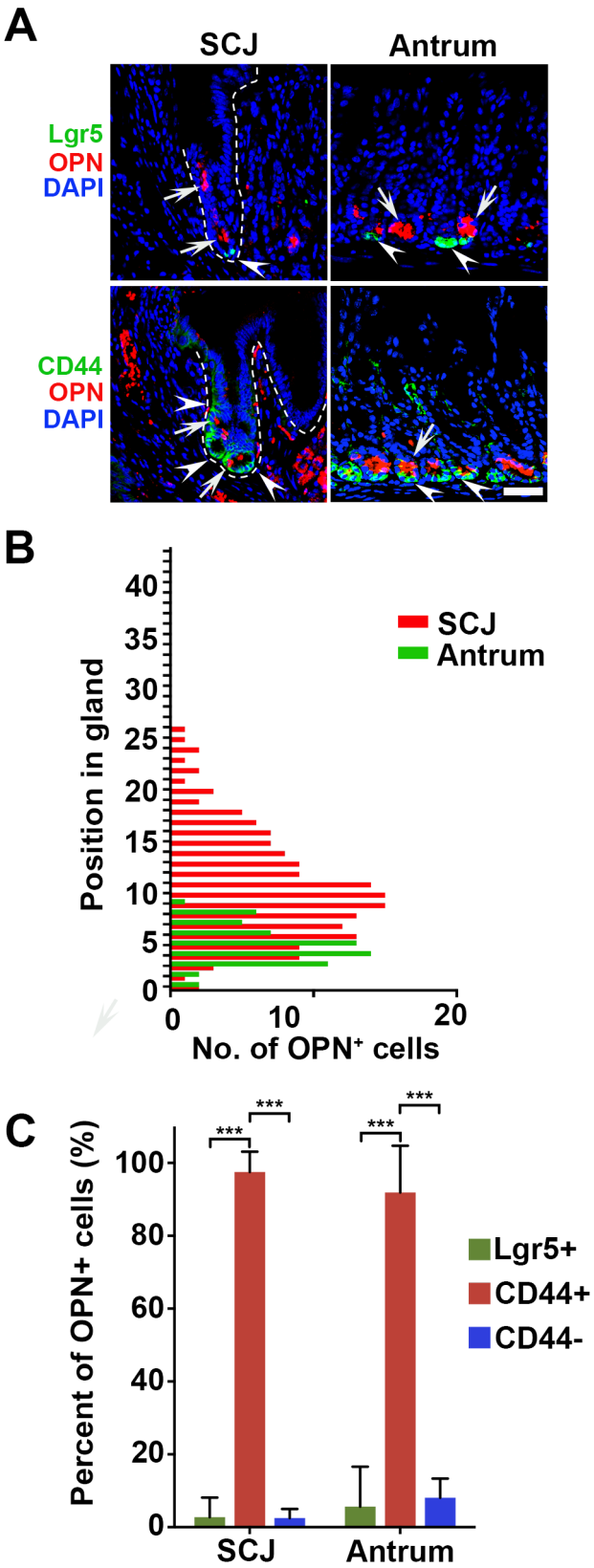
A
SCJ
Antrum
Lgr5
OPN
DAPI
CD44
OPN
DAPI
B
SCJ
Antrum
Position in gland
0
5
10
15
20
25
30
35
40
0
10
20
No. of OPN+ cells
C
Percent of OPN+ cells (%)
0
20
40
60
80
100
***
***
***
***
Lgr5+
CD44+
CD44-
SCJ
Antrum

Figure 4.1 Distribution of the OPN$^+$ cells in the gastric SCJ and antrum. (A) Detection of OPN (red, arrows in all panels), Lgr5-eGFP (green, arrowheads in top panels) and CD44 (green, arrowheads in bottom panels) in the SCJ and antrum of wild-type mice. (B) Number of OPN$^+$ cells located at specific positions in glands SCJ and antrum (n=20, each). (C) Fractions of the OPN$^+$ cells that express Lgr5 or CD44 within the regions as shown. Nuclear counterstained with DAPI (A). Scale bar represents 50 μm (A). *P<0.05. **P<0.01. ***P<0.00

cells derived from the SCJ and antral regions of the *Lgr5*$^{eGFP\text{-}Ires\text{-}CreERT2}$*Trp53*$^{loxP/loxP}$*Rb1*$^{loxP/loxP}$Ai9 mice, followed by the treatment with exogenous OPN and Adenovirus-*Cre* (Ad-*Cre*) -mediated inactivation of *Trp53* and *Rb1* genes. As expected, OPN promoted the growth of the wild-type (Ad-*Cre*$^{-}$) and *Trp53/Rb1*-deficient (Ad-*Cre*$^{+}$) SCJ organoids (Figure 4.2). Importantly, deprivation of CD44 using CRISPR/Cas9-mediated genetic editing diminished the OPN-mediated effect, supporting critical role of the CD44 in OPN-initiated signaling (Figure 4.3). On the contrary, organoids derived from the antral epithelium were not responsive to the OPN stimulation, regardless of Ad-*Cre*-mediated *Trp53* and *Rb1* inactivation (Figure 4.2B). These findings indicate that OPN epithelial regeneration and transformation of gastric SCJ epithelium in CD44 dependent manner.

It has been reported that the OPN-CD44 signaling regulates the stem/progenitor cell proliferation and differentiation in liver and hematopoietic systems, and also promotes stemness of melanoma, glioma and colon cancers (Katagiri et al., 1999; Liu et al., 2015; Nilsson et al., 2005; Pietras et al., 2014; Todaro et al., 2014). To assess if OPN has similar roles in gastric SCJ cells, we compared the relevant gene expression in the SCJ organoids before and after OPN treatment. OPN exposure

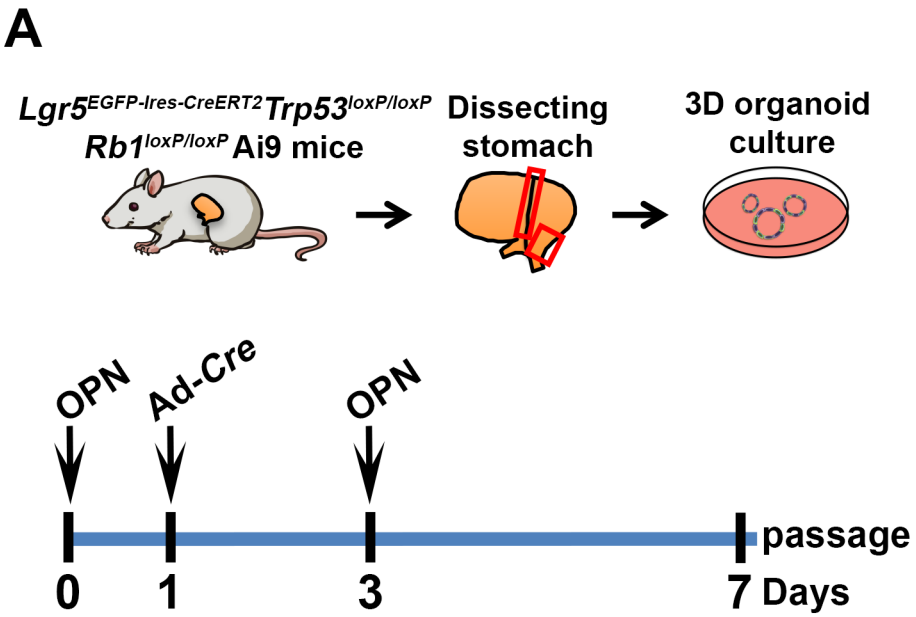
A
Lgr5EGFP-Ires-CreERT2 Trp53loxP/loxP
Rb1loxP/loxP Ai9 mice
Dissecting stomach
3D organoid culture
OPN
Ad-Cre
OPN
passage
0
1
3
7 Days

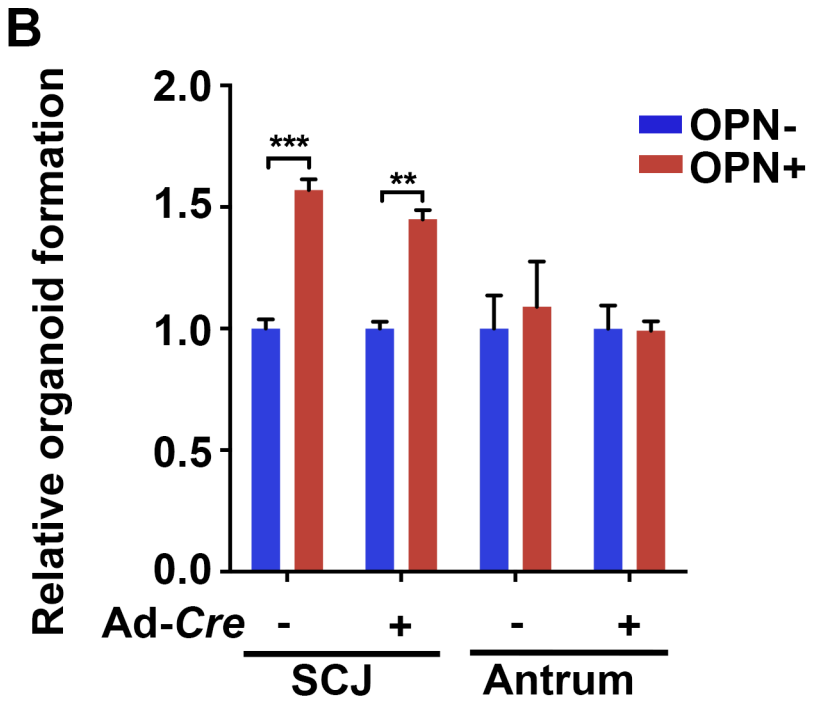
B
Relative organoid formation
2.0
1.5
1.0
0.5
0.0
***
**
OPN-
OPN+
Ad-Cre
-
+
-
+
SCJ
Antrum

OPN promotes the formation of organoids derived from the gastric SCJ region but not the antrum. (A) Experimental design. The rectangles indicate regions used for organoid preparation. (B) The relative numbers of gastric organoids before (OPN-) and after (OPN+) exogenous OPN treatment. The organoid numbers were normalized to non-treated control in each group.

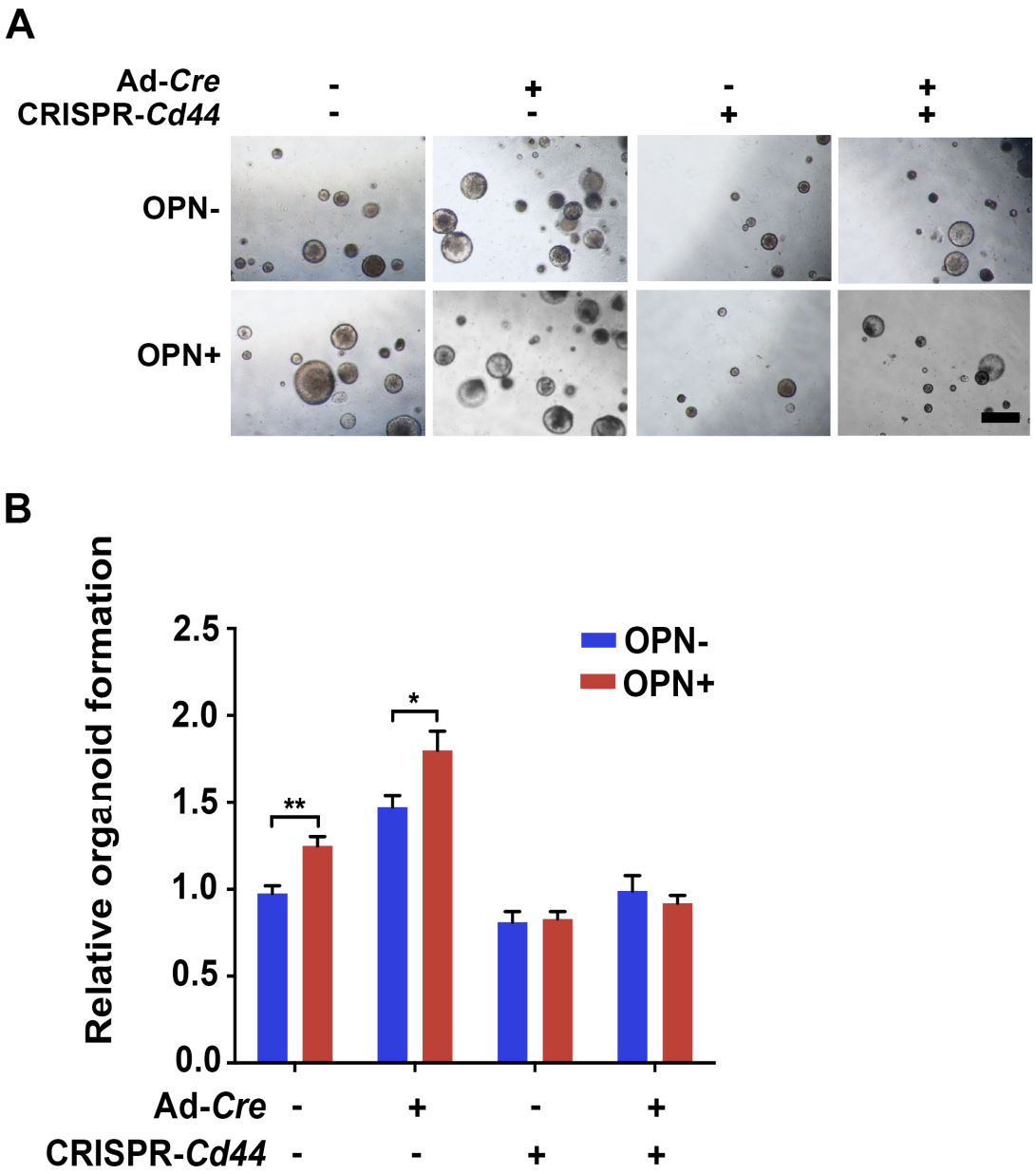

Figure 4.3 Effect of OPN-CD44 signaling on the gastric organoid formation. (A) Representative gastric organoids under various treatments as shown. (B) The relative numbers of gastric organoids before (OPN-) and after (OPN+) exogenous OPN treatment. The organoid numbers were normalized to non-treated control in each group. Scale bar represents 500 μm (A).

increased the expression of stem/progenitor markers *Cd44*, *Sox2*, and *Sox9*, but surprisingly, decreased *Lgr5* expression in primary organoids. At the same time, differentiation markers *Muc5ac, Mist1*, and *ChgA* were also decreased after the OPN treatment (Figure 4.4). Thus exposure to OPN may allow the gastric SCJ cells to maintain their immature progenitor properties.

4.4.3 OPN-CD44 signaling potentiates the carcinogenesis in human gastroesophageal junction

Expression of both OPN and CD44 has been reported to correlate with the worse prognosis for human gastric cancer patients (Chen et al., 2014; Gu et al., 2016). To determine the clinical relevance of the OPN and CD44 expression in human gastroesophageal junction (GEJ) cancer, we performed the immunohistochemistry (IHC) analysis of OPN and CD44 expression on total 21 samples from GEJ cancer patients. Positive immunoreaction with OPN and CD44 was observed in 61.9% (13/21) and 57.1% (12/21) of cases, respectively (Figure 4.5A and B). Expression of both proteins highly correlated with shorter post-operative survival time of patients with GEJ cancers (Figure 4.5C). Importantly, significant correlation was found between OPN and CD44 expression (P=0.0011).

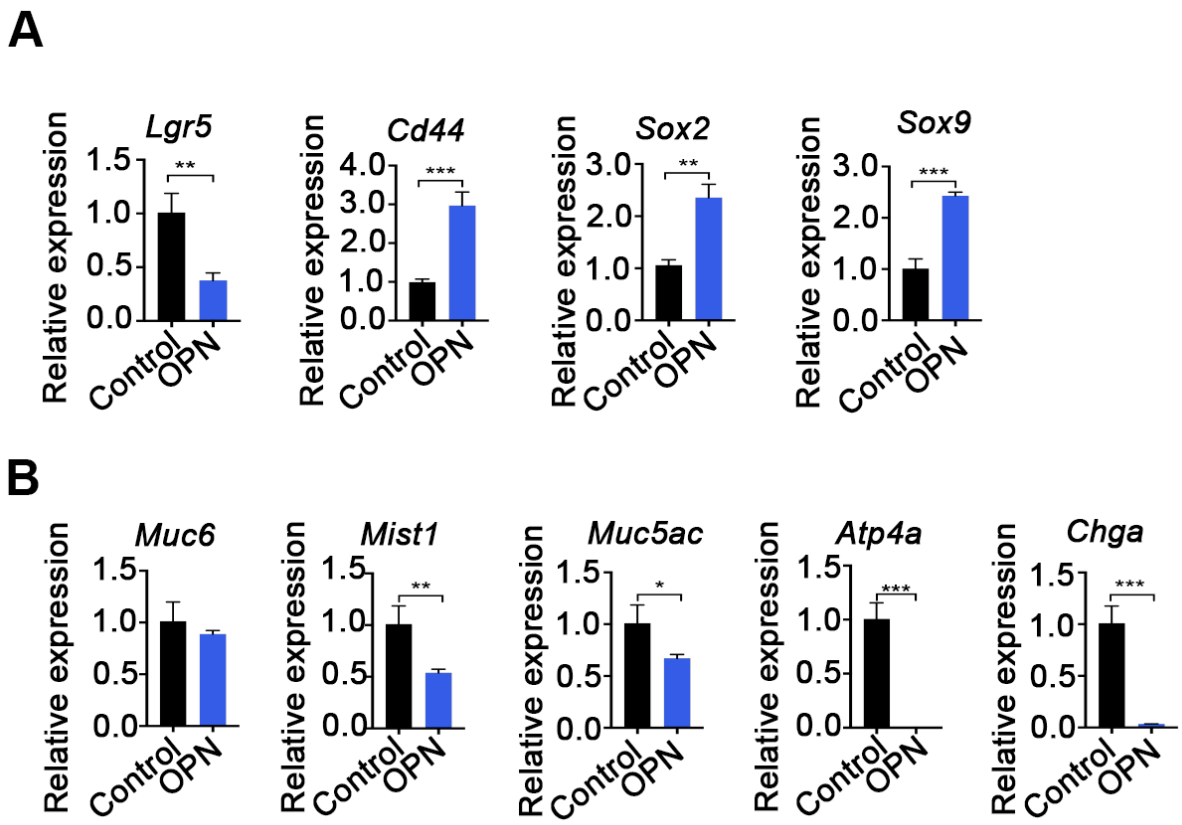

Figure 4.4 p. (A) The relative expression of stem/progenitor markers in the organoids with or without OPN treatment. (B) The relative expression of differentiation markers in the organoids with or without OPN treatment.

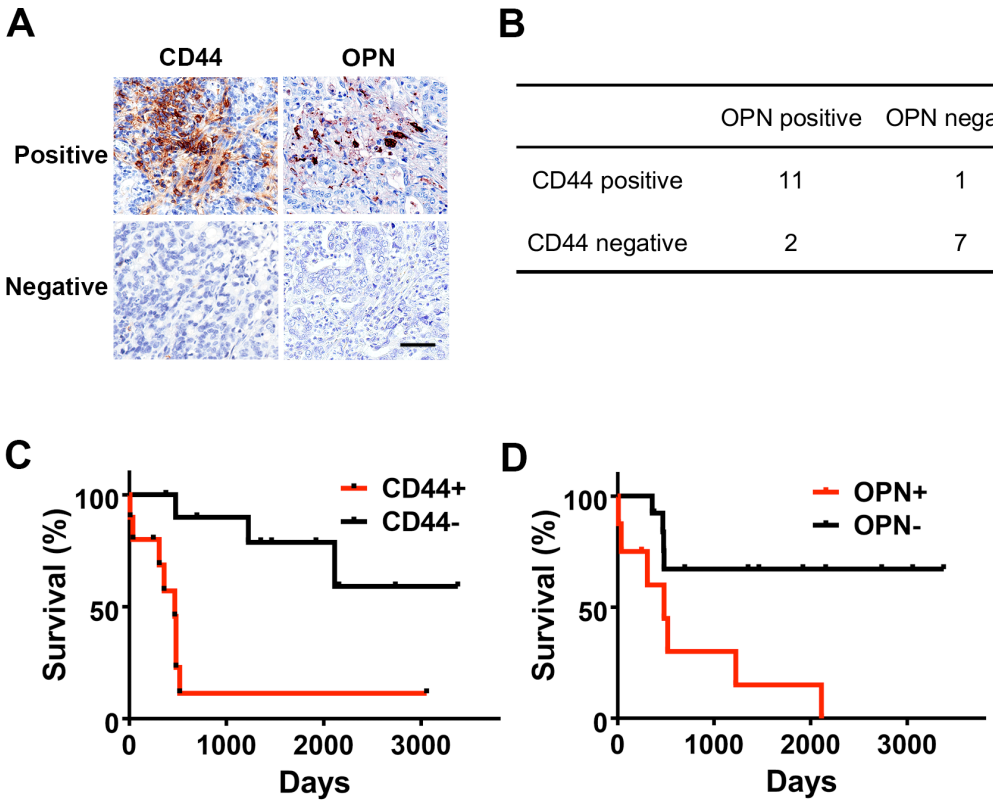

	OPN positive	OPN negative	*P*
CD44 positive	11	1	0.0011
CD44 negative	2	7	

Figure 4.5 CD44 and OPN expression in human GEJ cancer correlates with the worse survival of patients. (A) Detection of CD44 and OPN on human cancers arising from the GEJ regions. (B) Correlation between CD44 and OPN expression in human GEJ cancer patients. Chi-square analysis, P=0.0011. (C and D) Survival of patients with GEJ carcinoma stratified according to CD44 (C) and OPN (D) expression. Kaplan–Meier survival analysis, P=0.0018 (C) and P=0.0081 (D). Immunostaining, ABC Elite method, counterstaining with hematoxylin (A). The scale bar represents 120 μm for all images (A). *P<0.05. **P<0.01. ***P<0.001. All images and analysis are courtesy of Dr. Lianghai Wang, Shihezi University School of Medicine, Shihezi, Xinjiang, China

To determine the role of OPN-CD44 signaling in human disease, the ESO26 human GEJ cells were treated with exogenous OPN for 4 days and subsequently transplanted into immunodeficient mice. Exposure to OPN increased both the tumor volume and weight by the time of animal euthanasia at 6 weeks post injection (p.i.; Figure 4.6A-C)**.** To understand the mechanism by which OPN promotes the tumorigenic potential, we evaluated the expression of stem/progenitor markers such as *SOX2*, *SOX9*, and *CD44* in the ESO26 cells before and after OPN treatment. Consistent with the observations in primary mouse organoids (Figure 4.4), exposure to OPN upregulated expression of these stem/progenitor genes (Figure 4.6D). Moreover, the $CD44^+$ fraction of ESO26 cells demonstrated a higher tumorigenicity than the $CD44^-$ fraction, suggesting the $CD44^+$ cancer cells may serve as the cancer-propagating population to drive the tumor growth and even metastasis (Figure 4.7). In sum, these findings reveal the important role of OPN-CD44 signaling in the initiation and progression of GEJ cancer that may have clinical relevance.

4.4.4 WNT signaling receptor LGR5 serves as a tumor suppressor via regulating OPN expression

Previous study has suggested that WNT signaling suppresses the transcription of OPN encoding gene *Spp1* through the binding of WNT downstream effector TCF-4

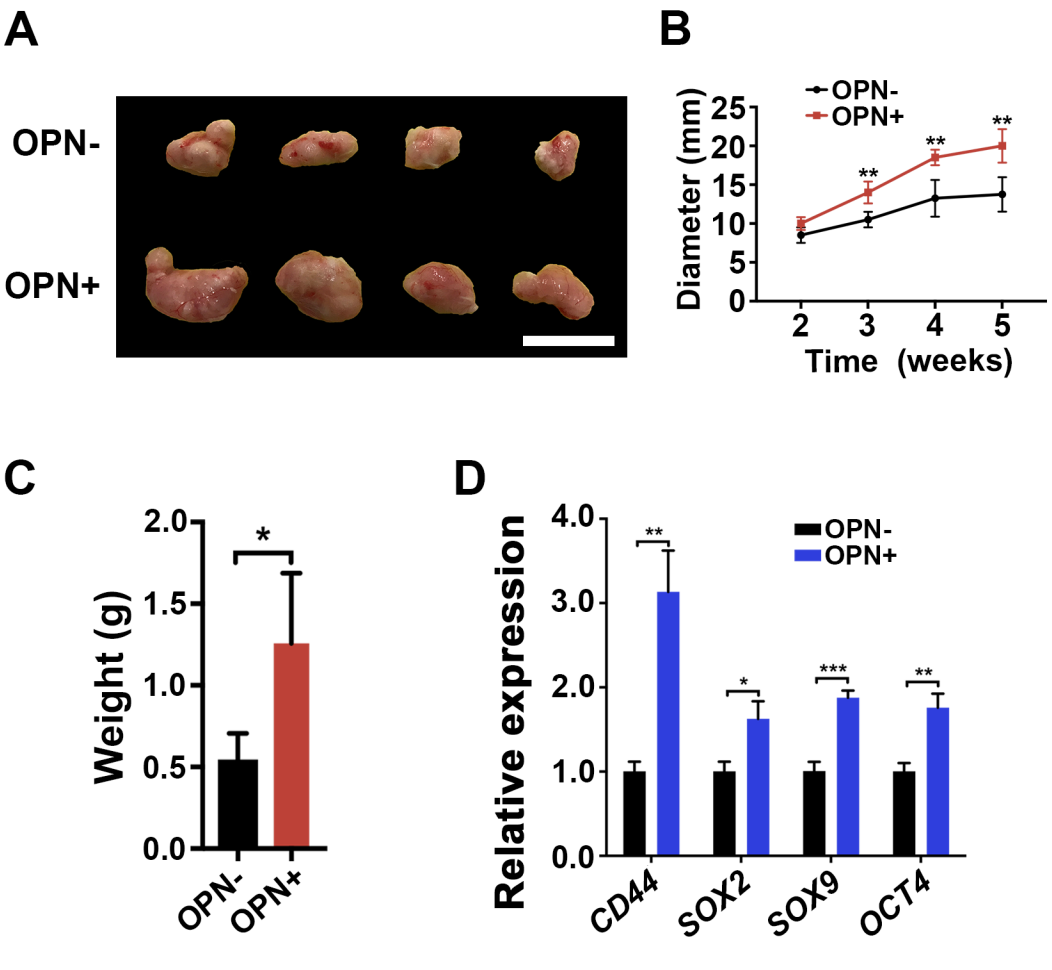
A
OPN-
OPN+
B
OPN-
OPN+
Diameter (mm)
25
20
15
10
5
0
2
3
4
5
Time (weeks)
**
**
**
C
Weight (g)
2.0
1.5
1.0
0.5
0.0
*
OPN-
OPN+
D
Relative expression
4.0
3.0
2.0
1.0
0.0
OPN-
OPN+
**
*
***
**
CD44
SOX2
SOX9
OCT4

Figure 4.6 OPN promotes the stemness and tumorigenicity of human GEJ cancers. (A to C) The size (A), growth (B), and weight (C) of subcutaneous ESO26 xenograft with or without OPN treatment prior to transplantation. (D) The relative gene expressions of ESO26 cells with or without OPN treatment. The scale bars represent 2 cm (A). *P<0.05. **P<0.01. ***P<0.001.

A

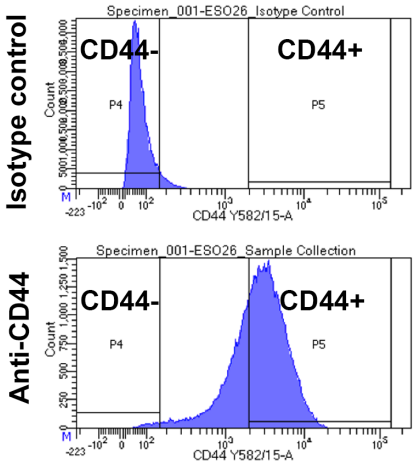

B

	CD44+	CD44-
10^5 cells	3/3 (100%)	1/3 (33.3%)
10^4 cells	2/3 (66.6%)	0/3 (0%)
10^3 cells	1/3 (33.3%)	0/3 (0%)

C

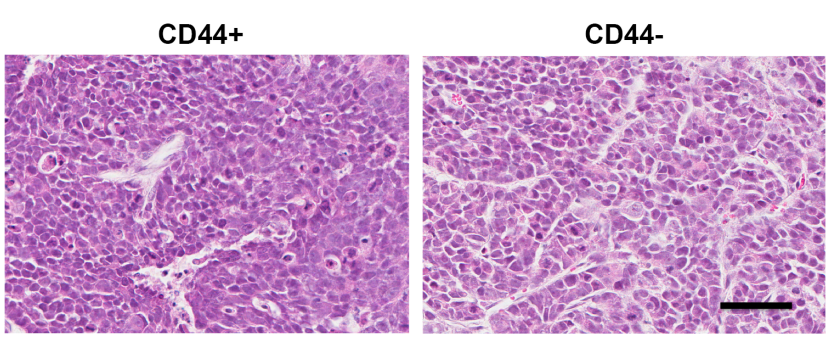

Figure 4.7. Preferential tumorigenicity of $CD44^+$ ESO26 cells. (A) Isolation of $CD44^+$ and $CD44^-$ ESO26 cells using Fluorescence-Activated Cell Sorting (FACS). (B) Tumorigenicity of serially diluted $CD44^+$ or $CD44^-$ ESO26 cells at 5-week post-injection. (C) Histology of tumors formed by either $CD44^+$ or $CD44^-$ ESO26 cells. Hematoxylin and eosin staining. Scale bar represents 60 μm in both images.

on the *Spp1* promoter sequence (Denhardt et al., 2003). Consistently, we found that the location of the OPN^+ cells in the first gland of SCJ regions mostly overlaps with the $Lgr5^-CD44^+$ immature populations rather than the $Lgr5^+$ stem cell niches (Figure 4.1). Importantly, our previous findings have shown that the $Lgr5^-CD44^+$ immature cells have significantly greater susceptibility to malignant transformation than the $Lgr5^+$ stem cell populations at the gastric SCJ region (Chapter 3). On the basis of these findings, we hypothesized that *LGR5* gene may functions as a tumor suppressor through downregulating OPN expression. To test this hypothesis we overexpressed the *LGR5* in ESO26 cells and analyzed their growth ability, gene expression and tumorigenicity. Overexpression of LGR5 downregulated the *SPP1* expression and also inhibited the growth and tumorigenicity of the ESO26 cells (Figure 4.8A to C). At the same time, shRNA-mediated knockdown of the WNT signaling downstream effector TCF4 restored the *SPP1* expression (Figure 4.8D). Conversely, deletion of *LGR5* using CRISPR/cas9-mediated gene editing promoted the ESO26 cell growth and tumorigenicity (Figure 4.9). These findings suggest that the Lgr5 signaling indeed has a tumor-suppressive function by negatively regulating the expression of cancer-promoting OPN.

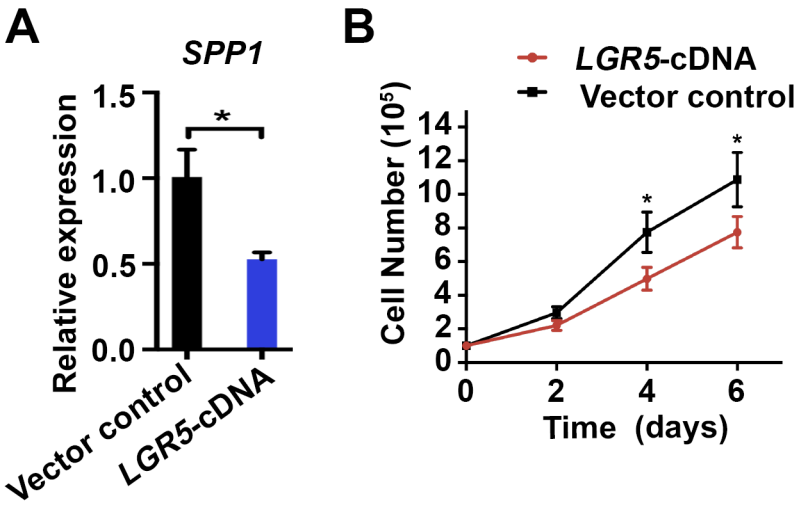

C

7-week p.i.

	LGR5-cDNA	Vector control
10^5 cells	3/3 (100%)	3/3 (100%)
10^4 cells	0/3 (0%)	2/3 (66.7%)
10^3 cells	1/3 (33.3%)	3/3 (100%)

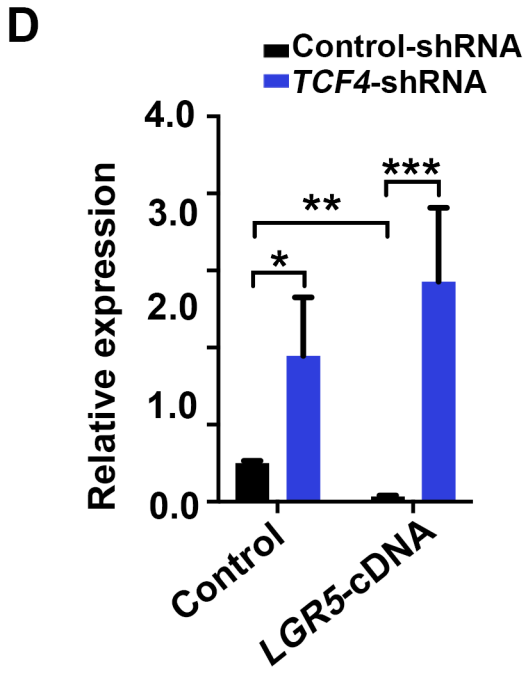

Figure 4.8 WNT signaling reduces the growth and tumorigenicity of human GEJ cancer through downregulation of *SPP1* expression. (A to C) LGR5 overexpression in ESO26 cells leads to *SPP1* downregulation (A), growth reduction (B), and tumorigenicity suppression (C). Normalized to vector control. (D) TCF-4 knockdown upregulates *SPP1* expression in ESO26 cells regardless of *LGR5* overexpression or not. Normalized to the control-shRNA before *LGR5* overexpression. *P<0.05. **P<0.01. ***P<0.001.

A

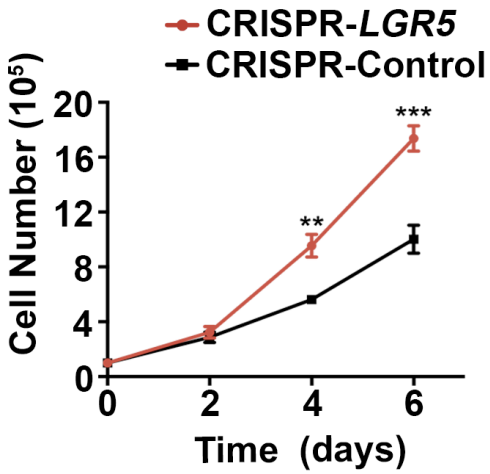

B

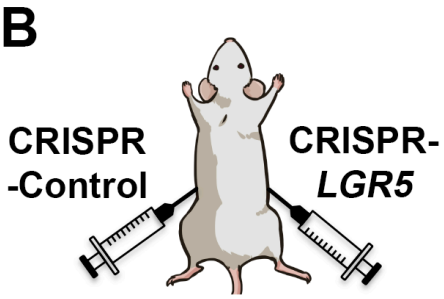

4 weeks p.i.

	CRISPR-Control	CRISPR-*LGR5*
10^5 cells	3/3 (100%)	3/3 (100%)
10^4 cells	0/3 (0%)	3/3 (100%)
10^3 cells	0/3 (0%)	0/3 (0%)

Figure 4.9 Effect of *LGR5* deletion on the growth and tumorigenicity of human GEJ cancer. (A and B) Comparison of growth (A) and tumorigenicity (B) of ESO26 cells before (CRISPR-Control) and after (CRISPR-*LGR5*) *LGR5* inactivation using CRISPR-mediated genetic editing. *P<0.05. **P<0.01. ***P<0.001.

4.5 Discussion

Our study provides several lines of direct evidence supporting the critical role of OPN-CD44 signaling in the initiation and progression of gastric SCJ cancers. First, the OPN is predominantly expressed by the pool of immature progenitor cells, which have shown to be highly susceptible to malignant transformation in our previous study (Chapter 3). Second, OPN appears to be a niche-derived factor promoting the tumorigenic potential of the gastric SCJ cells by enhancing their stem/progenitor cell properties. Third, the OPN and CD44 expression in human GEJ cancers correlate with the poor prognosis. Fourth, increased concentrations of OPN promote the stemness of human GEJ cancer, resulting in a higher tumorigenicity and more aggressive growth in immunodeficient mice. Collectively, these findings indicate that OPN-CD44 signaling may be a valuable target for designing new effective intervention strategies for treatment of SCJ cancer.

OPN has been shown to play an important role in tissue homeostasis and repair in a number of organs due to its pivotal effect on maintaining the stem cell properties in these tissues (Guidi et al., 2017; Liu et al., 2015; Nilsson et al., 2005; Stier et al., 2005; Wang et al., 2015; Wang et al., 2017). For example, OPN promotes the proliferation and migration of the neural stem cells during the neurogenesis that is a critical step for cerebral repair following ischemic injury (Rabenstein et al., 2015). On the other hand, aberration of OPN expression is highly associated with the development of various diseases including cancer (Shevde and Samant, 2014).

Interestingly, OPN overexpression stimulates the mammary epithelial cell proliferation and alveologenesis and also alters the mammary cell differentiation toward an immature progenitor status that leads to an expansion of stem/progenitor populations in the mammary glands predisposed to malignant transformation (Hubbard et al., 2013). Consistent with these findings, we observed that the $CD44^{+}$ immature progenitor cells at the first gland of SCJ can produce OPN. In this context, OPN may function as an essential autocrine factor responsible for increasing the stem-like phenotype, thereby promoting gastric epithelial regeneration, but also facilitating malignant transformation. Importantly, we also found that OPN is involved in a positive feedback loop mechanism allowing to enhance the signaling by increasing the receptor CD44 expression in gastric SCJ cells. In concordance with our observations, the OPN effect on increasing CD44 expression has also been reported in the cancers of other organs, such as the colon (Todaro et al., 2014), breast (Khan et al., 2005), and liver (Gao et al., 2003). Thus it may represent a critical mechanism by which OPN promotes the tumorigenic and metastatic potential of cancers.

The role of Lgr5 in cancer development and metastasis remains controversial (Morgan et al., 2018). Lgr5 has been recognized as a stem cell marker expressed by the proliferating adult stem cells in the intestine. Such cells possibly represent the cells of origin of some intestinal neoplasms (Barker et al., 2009; Barker et al., 2007; Schepers et al., 2012). Being an enhancer of Wnt/β-catenin signaling pathway, Lgr5 is involved in oncogenic activities of this pathway, such as cell proliferation,

migration, colony formation, and tumorigenicity in a wide variety of cancers (Cao et al., 2017; Effendi et al., 2014; Hirsch et al., 2014; Liu et al., 2018; Yang et al., 2015). Conversely, the tumor-suppressive function of Lgr5 has also been described on the basis of several clinical and experimental studies. First, epigenetic methylation of *LGR5* is commonly observed in the colon cancer patients, who have higher tumor grades and poor prognosis (Felipe de Sousa et al., 2011). Re-expression of LGR5 allows cancer cells to decrease the clonogenicity and tumorigenicity (Felipe de Sousa et al., 2011). Second, through interaction with its ligand R-spondin 2 (Rspo-2), Lgr5 functions as a negative regulator of Wnt-signaling to suppress the cancer proliferation and metastasis (Wu et al., 2014). Third, LGR5 has shown to be directly involved in the activation of TGF-β signaling, which is a well-known tumor inhibitory pathway associated with colon cancer cell survival, clonogenicity, and metastasis (Zhou et al., 2017). Here, we have provided a new insight into the tumor suppressive mechanism of LGR5 that involves decrease in OPN expression. Our observations show that overexpression of LGR5 in the ESO26 cells not only downregulates the OPN-encoding *SPP1* gene expression in a Wnt-signaling effector TCF-4-dependent manner but also suppresses the cell culture growth and tumorigenicity after transplantation into NSG mice. Conversely, knockout of LGR5 accelerates the growth of human GEJ cancer cells ESO26 in cell culture and increased their tumorigenicity These findings suggest the critical role of LGR5 in suppressing SCJ cancer progression and metastasis. They also indicate that downregulation of LGR5 expression as a part of cancer propagating cell targeting may have oncogenic effect in some tissues.

In sum, our data support the notion that the niche factor OPN plays an essential role in the homeostasis and carcinogenesis of gastric SCJ region via interacting with its receptor CD44. Lgr5 signaling may prevent the tumorigenic potential of target cells by suppressing cancer-promoting OPN-CD44 signaling. Thus our findings provide the rationale for development of approaches based on targeting OPN-CD44 signaling in gastric SCJ cancer. They also caution against application of Lgr5-targeted therapies in cancers with activeOPN-CD44 pathway.

References

Ahmed, M., Sottnik, J.L., Dancik, G.M., Sahu, D., Hansel, D.E., Theodorescu, D., and Schwartz, M.A. (2016). An Osteopontin/CD44 Axis in RhoGDI2-Mediated Metastasis Suppression. Cancer cell *30*, 432-443.

Barker, N., Ridgway, R.A., van Es, J.H., van de Wetering, M., Begthel, H., van den Born, M., Danenberg, E., Clarke, A.R., Sansom, O.J., and Clevers, H. (2009). Crypt stem cells as the cells-of-origin of intestinal cancer. Nature … *457*, 608-611.

Barker, N., van Es, J.H., Kuipers, J., Kujala, P., van den Born, M., Cozijnsen, M., Haegebarth, A., Korving, J., Begthel, H., Peters, P.J.*, et al.* (2007). Identification of stem cells in small intestine and colon by marker gene Lgr5. Nature … *449*, 1003-1007.

Bellahcène, A., Castronovo, V., Ogbureke, K.U.E., Fisher, L.W., and Fedarko, N.S. (2008). Small integrin-binding ligand N-linked glycoproteins (SIBLINGs): multifunctional proteins in cancer. Nature reviews Cancer *8*, 212-226.

Botterweck, A.A., Schouten, L.J., Volovics, A., Dorant, E., and van den Brandt, P.A. (2000). Trends in incidence of adenocarcinoma of the oesophagus and gastric cardia in ten European countries. International journal of epidemiology *29*, 645-654.

Brown, L.F., Berse, B., Van de Water, L., Papadopoulos-Sergiou, A., Perruzzi, C.A., Manseau, E.J., Dvorak, H.F., and Senger, D.R. (1992). Expression and distribution of osteopontin in human tissues: widespread association with luminal epithelial surfaces. Mol Biol Cell *3*, 1169-1180.

Buas, M.F., and Vaughan, T.L. (2013). Epidemiology and risk factors for gastroesophageal junction tumors: understanding the rising incidence of this disease. Seminars in radiation oncology *23*, 3-9.

Cao, H.-Z., Liu, X.-F., Yang, W.-T., Chen, Q., and Zheng, P.-S. (2017). LGR5 promotes cancer stem cell traits and chemoresistance in cervical cancer. Nature Publishing Group *8*, e3039.

Chen, Y., Fu, Z., Xu, S., Xu, Y., and Xu, P. (2014). The prognostic value of CD44 expression in gastric cancer: a meta-analysis. Biomed Pharmacother *68*, 693-697.

Denhardt, D.T., Mistretta, D., Chambers, A.F., Krishna, S., Porter, J.F., Raghuram, S., and Rittling, S.R. (2003). Transcriptional regulation of osteopontin and the metastatic phenotype: evidence for a Ras-activated

enhancer in the human OPN promoter. Clinical and Experimental Metastasis *20*, 77-84.

Effendi, K., Yamazaki, K., Fukuma, M., and Sakamoto, M. (2014). Overexpression of Leucine-Rich Repeat-Containing G Protein-Coupled Receptor 5 (LGR5) Represents a Typical Wnt/β-Catenin Pathway-Activated Hepatocellular Carcinoma. Liver Cancer *3*, 451-457.

Felipe de Sousa, E.M., Colak, S., Buikhuisen, J., Koster, J., Cameron, K., de Jong, J.H., Tuynman, J.B., Prasetyanti, P.R., Fessler, E., and van den Bergh, S.P. (2011). Methylation of cancer-stem-cell-associated Wnt target genes predicts poor prognosis in colorectal cancer patients. Cell stem cell *9*, 476-485.

Festa, E., Fretz, J., Berry, R., Schmidt, B., Rodeheffer, M., Horowitz, M., and Horsley, V. (2011). Adipocyte lineage cells contribute to the skin stem cell niche to drive hair cycling. Cell *146*, 761-771.

Flesken-Nikitin, A., Odai-Afotey, A.A., and Nikitin, A.Y. (2014). Role of the stem cell niche in the pathogenesis of epithelial ovarian cancers. Molecular & cellular oncology *1*, e963435.

Franzén, A., and Heinegård, D. (1985). Isolation and characterization of two sialoproteins present only in bone calcified matrix. Biochem J *232*, 715-724.

Fu, D.-J., Miller, A.D., Southard, T.L., Flesken-Nikitin, A., Ellenson, L.H., and Nikitin, A.Y. (2018). Stem Cell Pathology. Annu Rev Pathol *13*, 71-92.

Gao, C., Guo, H., Downey, L., Marroquin, C., Wei, J., and Kuo, P.C. (2003). Osteopontin-dependent CD44v6 expression and cell adhesion in HepG2 cells. CARCIN *24*, 1871-1878.

Gu, X., Gao, X.-S., Ma, M., Qin, S., Qi, X., Li, X., Sun, S., Yu, H., Wang, W., and Zhou, D. (2016). Prognostic significance of osteopontin expression in gastric cancer: a meta-analysis. Oncotarget *7*, 69666-69673.

Guidi, N., Sacma, M., Ständker, L., Soller, K., Marka, G., Eiwen, K., Weiss, J.M., Kirchhoff, F., Weil, T., Cancelas, J.A.*, et al.* (2017). Osteopontin attenuates aging-associated phenotypes of hematopoietic stem cells. The EMBO journal *36*, 840-853.

Haga, R.B., and Ridley, A.J. (2016). Rho GTPases: Regulation and roles in cancer cell biology. Small GTPases *7*, 207-221.

Hirsch, D., Barker, N., McNeil, N., Hu, Y., Camps, J., McKinnon, K., Clevers, H., Ried, T., and Gaiser, T. (2014). LGR5 positivity defines stem-like cells in colorectal cancer. Carcin *35*, 849-858.

Hsu, Y.-C., and Fuchs, E. (2012). A family business: stem cell progeny join the niche to regulate homeostasis. Nature reviews Molecular cell biology *13*, 103.

Hu, Z.-D., Wei, T.-T., Yang, M., Ma, N., Tang, Q.-Q., Qin, B.-D., Fu, H.-T., and Zhong, R.-Q. (2015). Diagnostic value of osteopontin in ovarian cancer: A meta-analysis and systematic review. PLoS ONE *10*, e0126444.

Hubbard, N.E., Chen, Q.J., Sickafoose, L.K., Wood, M.B., Gregg, J.P., Abrahamsson, N.M., Engelberg, J.A., Walls, J.E., and Borowsky, A.D. (2013). Transgenic mammary epithelial osteopontin (spp1) expression induces proliferation and alveologenesis. Genes Cancer *4*, 201-212.

Hwang, C.-I., Matoso, A., Corney, D.C., Flesken-Nikitin, A., Körner, S., Wang, W., Boccaccio, C., Thorgeirsson, S.S., Comoglio, P.M., and Hermeking, H. (2011). Wild-type p53 controls cell motility and invasion by dual regulation of MET expression. Proceedings of the National Academy of Sciences *108*, 14240-14245.

Jiang, M., Li, H., Zhang, Y., Yang, Y., Lu, R., Liu, K., Lin, S., Lan, X., Wang, H., Wu, H.*, et al.* (2017). Transitional basal cells at the squamous-columnar junction generate Barrett's oesophagus. Nature *550*, 529-533

Katagiri, Y.U., Sleeman, J., Fujii, H., Herrlich, P., Hotta, H., Tanaka, K., Chikuma, S., Yagita, H., Okumura, K., and Murakami, M. (1999). CD44 variants but not CD44s cooperate with β1-containing integrins to permit cells to bind to osteopontin independently of arginine-glycine-aspartic acid, thereby stimulating cell motility and chemotaxis. Cancer research *59*, 219-226.

Khan, S.A., Cook, A.C., Kappil, M., Gunthert, U., Chambers, A.F., Tuck, A.B., and Denhardt, D.T. (2005). Enhanced cell surface CD44 variant (v6, v9) expression by osteopontin in breast cancer epithelial cells facilitates tumor cell migration: novel post-transcriptional, post-translational regulation. Clin Exp Metastasis *22*, 663-673.

Kim, M.A., Lee, H.S., Yang, H.-K., and Kim, W.H. (2005). Clinicopathologic and protein expression differences between cardia carcinoma and noncardia carcinoma of the stomach. Cancer *103*, 1439-1446.

Kusano, C., Gotoda, T., Khor, C.J., Katai, H., Kato, H., Taniguchi, H., and Shimoda, T. (2008). Changing trends in the proportion of adenocarcinoma of the esophagogastric junction in a large tertiary referral center in Japan. Journal of gastroenterology and hepatology *23*, 1662-1665.

Lau, E.Y.-T., Ho, N.P.-Y., and Lee, T.K.-W. (2017). Cancer Stem Cells and Their Microenvironment: Biology and Therapeutic Implications. Stem Cells Int *2017*, 3714190.

Li, Z., Bao, S., Wu, Q., Wang, H., Eyler, C., Sathornsumetee, S., Shi, Q., Cao, Y., Lathia, J., and McLendon, R.E. (2009). Hypoxia-inducible factors regulate tumorigenic capacity of glioma stem cells. Cancer cell *15*, 501-513.

Lin, J., Myers, A.L., Wang, Z., Nancarrow, D.J., Ferrer-Torres, D., Handlogten, A., Leverenz, K., Bao, J., Thomas, D.G., Wang, T.D.*, et al.* (2015). Osteopontin (OPN/SPP1) isoforms collectively enhance tumor cell invasion and dissemination in esophageal adenocarcinoma. Oncotarget *6*, 22239-22257.

Lin, Y.-H., and Yang-Yen, H.-F. (2001). The osteopontin-CD44 survival signal involves activation of the phosphatidylinositol 3-kinase/Akt signaling pathway. Journal of Biological Chemistry *276*, 46024-46030.

Liu, W., Zhang, J., Gan, X., Shen, F., Yang, X., Du, N., Xia, D., Liu, L., Qiao, L., and Pan, J. (2018). LGR 5 promotes epithelial ovarian cancer proliferation, metastasis, and epithelial–mesenchymal transition through the Notch1 signaling pathway. Cancer medicine.

Liu, Y., Cao, L., Chen, R., Zhou, X., Fan, X., Liang, Y., Jia, R., Wang, H., Liu, G., Guo, Y.*, et al.* (2015). Osteopontin Promotes Hepatic Progenitor Cell Expansion and Tumorigenicity via Activation of beta-Catenin in Mice. Stem Cells *33*, 3569-3580.

Mertens, A.E., Roovers, R.C., and Collard, J.G. (2003). Regulation of Tiam1-Rac signalling. FEBS Lett *546*, 11-16.

Mi, Z., Bhattacharya, S.D., Kim, V.M., Guo, H., Talbot, L.J., and Kuo, P.C. (2011). Osteopontin promotes CCL5-mesenchymal stromal cell-mediated breast cancer metastasis. Carcin *32*, 477-487.

Nemir, M., Bhattacharyya, D., Li, X., Singh, K., Mukherjee, A.B., and Mukherjee, B.B. (2000). Targeted inhibition of osteopontin expression in the mammary gland causes abnormal morphogenesis and lactation deficiency. J Biol Chem *275*, 969-976.

Nilsson, S.K., Johnston, H.M., Whitty, G.A., Williams, B., Webb, R.J., Denhardt, D.T., Bertoncello, I., Bendall, L.J., Simmons, P.J., and Haylock, D.N. (2005). Osteopontin, a key component of the hematopoietic stem cell niche and regulator of primitive hematopoietic progenitor cells. Blood *106*, 1232-1239.

Okamoto, I., Kawano, Y., Murakami, D., Sasayama, T., Araki, N., Miki, T., Wong, A.J., and Saya, H. (2001). Proteolytic release of CD44 intracellular domain and its role in the CD44 signaling pathway. J Cell Biol *155*, 755-762.

Ordonez, P., and Di Girolamo, N. (2012). Limbal epithelial stem cells: role of the niche microenvironment. Stem cells (Dayton, Ohio) *30*, 100-107.

Pietras, A., Katz, A.M., Ekström, E.J., Wee, B., Halliday, J.J., Pitter, K.L., Werbeck, J.L., Amankulor, N.M., Huse, J.T., and Holland, E.C. (2014). Osteopontin-CD44 signaling in the glioma perivascular niche enhances cancer stem cell phenotypes and promotes aggressive tumor growth. Cell Stem Cell *14*, 357-369.

Quante, M., Bhagat, G., Abrams, J.A., Marache, F., Good, P., Lee, M.D., Lee, Y., Friedman, R., Asfaha, S., Dubeykovskaya, Z*., et al.* (2012). Bile acid and inflammation activate gastric cardia stem cells in a mouse model of Barrett-like metaplasia. Cancer Cell *21*, 36-51.

Quante, M., Tu, S.P., Tomita, H., Gonda, T., Wang, S.S., Takashi, S., Baik, G.H., Shibata, W., DiPrete, B., and Betz, K.S. (2011). Bone marrow-derived myofibroblasts contribute to the mesenchymal stem cell niche and promote tumor growth. Cancer Cell *19*, 257-272.

Rabenstein, M., Hucklenbroich, J., Willuweit, A., Ladwig, A., Fink, G.R., Schroeter, M., Langen, K.-J., and Rueger, M.A. (2015). Osteopontin mediates survival, proliferation and migration of neural stem cells through the chemokine receptor CXCR4. Stem Cell Res Ther *6*, 99.

Rangaswami, H., Bulbule, A., and Kundu, G.C. (2006). Osteopontin: role in cell signaling and cancer progression. Trends in cell biology *16*, 79-87.

Reinholt, F.P., Hultenby, K., Oldberg, A., and Heinegård, D. (1990). Osteopontin--a possible anchor of osteoclasts to bone. Proceedings of the National Academy of Sciences *87*, 4473-4475.

Sato, T., Van Es, J.H., Snippert, H.J., Stange, D.E., Vries, R.G., Van Den Born, M., Barker, N., Shroyer, N.F., Van De Wetering, M., and Clevers, H. (2011). Paneth cells constitute the niche for Lgr5 stem cells in intestinal crypts. Nature *469*, 415.

Schepers, A.G., Snippert, H.J., Stange, D.E., van den Born, M., van Es, J.H., van de Wetering, M., and Clevers, H. (2012). Lineage tracing reveals Lgr5+ stem cell activity in mouse intestinal adenomas. Science *337*, 730-735.

Shevde, L.A., and Samant, R.S. (2014). Role of osteopontin in the pathophysiology of cancer. Matrix Biol *37*, 131-141.

Singh, K., Balligand, J.L., Fischer, T.A., Smith, T.W., and Kelly, R.A. (1995). Glucocorticoids increase osteopontin expression in cardiac myocytes and microvascular endothelial cells. Role in regulation of inducible nitric oxide synthase. J Biol Chem *270*, 28471-28478.

Stier, S., Ko, Y., Forkert, R., Lutz, C., Neuhaus, T., Grunewald, E., Cheng, T., Dombkowski, D., Calvi, L.M., Rittling, S.R.*, et al.* (2005). Osteopontin is a hematopoietic stem cell niche component that negatively regulates stem cell pool size. The Journal of experimental medicine *201*, 1781-1791.

Sun, B.-S., Li, Y., Zhang, Z.-F., You, J., and Wang, C.-L. (2013). Osteopontin combined with CD44v6, a novel prognostic biomarker in non-small cell lung cancer undergoing curative resection. Ann Thorac Surg *96*, 1943-1951.

Tilli, T.M., Franco, V.F., Robbs, B.K., Wanderley, J.L.M., da Silva, F.R.d.A., de Mello, K.D., Viola, J.P.B., Weber, G.F., and Gimba, E.R. (2011). Osteopontin-c splicing isoform contributes to ovarian cancer progression. Mol Cancer Res *9*, 280-293.

Todaro, M., Gaggianesi, M., Catalano, V., Benfante, A., Iovino, F., Biffoni, M., Apuzzo, T., Sperduti, I., Volpe, S., Cocorullo, G.*, et al.* (2014). CD44v6 Is a Marker of Constitutive and Reprogrammed Cancer Stem Cells Driving Colon Cancer Metastasis. Stem Cell *14*, 342-356.

Wang, G., Li, X., Chen, S., Zhao, W., Yang, J., Chang, C., and Xu, C. (2015). Expression profiles uncover the correlation of OPN signaling pathways with rat liver regeneration at cellular level. Cell biology international *39*, 1329-1340.

Wang, W., Li, P., Li, W., Jiang, J., Cui, Y., Li, S., and Wang, Z. (2017). Osteopontin activates mesenchymal stem cells to repair skin wound. PLoS ONE *12*, e0185346.

Wei, R., Wong, J.P.C., and Kwok, H.F. (2017). Osteopontin -- a promising biomarker for cancer therapy. Journal of Cancer *8*, 2173-2183.

White, A.C., and Lowry, W.E. (2015). Refining the role for adult stem cells as cancer cells of origin. Trends in cell biology *25*, 11-20.

Wu, C., Qiu, S., Lu, L., Zou, J., Li, W.-f., Wang, O., Zhao, H., Wang, H., Tang, J., Chen, L.*, et al.* (2014). RSPO2-LGR5 signaling has tumour-suppressive activity in colorectal cancer. Nat Commun *5*, 3149.

Xie, Z., Singh, M., Siwik, D.A., Joyner, W.L., and Singh, K. (2003). Osteopontin Inhibits Interleukin-1-stimulated Increases in Matrix Metalloproteinase Activity in Adult Rat Cardiac Fibroblasts. Journal of Biological Chemistry *278*, 48546-48552.

Yang, L., Tang, H., Kong, Y., Xie, X., Chen, J., Song, C., Liu, X., Ye, F., Li, N., and Wang, N. (2015). LGR5 Promotes Breast Cancer Progression and Maintains Stem-Like Cells Through Activation of Wnt/β-Catenin Signaling. Stem cells *33*, 2913-2924.

Zhang, Z.-X., Shek, K., Wang, S., Huang, X., Lau, A., Yin, Z., Sun, H., Liu, W., Garcia, B., and Rittling, S. (2010). Osteopontin expressed in tubular epithelial cells regulates NK cell-mediated kidney ischemia reperfusion injury. The Journal of Immunology *185*, 967-973.

Zhao, M., Liang, F., Zhang, B., Yan, W., and Zhang, J. (2015). The impact of osteopontin on prognosis and clinicopathology of colorectal cancer patients: a systematic meta-analysis. Scientific Reports *5*, 12713.

Zhou, X., Geng, L., Wang, D., Yi, H., Talmon, G., and Wang, J. (2017). R-Spondin1/LGR5 Activates TGFβ Signaling and Suppresses Colon Cancer Metastasis. Cancer research *77*, 6589-6602.

CHAPTER 5

SUMMARY AND FUTURE DIRECTIONS

5.1 Summary

In Chapter 2, we have found that the *Lgr5*$^{+}$ stem cell lineage in the first pit of gastric squamous-columnar junction (SCJ) is highly susceptible to the malignant transformation following inactivation of tumor suppressors *Trp53* and *Rb1.* Through lineage tracing experiments, *Lgr5*$^{+}$ stem cells were identified as the adult stem cells responsible for routine epithelial homeostasis of the first pit of gastric squamous-columnar junction (SCJ) as well as the antrum region, consistent with the previous report (Barker et al., 2010). However, the metastatic poorly differentiated carcinomas arose only from the SCJ region, while only few benign neoplasms were observed in the antrum after identical conditional inactivation of *Trp53* and *Rb1*. These findings support the notion that epithelial transitional zones (TZ)/junctional regions are highly cancer-prone (Botterweck et al., 2000; Buas and Vaughan, 2013; Fu et al., 2018; Jiang et al., 2017; Kim et al., 2005; Kusano et al., 2008; Quante et al., 2012). Moreover, the gastric SCJ cancer in our mouse model represented histologic and genetic characteristics resembling human disease (Isinger-Ekstrand et al., 2010; Kim et al., 2005). Of note, Lgr5 expression was detected in neither primary nor metastatic carcinomas in our mouse model, indicating a dispensable role for Lgr5 in the SCJ carcinogenesis. On the other hand, a number of cancer cells have expressed another stem/progenitor-associated marker, CD44, which is highly associated with the

pathogenesis of various cancers including those of the prostate, ovary, liver, intestine and stomach (Alam et al., 2004; Ghaffarzadehgan et al., 2008; Morath et al., 2016; Noordzij et al., 1997).

To further explore the critical role of CD44 in cancer initiation and progression, in Chapter 3, we inactivated *Cd44* in the primary mouse gastric organoids using CRISPR/cas9-mediated genetic editing. The results revealed that the *Trp53/Rb1*-mediated transformation phenotypes were abrogated by *Cd44* inactivation. Moreover, we have also found that, unlike glands of the antral region, the first gland of gastric SCJ contains a large fraction of highly proliferative $Lgr5^{-}CD44^{+}$ immature progenitor cells. Of note, these $Lgr5^{-}CD44^{+}$ immature cells were most susceptible to malignant transformation following oncogenic mutations, as compared to other stages of Lgr5 lineage differentiation. By characterization of sequential stages of carcinogenesis and organoid cultures, we identified the $Lgr5^{-}CD44^{+}$ immature cells as the most likely target for malignant transformation of gastric SCJ epithelium. Thus, our findings support the notion that the preferential susceptibility of epithelial junctions to the cancer formation may be attributed to the presence of expanded pools of immature cells (Figure 5.1).

The niche factors are known to play important roles in determining the fate of stem/progenitor cells and enhancing the tumorigenic potentials of transformed cells

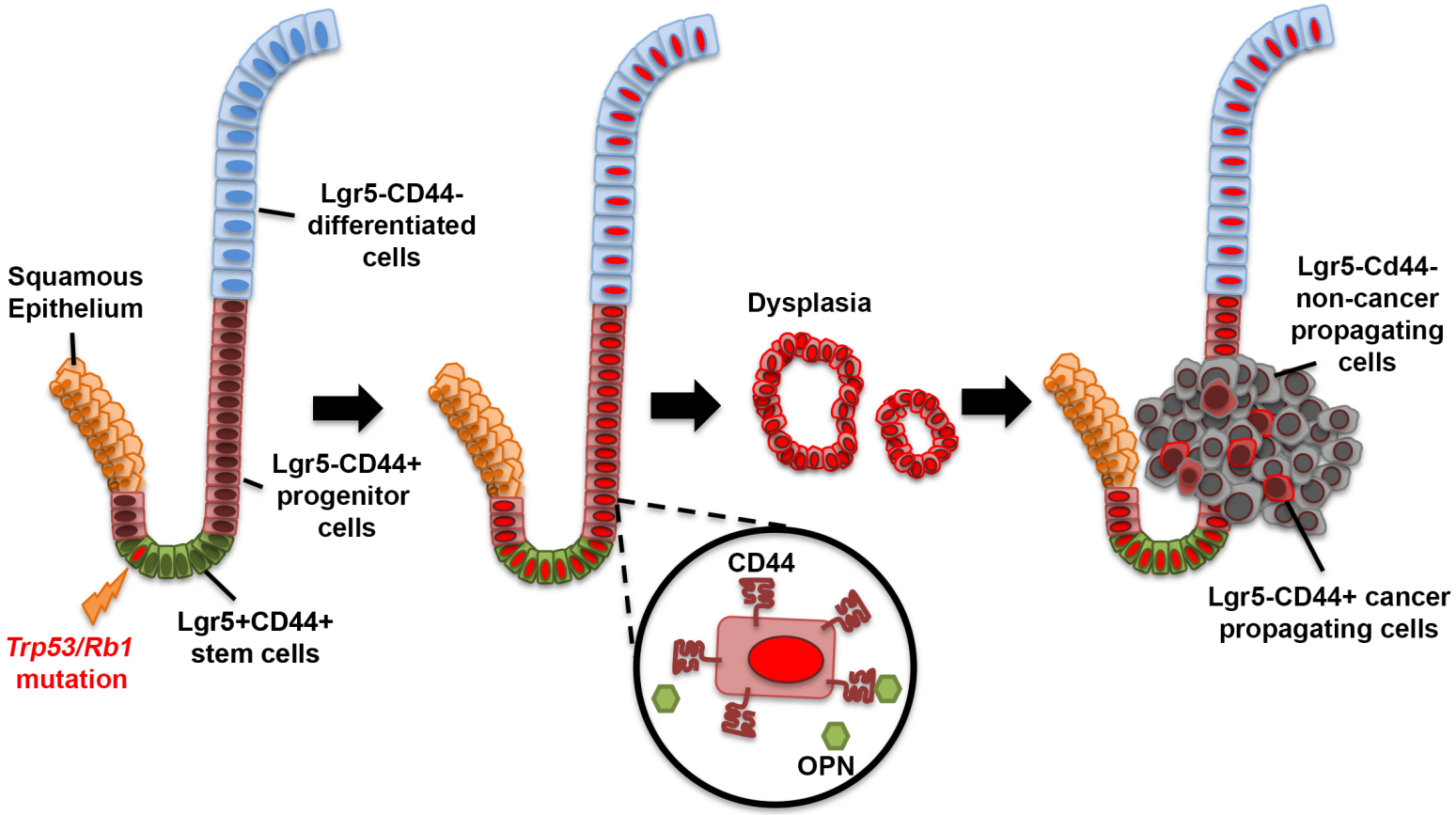

Figure 5.1 Carcinogenesis at the gastric squamous-columnar junction.

(Festa et al., 2011; Flesken-Nikitin et al., 2014; Hsu and Fuchs, 2012; Lau et al., 2017; Ordonez and Di Girolamo, 2012; Quante et al., 2012; Quante et al., 2011; Sato et al., 2011; White and Lowry, 2015). Based on the findings described in Chapter 4, CD44 ligand osteopontin (OPN) is preferentially expressed by the cancer-prone immature progenitor cells at the gastric SCJ. In such cells OPN promotes both the physiological epithelial regeneration and malignant transformation (Figure 5.2). These OPN-mediated effects can be abrogated by inactivation of *Cd44*, suggesting that CD44 may be the main effector of the OPN signaling. Consistent with our findings in mouse experiments, the exogenous OPN was sufficient to promote the stemness, growth, and tumorigenicity of human gastroesophageal junction (GEJ) cancer cells. Furthermore, supporting critical roles of OPN-CD44 signaling in the gastric SCJ carcinogenesis, CD44 and OPN expression correlated with shorter post-operative survival time observed in patients with GEJ cancers. Consistent with the observation in the previous study (Denhardt et al., 2003), we have found that LGR5 expression downregulates the expression of OPN-encoding gene *SPP1* and knockdown of the WNT downstream effector TCF4 restores the *SPP1* expression (Figure 5.2), Moreover, we have also found that CRISPR-Cas9-mediated knockout of LGR5 accelerates the growth of human GEJ cancer cells and increases their tumorigenicity after transplantation into NSG mice. Conversely, overexpression of *LGR5* in the cancer cells suppressed both phenotypes. These results provide a new perspective on the tumor-inhibitory role for Lgr5, indicating that Lgr5 may be a potential molecular marker

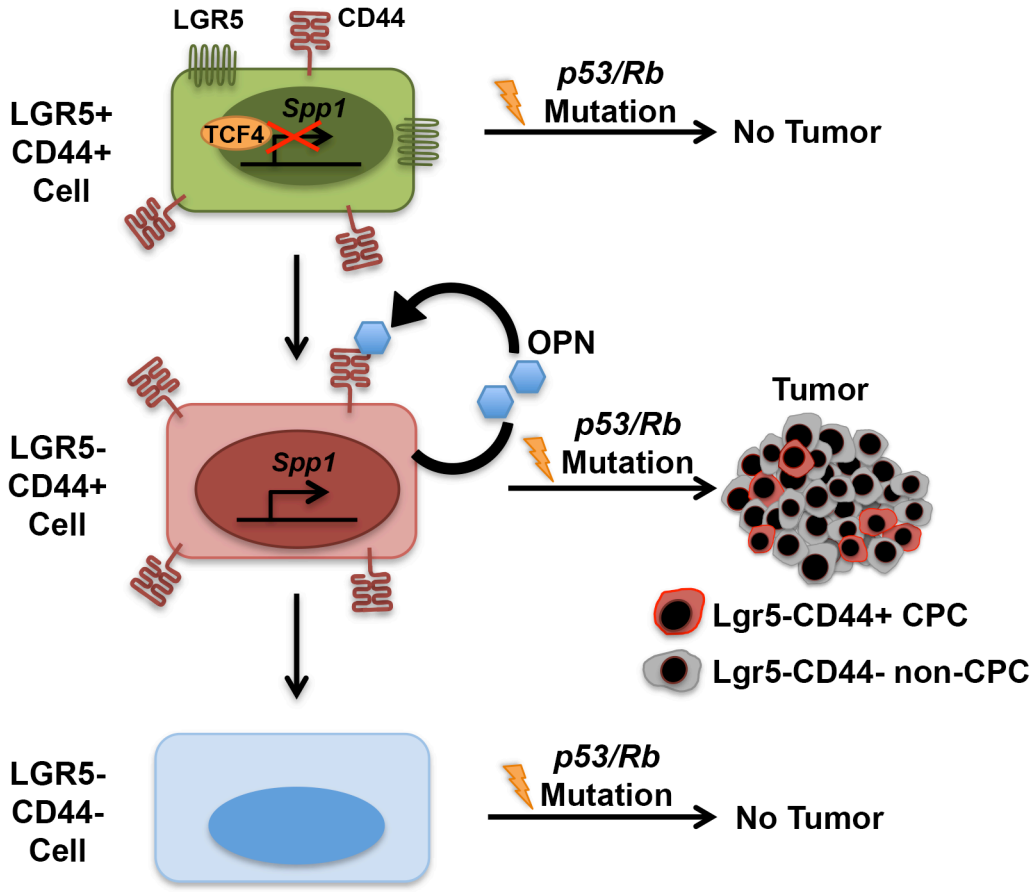

Figure 5.2 Proposed model of OPN-mediated oncogenic mechanism

for prognosis prediction of patients with gastric SCJ cancer. At the same time, insufficiently specific therapeutic targeting of $LGR5^+$ cancer propagating cells observed in other cancer types may lead to the increased risk of carcinogenesis in organs where LGR5 plays tumor suppressive role.

5.2 Future directions

5.2.1 Characterization of $Lgr5^-CD44^+$ immature progenitor cells

In rapidly self-renewing tissues, such as gastrointestinal epithelium, the tissue homeostasis and regeneration are fueled by a small population of adult stem cells, which resides at specialized anatomical locations and possess capacity to generate all differentiated lineages throughout life (Barker et al., 2010; Díaz-Flores et al., 2006). During this normal physiological process, the adult stem cells routinely produce the highly proliferating progenitors, often called transit amplifying (TA) cells, and commit to further differentiation into terminal multi-lineages with specialized functions (Barker, 2014; Tetteh et al., 2015). In Chapter 3, we identified a cancer-prone immature population that positions between the $Lgr5^+$ stem cell niche and terminally differentiated cells in the first gland of gastric SCJ region. Our lineage tracing results also demonstrated that these $Lgr5^-CD44^+$ immature progenitors represent the transient progeny of $Lgr5^+$ stem cells during physiological homeostasis. Therefore, the $Lgr5^-CD44^+$ immature cells may function as the TA cells in the first gland of SCJ. Of note, the role of TA cells in carcinogenesis varies among tissues. In

the hair follicle, for example, oncogenic mutations such as expression of *Kras*^{D12} and inactivation of *Trp53* in the TA cell are not sufficient to initiate tumor formation, while the adult stem cells which have been exposed to similar genetic alterations can be transformed to malignancy (Lapouge et al., 2011; White et al., 2011). On the other hand, the multiple progenitor (MPP), which is the TA population in bone marrow, has been implicated in the tumorigenesis of hematopoietic system (Yang et al., 2017). Through large-scale analysis of leukemia patient samples, the predominant population of leukemic cells has proven most similar to normal MPP cells among all hematopoietic lineage hierarchies, indicating that MPP population may be the cellular origin of leukemia (Goardon et al., 2011).

Our data support a possibility that the TA cells, at least in some cases, can be preferentially transformed. At the same time, we cannot exclude that the Lgr5^{-}CD44^{+} cells function as a distinct population of stem cell in the first gland of the gastric SCJ region. With *in vitro* 3D culture system, the Lgr5^{-}CD44^{+} cells can propagate and generate new organoids over long-term consecutive passages, suggesting a possible self-renewing capacity of this population. To gain a better understanding of the lineage hierarchy of Lgr5^{-}CD44^{+} immature cell in gastric epithelium, we will generate transgenic *Cd44-CreERT2* mice in which the inducible Cre recombinase (CreERT2) is driven by the *Cd44* promoter (Figure 5.3). These mice will be crossbred with *Lgr5-DTR* and Ai9 reporter mice. These *Cd44-CreERT2:Lgr5-DTR:*Ai9 mice can be used to trace the fate of Lgr5^{-}CD44^{+} cells after a single pulse of tamoxifen, which can induce tdTomato fluorescence expression via Cre-mediated which can induce

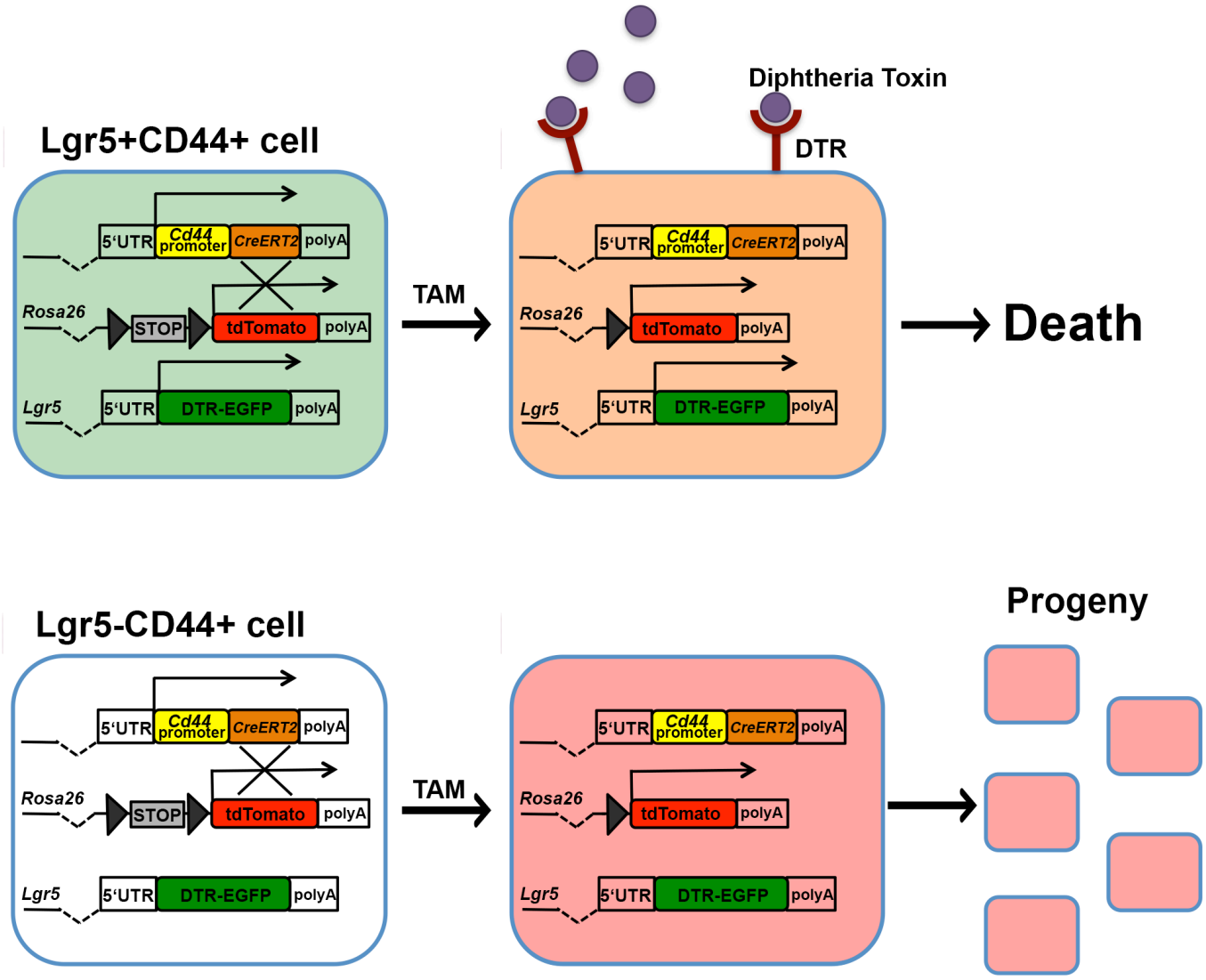

Figure 5.3 Experimental design for lineage tracing of Lgr5^{-}CD44^{+} immature progenitor cells using Cd44-*CreERT2:Lgr5-DTR:*Ai9 mice

tdTomato fluorescence expression via Cre-mediated recombination. Furthermore, the full regenerative potential of $Lgr5^{-}CD44^{+}$ cells can be explored after depletion of $Lgr5^{+}$ cells by diphtheria toxin injection (Figure 5.3).

CD44+ is expressed in many tissues, including hematopoietic cells, which may limit the use of Cd44-*CreERT2* mice in carcinogenesis studies. To identify promoters specific for SCJ $Lgr5^{-}CD44^{+}$ cells. To achieve this goal, we will isolate $Lgr5^{+}CD44^{+}$, $Lgr5^{-}CD44^{+}$, and $Lgr5^{-}CD44^{-}$ cells derived from mouse gastric SCJ epithelium using fluorescence-activated cell sorting (FACS), and then identify the genes which are specifically expressed in $Lgr5^{-}CD44^{+}$ cells through RNA-sequencing analysis of the genetic expression profiles. Computational promoter analysis of selected genes will be performed, following by preparation of transgenes in which CreERT2 is driven by $Lgr5^{-}CD44^{+}$-cell specific promoter. Crossing the $Lgr5^{-}CD44^{+}$ cell-specific CreERT2 mice with the mice carrying conditional alleles of *Trp53* and *Rb1* will allow us to examine the role of $Lgr5^{-}CD44^{+}$ cells in gastric SCJ carcinogenesis. Generation of the $Lgr5^{-}CD44^{+}$ cell-specific inducible Cre mice would be a promising approach for in-depth study of the role of this immature population in normal homeostasis and carcinogenesis.

5.2.2 Translation from animal model to human disease

One of the major challenges in the field of current biomedical research is how to bridge the gap between the laboratory and clinic, because many animal models do not faithfully recapitulate the pathological features of human disease. As a consequence, many novel therapeutic regimens based on results of laboratory experiments ultimately fail in clinical trials (Barré-Sinoussi and Montagutelli, 2015; Matthews, 2008; McGonigle and Ruggeri, 2014; van der Worp et al., 2010). Thus the discoveries obtained from animal models should be interpreted and validated more cautiously before applying to human clinical medicine.

Recently, the rapid advances in organoid culture have opened new avenues for translation of basic medical research into clinical application in an efficient way (Drost and Clevers, 2018). Unlike conventional *in vitro* two-dimensional (2D) culture, the organoids show the near-physiological characteristics resembling the organ they are derived from via mimicking their architectures and cellular compositions (Antoni et al., 2015; Fatehullah et al., 2016). These *in vitro* 3D culture systems provide an in-depth analysis of a range of biological processes including the organ development, tissue renewal from single stem cell, niche factor functions, and tissue responses to injury, infection, oncogenic stress, and drugs (Bartfeld et al., 2015; Boj et al., 2015; Cruz-Acuña et al., 2017; Dedhia et al., 2016; Drost et al., 2017; McCracken et al., 2014; Sato et al., 2011; Sato et al., 2009; Vlachogiannis et al., 2018; Voges et al., 2017; Weeber et al., 2017). Moreover, organoid technology allows for long-term expansion of some normal, untransformed, primary human tissues which usually do not grow in conventional 2D culture conditions (Boj et al., 2015; Li et al., 2016). For cancer

research, the 3D culture models have been widely used in various studies such as identification of cancer-propagating cells (Shimokawa et al., 2017), investigation for the mutation process underlying tumorigenesis (Blokzijl et al., 2016; De Sousa E Melo et al., 2017; Roerink et al., 2018), and high-throughput drug screen for development of novel and personalized medicine (Cristobal et al., 2017; Gao et al., 2014; Sachs et al., 2018; van de Wetering et al., 2015). Furthermore, multiple genetic mutations can be readily introduced in organoids using CRISPR-Cas9-mediated genome editing that facilitates the studies of cancer initiation and progression (Drost et al., 2017; Drost et al., 2015; Matano et al., 2015). Through this genetic modification strategy, we can inactivate *Trp53* and *Rb1* in healthy human organoids derived from gastric SCJ tissue, and study the process by which the normal human SCJ cells can be transformed to cancer. Additionally, previous genome-wide studies have reported a range of genetic mutations that may be associated with human gastric SCJ carcinomas (Network, 2014, 2017). We can implement a large-scale genetic screening using a CRISPR/Cas9 library targeting the relevant mutations to identify the signature combination of drivers essential for human gastric SCJ organoid transformation.

To identify the most likely cellular origin of gastric SCJ cancer, we have tracked the CD44 and Lgr5 expression during the SCJ carcinogenesis in *Lgr5*$^{EGFP\text{-}Ires\text{-}CreERT2}$*Trp53*$^{loxP/loxP}$*Rb1*$^{loxP/loxP}$Ai9 mouse model (Chapter 3). The results demonstrated that both the early dysplastic lesions and advanced tumors showed CD44 but not Lgr5 expression, supporting the notion that Lgr5^{-}CD44^{+} cells are the cells of gastric

SCJ carcinoma origin. To determine if the $LGR5^{-}CD44^{+}$ cells are also located at human gastric SCJ and contribute to cancer initiation and progression, we utilized *in situ* hybridization and immunohistochemistry to detect *LGR5* and CD44 expression, respectively, in the human tissue (Figure 5.4). Our preliminary results suggest that *LGR5* and CD44 expression are observed in the normal SCJ glands. However, the dysplastic lesion and advanced carcinoma appeared to show CD44 but not *LGR5* expression, which is consistent with the findings in mouse model. We plan to further extend this study by detection of LGR5 and CD44 expression in a cohort of patients with known survival.

5.2.3 Targeting of OPN-CD44 signaling for gastric SCJ cancer therapy

OPN-CD44 signaling has been known as a key oncogenic player involved in promotion of neoplasm into a high grade malignancy by mediating various facets of tumor behavior including cell proliferation, invasion, metastasis, angiogenesis, and stemness (Chakraborty et al., 2008; Lee et al., 2007; Mi et al., 2011; Tilli et al., 2011; Todaro et al., 2014). In Chapter 4, our data demonstrated that both OPN and CD44 expression are highly associated with poor survival time of the patient who had gastric SCJ cancer. Additionally, we also provided direct experimental evidence that OPN can promote the cancer initiation, growth, and tumorigenicity by regulating the stem-like properties of recipient cells. Thus OPN-CD44 signaling could be an appealing therapeutic target for managing the gastric SCJ cancer.

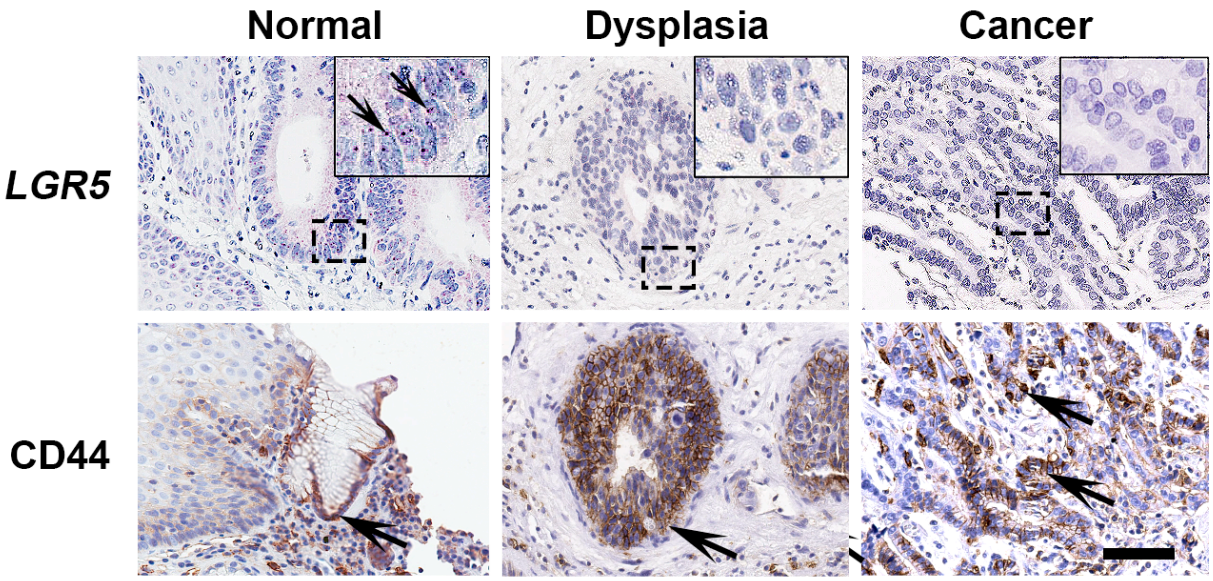

Figure 5.4 Detection of *LGR5* and CD44 expression in human tissue. *LGR5* mRNA (arrows in insets) and CD44 (arrows) are indicated. Rectangles in the images indicate respective locations of inset images. *In situ* hybridization (top panel) and Immunostaining, Elite ABC method (bottom panel). Counterstaining with hematoxylin. Scale bar represents 50 μm and 18 μm (insets), **P<0.01, ***P<0.001.

There are several potential approaches for the interruption of OPN-CD44 signaling pathway (Bandopadhyay et al., 2014; Wei et al., 2017). First, we can exploit small-molecule inhibitors to downregulate OPN and CD44 expression in the cancer cells (Mason et al., 2008; Sharma et al., 2010; Zagani et al., 2009; Zhao et al., 2018). Treatment of Agelastatin A, which is a brominated oroidin alkaloid extracted from marine animals, inhibits OPN expression through upregulation of OPN inhibitor TCF-4 and thereby suppresses tumor cell adhesion, colony formation, and migration (Mason et al., 2008). Moreover, downregulation of OPN and CD44 expression upon employment of Curcumin, which is a polysaccharide extract obtained from plants, significantly inhibit cancer invasion (Lv et al., 2013). Second, RNA aptamers, which are stable single-stranded oligonucleotides designed against specific proteins or peptides, can be used to inactivate extracellular OPN leading to the repression of cancer growth and metastasis (Mi et al., 2009; Talbot et al., 2011). Third, blocking antibodies to OPN and CD44 have also shown a promising result that inhibit the cancer cell proliferation, adhesion, and invasion by disturbing the bindings of OPN to CD44 (Ahmed et al., 2016; Dai et al., 2010; Teramoto et al., 2005). If successful, these approaches will provide the necessary rationale for planning of clinical trials.

References

Ahmed, M., Sottnik, J.L., Dancik, G.M., Sahu, D., Hansel, D.E., Theodorescu, D., and Schwartz, M.A. (2016). An Osteopontin/CD44 Axis in RhoGDI2-Mediated Metastasis Suppression. Cancer cell *30*, 432-443.

Alam, T.N., O'Hare, M.J., Laczkó, I., Freeman, A., Al-Beidh, F., Masters, J.R., and Hudson, D.L. (2004). Differential expression of CD44 during human prostate epithelial cell differentiation. Journal of Histochemistry & Cytochemistry *52*, 1083-1090.

Antoni, D., Burckel, H., Josset, E., and Noel, G. (2015). Three-dimensional cell culture: a breakthrough in vivo. Int J Mol Sci *16*, 5517-5527.

Bandopadhyay, M., Bulbule, A., Butti, R., Chakraborty, G., Ghorpade, P., Ghosh, P., Gorain, M., Kale, S., Kumar, D., Kumar, S.*, et al.* (2014). Osteopontin as a therapeutic target for cancer. Expert Opin Ther Targets *18*, 883-895.

Barker, N. (2014). Adult intestinal stem cells: critical drivers of epithelial homeostasis and regeneration. Nature reviews Molecular cell biology *15*, 19.

Barker, N., Huch, M., Kujala, P., van de Wetering, M., Snippert, H.J., van Es, J.H., Sato, T., Stange, D.E., Begthel, H., van den Born, M.*, et al.* (2010). Lgr5(+ve) stem cells drive self-renewal in the stomach and build long-lived gastric units in vitro. Cell stem cell *6*, 25-36.

Barré-Sinoussi, F., and Montagutelli, X. (2015). Animal models are essential to biological research: issues and perspectives. Future Sci OA *1*, FSO63.

Bartfeld, S., Bayram, T., van de Wetering, M., Huch, M., Begthel, H., Kujala, P., Vries, R., Peters, P.J., and Clevers, H. (2015). In vitro expansion of human gastric epithelial stem cells and their responses to bacterial infection. Gastroenterology *148*, 126-136. e126.

Blokzijl, F., de Ligt, J., Jager, M., Sasselli, V., Roerink, S., Sasaki, N., Huch, M., Boymans, S., Kuijk, E., Prins, P.*, et al.* (2016). Tissue-specific mutation accumulation in human adult stem cells during life. Nature … *538*, 260-264.

Boj, S.F., Hwang, C.-I., Baker, L.A., Chio, I.I.C., Engle, D.D., Corbo, V., Jager, M., Ponz-Sarvise, M., Tiriac, H., and Spector, M.S. (2015). Organoid models of human and mouse ductal pancreatic cancer. Cell *160*, 324-338.

Botterweck, A.A., Schouten, L.J., Volovics, A., Dorant, E., and van den Brandt, P.A. (2000). Trends in incidence of adenocarcinoma of the oesophagus and gastric

cardia in ten European countries. International journal of epidemiology *29*, 645-654.

Buas, M.F., and Vaughan, T.L. (2013). Epidemiology and risk factors for gastroesophageal junction tumors: understanding the rising incidence of this disease. Seminars in radiation oncology *23*, 3-9.

Chakraborty, G., Jain, S., and Kundu, G.C. (2008). Osteopontin promotes vascular endothelial growth factor-dependent breast tumor growth and angiogenesis via autocrine and paracrine mechanisms. Cancer research *68*, 152-161.

Cristobal, A., van den Toorn, H.W.P., van de Wetering, M., Clevers, H., Heck, A.J.R., and Mohammed, S. (2017). Personalized Proteome Profiles of Healthy and Tumor Human Colon Organoids Reveal Both Individual Diversity and Basic Features of Colorectal Cancer. Cell reports *18*, 263-274.

Cruz-Acuña, R., Quirós, M., Farkas, A.E., Dedhia, P.H., Huang, S., Siuda, D., García-Hernández, V., Miller, A.J., Spence, J.R., and Nusrat, A. (2017). Synthetic hydrogels for human intestinal organoid generation and colonic wound repair. Nature cell biology *19*, 1326.

Dai, J., Li, B., Shi, J., Peng, L., Zhang, D., Qian, W., Hou, S., Zhao, L., Gao, J., Cao, Z.*, et al.* (2010). A humanized anti-osteopontin antibody inhibits breast cancer growth and metastasis in vivo. Cancer Immunol Immunother *59*, 355-366.

De Sousa E Melo, F., Kurtova, A.V., Harnoss, J.M., Kljavin, N., Hoeck, J.D., Hung, J., Anderson, J.E., Storm, E.E., Modrusan, Z., Koeppen, H.*, et al.* (2017). A distinct role for Lgr5+ stem cells in primary and metastatic colon cancer. Nature … *543*, 676-680.

Dedhia, P.H., Bertaux-Skeirik, N., Zavros, Y., and Spence, J.R. (2016). Organoid Models of Human Gastrointestinal Development and Disease. Gastroenterology *150*, 1098-1112.

Denhardt, D.T., Mistretta, D., Chambers, A.F., Krishna, S., Porter, J.F., Raghuram, S., and Rittling, S.R. (2003). Transcriptional regulation of osteopontin and the metastatic phenotype: evidence for a Ras-activated enhancer in the human OPN promoter. Clinical and Experimental Metastasis *20*, 77-84.

Díaz-Flores, L., Madrid, J.F., Gutiérrez, R., Varela, H., Valladares, F., Alvarez-Argüelles, H., and Díaz-Flores, L. (2006). Adult stem and transit-amplifying cell location. Histol Histopathol *21*, 995-1027.

Drost, J., and Clevers, H. (2018). Organoids in cancer research. Nature reviews Cancer, 1-12.

Drost, J., van Boxtel, R., Blokzijl, F., Mizutani, T., Sasaki, N., Sasselli, V., de Ligt, J., Behjati, S., Grolleman, J.E., van Wezel, T.*, et al.* (2017). Use of CRISPR-modified human stem cell organoids to study the origin of mutational signatures in cancer. Science (New York, NY) *358*, 234-238.

Drost, J., van Jaarsveld, R.H., Ponsioen, B., Zimberlin, C., van Boxtel, R., Buijs, A., Sachs, N., Overmeer, R.M., Offerhaus, G.J., Begthel, H.*, et al.* (2015). Sequential cancer mutations in cultured human intestinal stem cells. Nature … *521*, 43-47.

Fatehullah, A., Tan, S.H., and Barker, N. (2016). Organoids as an in vitro model of human development and disease. Nature cell biology *18*, 246.

Felipe de Sousa, E.M., Colak, S., Buikhuisen, J., Koster, J., Cameron, K., de Jong, J.H., Tuynman, J.B., Prasetyanti, P.R., Fessler, E., and van den Bergh, S.P. (2011). Methylation of cancer-stem-cell-associated Wnt target genes predicts poor prognosis in colorectal cancer patients. Cell stem cell *9*, 476-485.

Festa, E., Fretz, J., Berry, R., Schmidt, B., Rodeheffer, M., Horowitz, M., and Horsley, V. (2011). Adipocyte lineage cells contribute to the skin stem cell niche to drive hair cycling. Cell *146*, 761-771.

Flesken-Nikitin, A., Odai-Afotey, A.A., and Nikitin, A.Y. (2014). Role of the stem cell niche in the pathogenesis of epithelial ovarian cancers. Molecular & cellular oncology *1*, e963435.

Fu, D.-J., Miller, A.D., Southard, T.L., Flesken-Nikitin, A., Ellenson, L.H., and Nikitin, A.Y. (2018). Stem Cell Pathology. Annu Rev Pathol *13*, 71-92.

Gao, D., Vela, I., Sboner, A., Iaquinta, P.J., Karthaus, W.R., Gopalan, A., Dowling, C., Wanjala, J.N., Undvall, E.A., and Arora, V.K. (2014). Organoid cultures derived from patients with advanced prostate cancer. Cell *159*, 176-187.

Ghaffarzadehgan, K., Jafarzadeh, M., Raziee, H.R., Sima, H.R., Esmaili-Shandiz, E., Hosseinnezhad, H., Taghizadeh-Kermani, A., Moaven, O., and Bahrani, M. (2008). Expression of cell adhesion molecule CD44 in gastric adenocarcinoma and its prognostic importance. World journal of gastroenterology: WJG *14*, 6376.

Goardon, N., Marchi, E., Atzberger, A., Quek, L., Schuh, A., Soneji, S., Woll, P., Mead, A., Alford, K.A., Rout, R.*, et al.* (2011). Coexistence of LMPP-like and GMP-like leukemia stem cells in acute myeloid leukemia. Cancer cell *19*, 138-152.

Hsu, Y.-C., and Fuchs, E. (2012). A family business: stem cell progeny join the niche to regulate homeostasis. Nature reviews Molecular cell biology *13*, 103.

Isinger-Ekstrand, A., Johansson, J., Ohlsson, M., Francis, P., Staaf, J., Jonsson, M., Borg, A., and Nilbert, M. (2010). Genetic profiles of gastroesophageal cancer: combined analysis using expression array and tiling array--comparative genomic hybridization. Cancer genetics and cytogenetics *200*, 120-126.

Jiang, M., Li, H., Zhang, Y., Yang, Y., Lu, R., Liu, K., Lin, S., Lan, X., Wang, H., Wu, H.*, et al.* (2017). Transitional basal cells at the squamous-columnar junction generate Barrett's oesophagus. Nature ….

Kim, M.A., Lee, H.S., Yang, H.-K., and Kim, W.H. (2005). Clinicopathologic and protein expression differences between cardia carcinoma and noncardia carcinoma of the stomach. Cancer *103*, 1439-1446.

Kusano, C., Gotoda, T., Khor, C.J., Katai, H., Kato, H., Taniguchi, H., and Shimoda, T. (2008). Changing trends in the proportion of adenocarcinoma of the esophagogastric junction in a large tertiary referral center in Japan. Journal of gastroenterology and hepatology *23*, 1662-1665.

Lapouge, G., Youssef, K.K., Vokaer, B., Achouri, Y., Michaux, C., Sotiropoulou, P.A., and Blanpain, C. (2011). Identifying the cellular origin of squamous skin tumors. Proceedings of the National Academy of Sciences of the United States of America *108*, 7431-7436.

Lau, E.Y.-T., Ho, N.P.-Y., and Lee, T.K.-W. (2017). Cancer Stem Cells and Their Microenvironment: Biology and Therapeutic Implications. Stem Cells Int *2017*, 3714190.

Lee, J.-L., Wang, M.-J., Sudhir, P.-R., Chen, G.-D., Chi, C.-W., and Chen, J.-Y. (2007). Osteopontin promotes integrin activation through outside-in and inside-out mechanisms: OPN-CD44V interaction enhances survival in gastrointestinal cancer cells. Cancer research *67*, 2089-2097.

Li, Z., Araoka, T., Wu, J., Liao, H.-K., Li, M., Lazo, M., Zhou, B., Sui, Y., Wu, M.-Z., Tamura, I.*, et al.* (2016). 3D Culture Supports Long-Term Expansion of Mouse and Human Nephrogenic Progenitors. Cell stem cell *19*, 516-529.

Lv, J., Shao, Q., Wang, H., Shi, H., Wang, T., Gao, W., Song, B., Zheng, G., Kong, B., and Qu, X. (2013). Effects and mechanisms of curcumin and basil polysaccharide on the invasion of SKOV3 cells and dendritic cells. Mol Med Rep *8*, 1580-1586.

Mason, C.K., McFarlane, S., Johnston, P.G., Crowe, P., Erwin, P.J., Domostoj, M.M., Campbell, F.C., Manaviazar, S., Hale, K.J., and El-Tanani, M. (2008). Agelastatin A: a novel inhibitor of osteopontin-mediated adhesion, invasion, and colony formation. Mol Cancer Ther *7*, 548-558.

Matano, M., Date, S., Shimokawa, M., Takano, A., Fujii, M., Ohta, Y., Watanabe, T., Kanai, T., and Sato, T. (2015). Modeling colorectal cancer using CRISPR-Cas9-mediated engineering of human intestinal organoids. Nature medicine *21*, 256-262.

Matthews, R.A.J. (2008). Medical progress depends on animal models - doesn't it? J R Soc Med *101*, 95-98.

McCracken, K.W., Catá, E.M., Crawford, C.M., Sinagoga, K.L., Schumacher, M., Rockich, B.E., Tsai, Y.-H., Mayhew, C.N., Spence, J.R., and Zavros, Y. (2014). Modelling human development and disease in pluripotent stem-cell-derived gastric organoids. Nature *516*, 400.

McGonigle, P., and Ruggeri, B. (2014). Animal models of human disease: challenges in enabling translation. Biochem Pharmacol *87*, 162-171.

Mi, Z., Bhattacharya, S.D., Kim, V.M., Guo, H., Talbot, L.J., and Kuo, P.C. (2011). Osteopontin promotes CCL5-mesenchymal stromal cell-mediated breast cancer metastasis. CARCIN *32*, 477-487.

Mi, Z., Guo, H., Russell, M.B., Liu, Y., Sullenger, B.A., and Kuo, P.C. (2009). RNA aptamer blockade of osteopontin inhibits growth and metastasis of MDA-MB231 breast cancer cells. Mol Ther *17*, 153-161.

Morath, I., Hartmann, T.N., and Orian-Rousseau, V. (2016). CD44: more than a mere stem cell marker. The international journal of biochemistry & cell biology.

Network, C.G.A.R. (2014). Comprehensive molecular characterization of gastric adenocarcinoma. Nature *513*, 202-209.

Network, C.G.A.R. (2017). Integrated genomic characterization of oesophageal carcinoma. Nature *541*, 169-175.

Noordzij, M.A., van Steenbrugge, G.J., Verkaik, N.S., Schröder, F.H., and van der Kwast, T.H. (1997). The prognostic value of CD44 isoforms in prostate cancer patients treated by radical prostatectomy. Clin Cancer Res *3*, 805-815.

Ordonez, P., and Di Girolamo, N. (2012). Limbal epithelial stem cells: role of the niche microenvironment. Stem cells *30*, 100-107.

Quante, M., Bhagat, G., Abrams, J.A., Marache, F., Good, P., Lee, M.D., Lee, Y., Friedman, R., Asfaha, S., Dubeykovskaya, Z*., et al.* (2012). Bile acid and inflammation activate gastric cardia stem cells in a mouse model of Barrett-like metaplasia. Cancer cell *21*, 36-51.

Quante, M., Tu, S.P., Tomita, H., Gonda, T., Wang, S.S., Takashi, S., Baik, G.H., Shibata, W., DiPrete, B., and Betz, K.S. (2011). Bone marrow-derived

myofibroblasts contribute to the mesenchymal stem cell niche and promote tumor growth. Cancer cell *19*, 257-272.

Roerink, S.F., Sasaki, N., Lee-Six, H., Young, M.D., Alexandrov, L.B., Behjati, S., Mitchell, T.J., Grossmann, S., Lightfoot, H., Egan, D.A.*, et al.* (2018). Intra-tumour diversification in colorectal cancer at the single-cell level. Nature … *556*, 457-462.

Sachs, N., de Ligt, J., Kopper, O., Gogola, E., Bounova, G., Weeber, F., Balgobind, A.V., Wind, K., Gracanin, A., Begthel, H.*, et al.* (2018). A Living Biobank of Breast Cancer Organoids Captures Disease Heterogeneity. Cell *172*, 373-386.e310.

Sato, T., Van Es, J.H., Snippert, H.J., Stange, D.E., Vries, R.G., Van Den Born, M., Barker, N., Shroyer, N.F., Van De Wetering, M., and Clevers, H. (2011). Paneth cells constitute the niche for Lgr5 stem cells in intestinal crypts. Nature *469*, 415.

Sato, T., Vries, R.G., Snippert, H.J., van de Wetering, M., Barker, N., Stange, D.E., van Es, J.H., Abo, A., Kujala, P., Peters, P.J.*, et al.* (2009). Single Lgr5 stem cells build crypt-villus structures in vitro without a mesenchymal niche. Nature … *459*, 262-265.

Sharma, P., Kumar, S., and Kundu, G.C. (2010). Transcriptional regulation of human osteopontin promoter by histone deacetylase inhibitor, trichostatin A in cervical cancer cells. Molecular Cancer *9*, 178.

Shimokawa, M., Ohta, Y., Nishikori, S., Matano, M., Takano, A., Fujii, M., Date, S., Sugimoto, S., Kanai, T., and Sato, T. (2017). Visualization and targeting of LGR5+ human colon cancer stem cells. Nature … *545*, 187-192.

Talbot, L.J., Mi, Z., Bhattacharya, S.D., Kim, V., Guo, H., and Kuo, P.C. (2011). Pharmacokinetic characterization of an RNA aptamer against osteopontin and demonstration of in vivo efficacy in reversing growth of human breast cancer cells. Surgery *150*, 224-230.

Teramoto, H., Castellone, M.D., Malek, R.L., Letwin, N., Frank, B., Gutkind, J.S., and Lee, N.H. (2005). Autocrine activation of an osteopontin-CD44-Rac pathway enhances invasion and transformation by H-RasV12. Oncogene *24*, 489-501.

Tetteh, P.W., Farin, H.F., and Clevers, H. (2015). Plasticity within stem cell hierarchies in mammalian epithelia. Trends in cell biology *25*, 100-108.

Tilli, T.M., Franco, V.F., Robbs, B.K., Wanderley, J.L.M., da Silva, F.R.d.A., de Mello, K.D., Viola, J.P.B., Weber, G.F., and Gimba, E.R. (2011). Osteopontin-c splicing isoform contributes to ovarian cancer progression. Mol Cancer Res *9*, 280-293.

Todaro, M., Gaggianesi, M., Catalano, V., Benfante, A., Iovino, F., Biffoni, M., Apuzzo, T., Sperduti, I., Volpe, S., Cocorullo, G.*, et al.* (2014). CD44v6 Is a Marker of Constitutive and Reprogrammed Cancer Stem Cells Driving Colon Cancer Metastasis. Stem Cell *14*, 342-356.

van de Wetering, M., Francies, H.E., Francis, J.M., Bounova, G., Iorio, F., Pronk, A., van Houdt, W., van Gorp, J., Taylor-Weiner, A., and Kester, L. (2015). Prospective derivation of a living organoid biobank of colorectal cancer patients. Cell *161*, 933-945.

van der Worp, H.B., Howells, D.W., Sena, E.S., Porritt, M.J., Rewell, S., O'Collins, V., and Macleod, M.R. (2010). Can Animal Models of Disease Reliably Inform Human Studies? PLoS Med *7*, e1000245.

Vlachogiannis, G., Hedayat, S., Vatsiou, A., Jamin, Y., Fernández-Mateos, J., Khan, K., Lampis, A., Eason, K., Huntingford, I., and Burke, R. (2018). Patient-derived organoids model treatment response of metastatic gastrointestinal cancers. Science *359*, 920-926.

Voges, H.K., Mills, R.J., Elliott, D.A., Parton, R.G., Porrello, E.R., and Hudson, J.E. (2017). Development of a human cardiac organoid injury model reveals innate regenerative potential. Development *144*, 1118-1127.

Wang, T., Yeoh, K.G., and Salto-Tellez, M. (2012). Lgr5 expression is absent in human premalignant lesions of the stomach. Gut *61*, 1777-1778.

Weeber, F., Ooft, S.N., Dijkstra, K.K., and Voest, E.E. (2017). Tumor Organoids as a Pre-clinical Cancer Model for Drug Discovery. Cell Chem Biol *24*, 1092-1100.

Wei, R., Wong, J.P.C., and Kwok, H.F. (2017). Osteopontin -- a promising biomarker for cancer therapy. Journal of Cancer *8*, 2173-2183.

White, A.C., and Lowry, W.E. (2015). Refining the role for adult stem cells as cancer cells of origin. Trends in cell biology *25*, 11-20.

White, A.C., Tran, K., Khuu, J., Dang, C., Cui, Y., Binder, S.W., and Lowry, W.E. (2011). Defining the origins of Ras/p53-mediated squamous cell carcinoma. Proceedings of the National Academy of Sciences of the United States of America *108*, 7425-7430.

Yang, H., Adam, R.C., Ge, Y., Hua, Z.L., and Fuchs, E. (2017). Emerging roles of transit-amplifying cells in tissue regeneration and cancer. Cell *169*, 483-496.e413.

Zagani, R., Hamzaoui, N., Cacheux, W., de Reyniès, A., Terris, B., Chaussade, S., Romagnolo, B., Perret, C., and Lamarque, D. (2009). Cyclooxygenase-2

inhibitors down-regulate osteopontin and Nr4A2-new therapeutic targets for colorectal cancers. Gastroenterology *137*, 1358-1366.e1351-1353.

Zhao, H., Chen, Q., Alam, A., Cui, J., Suen, K.C., Soo, A.P., Eguchi, S., Gu, J., and Ma, D. (2018). The role of osteopontin in the progression of solid organ tumour. Cell Death Dis *9*, 1-15.

APPENDIX

SUMMARY OF ADDITIONAL RELEVANT PUBLICATIONS WITH CONTRIBUTIONS BY THE AUTHOR

STEM CELL PATHOLOGY

Dah-Jiun Fu, Andrew D. Miller, Teresa L. Southard, Andrea Flesken-Nikitin, Lora H. Ellenson, and Alexander Yu. Nikitin (2018) Annual Review of Pathology: Mechanisms of Disease: 13:71-92. PMID: 29059010

Abstract

Rapid advances in stem cell biology and regenerative medicine have opened new opportunities for better understanding disease pathogenesis and the development of new diagnostic, prognostic, and treatment approaches. Many stem cell niches are well defined anatomically, thereby allowing their routine pathological evaluation during disease initiation and progression. Evaluation of the consequences of genetic manipulations in stem cells and investigation of the roles of stem cells in regenerative medicine and pathogenesis of various diseases such as cancer require significant expertise in pathology for accurate interpretation of novel findings. Therefore, there is an urgent need for developing stem cell pathology as a discipline to facilitate stem cell research and regenerative medicine. This review provides examples of anatomically defined niches suitable for evaluation by diagnostic pathologists, describes neoplastic lesions associated with them, and discusses further directions of stem cell pathology.

SCALABLE PRODUCTION AND CRYO-STORAGE OF ORGANOIDS USING CORE-SHELL DECOUPLED HYDROGEL CAPSULES

Yen-Chun Lu, Dah-Jiun Fu, Duo An, Alan Chiu, Robert Schwartz, Alexander Yu. Nikitin, and Minglin Ma (2017) Adv Biosyst 1:1700165. PMID: 2960740

Abstract

Organoids, organ-mimicking multicellular structures derived from pluripotent stem cells or organ progenitors, have recently emerged as an important system for both studies of stem cell biology and development of potential therapeutics; however, a large-scale culture of organoids and cryopreservation for whole organoids, a prerequisite for their industrial and clinical applications, has remained a challenge. Current organoid culture systems relying on embedding the stem or progenitor cells in bulk extracellular matrix (ECM) hydrogels (e.g., Matrigel) have limited surface area for mass transfer and are not suitable for large-scale productions. Here, a capsule-based, scalable organoid production and cryopreservation platform is demonstrated. The capsules have a core-shell structure where the core consists of Matrigel that supports the growth of organoids, and the alginate shell forms robust spherical capsules, enabling suspension culture in stirred bioreactors. Compared with conventional, bulk ECM hydrogels, the capsules, which can be produced continuously by a two-fluidic electrostatic cospraying method, provide better mass transfer through both diffusion and convection. The core-shell structure of the capsules also leads to better cell recovery after cryopreservation of organoids probably through prevention of intracellular ice formation.